

**NASA Contractor Report 181819**

**Interior Noise Control  
Ground Test Studies for  
Advanced Turboprop  
Aircraft Applications**

**Myles A. Simpson, Mark R. Cannon,  
Paul L. Burge, and Robert P. Boyd**

**DOUGLAS AIRCRAFT COMPANY  
MCDONNELL DOUGLAS CORPORATION  
LONG BEACH, CA 90846**

**CONTRACT NAS1-18037  
APRIL 1989**



**National Aeronautics and  
Space Administration**

**Langley Research Center  
Hampton, Virginia 23665-5225**

## Preface

This report was prepared by McDonnell Douglas Corporation under Task Assignment 2 of Contract NAS1-18037 with NASA Langley Research Center. The NASA technical monitor was Dr. Kevin P. Shepherd.

Several individuals at Douglas Aircraft Company made major contributions to this study. The various tests described in this report were conducted under the direction of Don Daulton, with support from Dick Gordon, Debbie Murphy and Mike Sundquist. Glenn Hinote was responsible for the structural mode survey. Matt Salcius and Bill Gayle directed fuselage modification activities. Analysis software was developed by Carol Ritch, John Hatlestad, Robert Redfield and Jim Strong. Stuart McGregor, Bal Lahoti, Sandra Krauthamer, Kristy Warfield and Rhonda Cunningham assisted with data analysis and presentation. Inge Green, Marcello Cianciaruso and Karl Liehr contributed to test planning and interpretation of test results. Dr. Mahendra Joshi reviewed the report and offered many constructive comments. Special thanks go to Norris Haight for overseeing implementation and design of the FARF facility, and to Dr. Daryl May for initiating the FARF facility concept and providing support and guidance with the test program.

# Contents

<b>1</b>	<b>Introduction</b>	<b>1</b>
1.1	Background . . . . .	1
1.2	Objectives and Approach . . . . .	3
1.3	Report Overview . . . . .	4
<b>2</b>	<b>Description of the Test Facility</b>	<b>5</b>
2.1	Test Article . . . . .	5
2.2	Noise and Vibration Sources . . . . .	6
2.3	Measurement and Processing Instrumentation . . . . .	7
<b>3</b>	<b>Fuselage Structural Mode Surveys</b>	<b>23</b>
3.1	Measurement and Analysis Procedures . . . . .	23
3.2	Measurement Results . . . . .	24
<b>4</b>	<b>Cabin Cavity Mode Surveys</b>	<b>32</b>
4.1	Measurement and Analysis Procedures . . . . .	32
4.2	Measurement Results . . . . .	33
<b>5</b>	<b>Baseline Forced Response Tests</b>	<b>42</b>
5.1	Measurement and Analysis Procedures . . . . .	42
5.1.1	Transducers . . . . .	42
5.1.2	Acoustic Excitation Sources . . . . .	43
5.1.3	Vibration Excitation Sources . . . . .	45
5.1.4	Data Analysis and Normalization . . . . .	46
5.2	Measurement Results . . . . .	47
5.2.1	Baseline Response Levels, Acoustic Excitation . . . . .	47
5.2.2	Baseline Response Levels, Vibration Excitation . . . . .	47
<b>6</b>	<b>Noise Control Treatment Forced Response Tests</b>	<b>60</b>
6.1	Description of Treatments . . . . .	60
6.2	Measurement and Analysis Procedures . . . . .	62
6.3	Measurement Results . . . . .	63
6.3.1	Treatment Response Levels, Acoustic Excitation . . . . .	63
6.3.2	Treatment Response Levels, Vibration Excitation . . . . .	64
<b>7</b>	<b>Transmission Path Tests</b>	<b>90</b>
7.1	Pressure Bulkhead Path . . . . .	90
7.1.1	Measurement and Analysis Procedures . . . . .	91
7.1.2	Measurement Results . . . . .	91
7.2	Cabin Sidewall Path . . . . .	92

7.2.1	Measurement and Analysis Procedures . . . . .	93
7.2.2	Measurement Results . . . . .	93
7.3	Fuselage Structural Path . . . . .	94
7.3.1	Measurement and Analysis Procedures . . . . .	94
7.3.2	Measurement Results . . . . .	94
<b>8</b>	<b>Sound Intensity Surveys</b>	<b>116</b>
8.1	Measurement and Analysis Procedures . . . . .	116
8.1.1	Bare Cabin Survey . . . . .	116
8.1.2	Furnished Cabin Surveys . . . . .	117
8.2	Measurement Results . . . . .	117
8.2.1	Bare Cabin Survey . . . . .	117
8.2.2	Furnished Cabin Surveys . . . . .	118
<b>9</b>	<b>Summary and Conclusions</b>	<b>136</b>

## List of Tables

3-1. Measured Frame and Shell Modes .....	25
4-1. Measured Transverse and Longitudinal Modes .....	34
6-1. Forced Response Test Configurations .....	67

## List of Figures

2-1. Schematic of the Fuselage Acoustic Research Facility (FARF) .....	10
2-2. The DC-9 Aft Fuselage Section, Showing Frame and Longeron Numbering ...	11
2-3. Plan View of the Bare Cabin .....	12
2-4. The Test Section on its Transporter, Entering the Anechoic Chamber .....	13
2-5. Plan View of the Furnished Cabin .....	14
2-6. The Loudspeaker Array, Positioned at the UHB Prop Plane .....	15
2-7. The Shaker Mounted to the Left Pylon at the Engine Attachment Point .....	16
2-8. Comparison of the JT8D and UHB Pylons and Engine Installation .....	17
2-9. Exterior Microphones Mounted Around the Fuselage .....	18
2-10. Interior Microphones in the Bare Cabin .....	19
2-11. Interior Microphones in the Furnished Cabin .....	20
2-12. Tri-axial Accelerometers Mounted on the Pylon .....	21
2-13. View of the Control Room During Testing .....	22
3-1. Structural Mode Survey Measurement Locations .....	26
3-2. Frame and Shell Undeformed Structures .....	27
3-3. Frequency Response Function for Frame 766 at Longeron 4 (Input at Longeron 10) .....	28
3-4. Sample Frame Mode, Station 766 .....	29
3-5. Sample Shell Mode .....	30
3-6. Comparison of Predicted and Measured Frame Modes at Station 766 .....	31
4-1. Cavity Mode Measurement Locations .....	35
4-2. Cavity Mode Measurements in the Bare and Furnished Cabin .....	36
4-3. Identification of Modal Frequencies from Transfer Function Plots .....	37
4-4. Sample Transverse Cavity Mode in the Bare Cabin .....	38
4-5. Sample Transverse Cavity Mode in the Furnished Cabin .....	39
4-6. Sample Longitudinal Cavity Mode in the Furnished Cabin .....	40

4-7. Comparison of Predicted and Measured Transverse Cavity Modes in the Bare Cabin .....	41
5-1. Location of Microphones .....	48
5-2. Location of Accelerometers .....	49
5-3. Comparison of Predicted and Simulated UHB Level Distributions .....	50
5-4. Measured Sound Pressure Levels for Tonal Acoustic Excitation, Baseline Phase, Sta. 642 .....	51
5-5. Measured Sound Pressure Levels for Tonal Acoustic Excitation, Baseline Phase, Sta. 690 .....	52
5-6. Measured Sound Pressure Levels for Tonal Acoustic Excitation, Baseline Phase, Sta. 748 .....	53
5-7. Measured Sound Pressure Levels for Tonal Acoustic Excitation, Baseline Phase, Sta. 772 .....	54
5-8. Measured Sound Pressure Levels for Tonal Acoustic Excitation, Baseline Phase, Station Averages .....	55
5-9. Measured Acceleration Levels for Tonal Vibration Excitation, Baseline Phase, Longeron 10 .....	56
5-10. Measured Acceleration Levels for Tonal Vibration Excitation, Baseline Phase, Station 718 .....	57
5-11. Measured Sound Pressure Levels for Tonal Vibration Excitation, Baseline Phase, Stations 748, 772 .....	58
5-12. Measured Sound Pressure Levels for Tonal Vibration Excitation, Baseline Phase, Station Averages .....	59
6-1. Predicted Transmission Paths for UHB Aircraft .....	68
6-2. Torque Box Design .....	69
6-3. Frame Modification Details .....	70
6-4. Double Wall Pressure Bulkhead Design .....	71
6-5. Dynamic Tuned Absorber Installed on Frame .....	72
6-6. Selected Treatments Installed on the Fuselage Sidewall .....	73
6-7. Absorption Blanket Installed in Aft Section .....	73
6-8. The Fully Furnished Cabin .....	74
6-9. Measured Sound Pressure Levels for Tonal Acoustic Excitation, Structural Modifications Phase, Station 772 .....	75
6-10. Measured Sound Pressure Levels for Tonal Acoustic Excitation, Furnished Fuselage Phase, Station 772 .....	76
6-11. Comparison of Average Sound Pressure Levels for All Treatment Configurations, Tonal Acoustic Excitation, 169 Hz .....	77

6-12. Comparison of Average Sound Pressure Levels for All Treatment Configurations, Tonal Acoustic Excitation, 213 Hz .....	78
6-13. Comparison of Average Sound Pressure Levels for All Treatment Configurations, Tonal Acoustic Excitation, 338 Hz .....	79
6-14. Comparison of Average Sound Pressure Levels for All Treatment Configurations, Tonal Acoustic Excitation, 426 Hz .....	80
6-15. Comparison of Average Sound Pressure Levels for All Treatment Configurations, Tonal Acoustic Excitation, 507 Hz .....	81
6-16. Comparison of Average Sound Pressure Levels for All Treatment Configurations, Tonal Acoustic Excitation, 639 Hz .....	82
6-17. Measured Acceleration Levels for Tonal Vibration Excitation, Baseline and Structural Modifications Phases, 169 Hz .....	83
6-18. Measured Acceleration Levels for Tonal Vibration Excitation, Baseline and Furnished Fuselage Phases, 169 Hz .....	84
6-19. Comparison of Average Measured Acceleration Levels for All Treatment Configurations, Tonal Vibration Excitation, Station 718, 169 Hz .....	85
6-20. Comparison of Average Measured Acceleration Levels for All Treatment Configurations, Tonal Vibration Excitation, Longeron 10, 169 Hz .....	86
6-21. Comparison of Average Measured Acceleration Levels for All Treatment Configurations, Tonal Vibration Excitation, Station 718, 213 Hz .....	87
6-22. Comparison of Average Measured Acceleration Levels for All Treatment Configurations, Tonal Vibration Excitation, Longeron 10, 213 Hz .....	88
6-23. Measured Sound Pressure Levels for Tonal Vibration Excitation, Structural Modifications and Furnished Fuselage Phases, Stations 748, 772 .....	89
7-1. UHB Noise Transmission Paths (Based on Demo Data) .....	96
7-2. Pressure Bulkhead Path Test Configuration .....	97
7-3. Pressure Bulkhead "Through the Door" Noise Reduction .....	98
7-4. Pressure Bulkhead "Into the Cabin" Noise Reduction .....	99
7-5. Cabin Sidewall Path Test Configuration .....	100
7-6. Sidewall Noise Reduction (Average for all Mics) .....	101
7-7. Sidewall Noise Reduction (To Mic I-672-B) .....	102
7-8. Sidewall Noise Reduction (To Mic I-672-F) .....	103
7-9. Longeron 10 Acceleration Levels, Configuration 23 .....	104
7-10. Frame 718 Acceleration Levels, Configuration 23 .....	106
7-11. Longeron 10 Normalized Acceleration Levels (20 lb Force) .....	108
7-12. Frame 718 Normalized Acceleration Levels (20 lb Force) .....	110
7-13. Normalized Sound Pressure Levels (Average for all Mics) .....	112
7-14. Normalized Sound Pressure Levels (At Mics I-737-E or F) .....	114

8-1. Sound Intensity Survey Areas in the Bare Cabin .....	121
8-2. Survey Grid Cells, Bare Cabin .....	122
8-3. Sound Intensity Survey Areas in the Furnished Cabin .....	123
8-4. Survey Grid Cells, Furnished Cabin .....	124
8-5. View of the Furnished Cabin Survey Area .....	125
8-6. Sound Power Levels in the 160 Hz Band, Airborne Path Survey, Bare Cabin .....	126
8-7. Sound Power Levels in the 200 Hz Band, Airborne Path Survey, Bare Cabin .....	127
8-8. Sound Power Levels in the 160 Hz Band, Airborne Path Survey, Furnished Cabin .....	128
8-9. Sound Power Levels in the 200 Hz Band, Airborne Path Survey, Furnished Cabin .....	129
8-10. Sound Power Levels in the 160 Hz Band, Structureborne Path Survey, Furnished Cabin .....	130
8-11. Sound Power Levels in the 200 Hz Band, Structureborne Path Survey, Furnished Cabin .....	131
8-12. Comparison of Sidewall Intensity Levels, Airborne Path Surveys .....	132
8-13. Comparison of Pressure Bulkhead Intensity Levels, Airborne Path Surveys .....	133
8-14. Comparison of Pressure Bulkhead Intensity Levels, Structureborne Path Surveys .....	134
8-15. Comparison of Sidewall and Pylon Bulkhead Intensity Levels, Structureborne Path Surveys .....	135

# 1 Introduction

## 1.1 Background

Over the past fifteen years there has been a renewed interest in the use of fuel-efficient turboprop engines for aircraft powerplants, due to the concern over rising fuel costs and the accompanying desire for energy conservation. Advanced turboprop engines, which make use of recent developments in blade design and fabrication, have the potential for providing thrust that is comparable to today's turbofan engines with a significant reduction in fuel use.

McDonnell Douglas Corporation (MDC) is currently developing a new generation of commercial transport aircraft that would be powered by such advanced turboprop engines, designated as Ultra High Bypass (UHB) engines. MDC's plans are to develop a derivative of the MD-80 series aircraft, which would incorporate two aft-mounted UHB engines in place of the two turbofan engines now utilized.

One of the major technology issues associated with these UHB aircraft is the noise environment that may be experienced by passengers. The longest portion of a typical flight is spent at high altitude, high speed cruise. Under these conditions the UHB engine is expected to produce its highest noise levels since the tips of the propeller blades are moving at supersonic speeds.

The resulting acoustic energy is generated in discrete tones, at frequencies corresponding to the blade passage frequency and its multiples for each propeller rotor. These blade passage frequencies lie typically between 100 and 250 Hz, where the transmission loss characteristics of standard aircraft sidewalls are not sufficient to reduce exterior levels to acceptably low interior levels, and where traditional methods of noise control usually involve measures which adversely affect aircraft performance (i.e., add-on treatments which are bulky and massive). Since today's airline passenger expects a pleasant cabin noise environment, noise control treatments are required which result in satisfactory interior noise levels and which meet space and weight constraints.

In 1985, a UHB Technology Readiness Program was initiated at Douglas Aircraft Company to address the various technical issues associated with the development of UHB aircraft. Under this program a Fuselage Acoustic Research Facility (FARF), dedicated to the study and control of UHB interior noise, was constructed in Long Beach, California. FARF consists of the aft section of a DC-9 aircraft as the full scale test article, acoustic and vibration sources for the simulation of UHB excitation, a multi-channel digital data acquisition and processing system, and a large anechoic chamber to house the fuselage section.

FARF was designed to be the primary test facility for evaluating the effectiveness

of cabin noise control measures for UHB aircraft. The rationale for the construction and use of a full size fuselage ground test facility for this purpose was based on early expectations about the complexity of the cabin noise control problem. High noise levels in the cabin could arise from propagation along any of several airborne and structureborne paths, and the modal characteristics of both the fuselage structure and the cabin cavity could significantly influence the interior noise environment. These factors, combined with the complex structural characteristics in the aft section of the MD-80 aircraft, led to the belief that assessments based on either analytical models or testing at other than full scale would not produce accurate results. A further benefit of FARF is that the aft fuselage structure of the DC-9 test article is nearly identical to that of the MD-80.

The most desirable approach to study cabin noise and alternative control measures would be during actual flight conditions, however the high costs and severe time constraints associated with flight testing made this impractical except on a limited basis. The UHB Technology Readiness Program did, in fact, include a series of flight tests of an MD-80 aircraft which was modified by replacing one of its JT8D turbofan engines with a prototype UHB engine. The UHB engine used for these tests was a General Electric "Unducted Fan" (UDF) engine, which utilizes the exhaust from a small jet engine to drive two rows of highly swept, counter-rotating propeller blades. One of the major purposes of the flight tests of this UHB Demonstrator aircraft was to demonstrate that a "Quiet Cabin" could be achieved in a commercial transport aircraft powered by advanced turboprop engines. For these tests, a Quiet Cabin meant that the maximum noise level in the cabin during high altitude, high speed cruise conditions would not exceed 82 dBA.

In order to meet this interior noise goal for the UHB Demonstrator, the approach adopted was to:

1. Estimate interior noise levels for an untreated aircraft, using projections of UHB exterior noise levels and vibration loads;
2. Propose candidate noise control treatments applicable to the various expected airborne and structureborne transmission paths which would reduce interior noise levels to meet the goal of 82 dBA;
3. Evaluate the effectiveness of the candidate treatments using fuselage ground tests in FARF; and
4. Install the most promising treatments on the UHB Demonstrator aircraft to demonstrate that the Quiet Cabin could be achieved.

Starting in October 1986, a series of interior noise control tests was conducted in FARF to evaluate selected treatments planned for installation on the UHB Demonstra-

tor, and to study fuselage response characteristics. In conducting these tests, estimates of exterior acoustic and vibration loads were utilized since actual flight data to define these loads were not yet available. Flight tests of the Demonstrator powered by one JT8D engine and one UHB engine with eight blades on both the forward and aft rotors (an 8x8 configuration) began in June 1987, with a minimal noise control treatment package. Additional treatments were subsequently added, aided by the FARF test results. In July the installation of the full Quiet Cabin treatment package was completed, and the interior noise goal of 82 dBA was attained. In August, the 8x8 engine was replaced by a 10x8 engine (10 blades on the forward rotor and 8 blades on the aft rotor), and achievement of the 82 dBA interior noise goal was again demonstrated. Additional treatment evaluation tests have been conducted in FARF since that time, in order to better understand the effectiveness of the various treatments along individual transmission paths.

As one element of NASA's Advanced Turboprop (ATP) technology program, the NASA/Industry flight demonstration program was started in 1987 to work with the aircraft industry in the study of passenger cabin noise in advanced turboprop aircraft. Under this program, a contract with MDC required detailed analysis of the interior noise measurement data acquired during the several ground and flight tests described above. The results of the ground tests using FARF are documented herein. Analysis of the interior noise data measured on the UHB Demonstrator will be the subject of a subsequent report.

## 1.2 Objectives and Approach

The objectives of the analyses described in this report are to study the fuselage response characteristics of treated and untreated aircraft with aft-mount advanced turboprop engines, and to evaluate the effectiveness of selected noise control treatments in reducing passenger cabin noise.

In order to achieve these objectives, several sets of tests were conducted in FARF over a 1-1/2 year period. The majority of these tests were oriented towards measurement of treatment effectiveness, and were divided into three test phases. For each phase, the fuselage test article was exposed to both acoustic and vibration excitation designed to simulate the loads expected during high altitude, high speed cruise operations of an advanced turboprop aircraft (and specifically, a UHB aircraft powered by two Unducted Fan 10x8 engines); these tests are thus "forced response" tests, since the response of the aircraft to a particular forcing excitation is being evaluated.

The first or Baseline phase of the tests involved measurement of interior and exterior noise and vibration levels for a bare (unfurnished and untreated) test fuselage.

In the second or Structural Modifications phase, selected structural treatments were sequentially installed on the fuselage. Noise and vibration levels were measured at the same locations after each installation, and compared with the corresponding Baseline data in order to evaluate the effectiveness of each treatment. In the third or Furnished Fuselage phase, additional treatments were added including installation of the cabin furnishings and selected sidewall treatments. Again, after each installation noise and vibration levels were measured and compared with Baseline levels to evaluate treatment effectiveness.

Selected treatments were further assessed in a fourth phase, the Transmission Path phase. Here, acoustic and vibration excitation were applied along specific transmission paths to provide treatment effectiveness data appropriate to that path.

In addition to these various treatment effectiveness tests, three sets of measurement surveys were conducted to define the modal response of the test fuselage, and to identify major transmission paths. A proper understanding of modal and transmission path characteristics aids the development and application of cabin noise control techniques. At the start of the experimental program, structural mode surveys were conducted to measure frame and shell modes. At the same time, and again after the cabin furnishings were installed, acoustic mode surveys were conducted to measure cabin cavity modes. Finally, sound intensity surveys were also conducted on the bare and furnished fuselage, to help diagnose transmission path strengths and as a further measurement of the effectiveness of selected treatments.

### **1.3 Report Overview**

For the various tests described above, this report documents the measurement and analysis procedures, and summarizes the test results. In Section 2, the Fuselage Acoustic Research Facility is described. Sections 3 and 4 report on the structural and cavity mode surveys, respectively. The forced response tests are discussed in the following two sections, with the Baseline measurements covered in Section 5 and the Structural and Furnished Fuselage measurements covered in Section 6. Section 7 describes the Transmission Path tests, and Section 8 discusses the sound intensity surveys. The final section provides a summary of major conclusions. Tables and figures may be found at the end of each section.

## 2 Description of the Test Facility

All tests were conducted in the Douglas Aircraft Company (DAC) Fuselage Acoustics Research Facility (FARF). The facility consists of the aft section of a DC-9 aircraft fuselage, noise and vibration sources to simulate advanced turboprop excitation, a multi-channel digital data acquisition and processing system, and an anechoic chamber to house the fuselage section. A schematic of the experimental setup is shown in Figure 2-1. The individual components of the facility are described in the following sections.

### 2.1 Test Article

The aft 50 ft section of a DC-9 aircraft was utilized as the test article for all experiments. The DC-9 fuselage section was selected in order to permit full scale testing of a realistic structure representative of aft-engine mount configurations. Also, since the future MDC UHB aircraft will be a derivative of the MD-80 aircraft series, which itself is a derivative of the DC-9 aircraft series, the structural characteristics of the test article are expected to be similar to those of the UHB and MD-80 aircraft.

The test fuselage was originally a DC-9 series 10 aircraft used for passenger and then freight service; after a crash it was acquired by DAC for acoustic testing purposes and refurbished. To prepare the aircraft for experimentation, the forward portion of the vehicle was cut off at station 438 (see Figure 2-2), the wings were cut off, and the engines and vertical stabilizer were removed. A special flat bulkhead was installed at the forward end of the test section as a plug, in order to form a completely enclosed interior space (see Figure 2-3). Use of this plug eliminated acoustic flanking paths, and also permitted pressurization of the cabin. Two foot deep fiberglass wedges were attached to the interior side of the bulkhead, to limit reflections from the bulkhead wall.

The fuselage section was mounted on a wheeled transporter dolly so that it could be moved easily into and out of the chamber. To isolate the test section structurally, air bag type isolators were installed at the three points where the fuselage was mounted to the transporter. Figure 2-4 shows the fuselage section on the transporter as it is rolled into the anechoic chamber. The chamber itself has floor dimensions of 55 ft by 50 ft, and is 30 ft high; it is designed to provide anechoic conditions above 100 Hz.

For the Baseline, bare fuselage tests, the entire interior was removed so that only the bare skin, frame and longeron structural members, floor, and bulkheads (new front bulkhead, forward engine mount bulkheads and aft pressure bulkhead) were present. All the systems, ductwork and equipment in the aft portion of the fuselage section behind the pressure bulkhead were also removed. For the Furnished Fuselage tests, in addition

to the noise control treatments under evaluation, the cabin contained new carpeting, thermal insulation, trim and ceiling panels, and bag racks. The original seats, one of the original lavatories, and one new, modular lavatory were also installed (see Figure 2-5).

During all tests except the sound intensity and structural mode surveys (which required lab personnel to be in the cabin), the fuselage was pressurized to a pressure differential of 5 psi to better simulate in-flight conditions.

Additional details of the fuselage test section are shown in Figures 2-3 and 2-5.

## **2.2 Noise and Vibration Sources**

For those tests where simulation of advanced turboprop acoustic excitation was required (the forced response tests and the sound intensity surveys), two banks of 15 inch diameter loudspeakers (JBL model 2225H) were utilized. In each bank, 25 of these speakers were mounted in a specially fabricated rack in a 5 by 5 array (see Figure 2-6). The speaker rack permits the entire array to move vertically, and to rotate about its horizontal axis. During testing, each bank was positioned near the aft portion of the aircraft, one on each side, centered in the plane of the forward UHB propeller and rotated toward the fuselage (also shown in Figure 2-6).

The acoustic signal is created by one or more signal generators which feed either random, broadband noise or sine tones of selected frequencies through a series of amplifiers to any combination of speakers. By using different speaker combinations for different frequencies, the noise level distribution on the exterior surface of the fuselage could be adjusted (within limits) to simulate the distribution expected for a real UHB engine. This process will be described in more detail in Section 5.

A control panel permits independent gain control for each speaker. Time delay electronics are also incorporated into the signal generation circuitry to permit control over the phase of the signal, however for these tests the time delay feature of the system was not used.

With this speaker system, sound pressure levels on the fuselage surface for sine tones at specific frequencies were on the order of 130 dB. Although levels up to 150 dB were expected at the same locations on an actual UHB aircraft during high speed, high altitude operations, the acoustic loads generated in the facility were judged to be sufficiently high to study fuselage response characteristics in a relative sense, and to compare the effectiveness of noise control treatments tested at the same excitation level.

For those tests where simulation of UHB acoustic excitation was not required, a

single JBL model 2225H loudspeaker was used, located in accordance with the specific needs of the test.

Vibration excitation of the fuselage structure was generated by electrodynamic shakers (VTS-100) attached to either the engine pylon or directly to the fuselage frames. As for the acoustic excitation, signal generators provided either random or sine tone input to the shakers.

For UHB simulation, a single shaker attached to the forward engine mount on the left pylon was used. As shown in Figure 2-7, the shaker was mounted on a support structure external to the fuselage; vibration was imparted through a stinger connected to the pylon at a 45 degree angle. In an actual aft-mount UHB aircraft, each engine would be attached to a pylon which is much higher and wider than the pylon on either an MD-80 or the DC-9 test article (see Figure 2-8). However, for both the DC-9/MD-80 aircraft and the UHB Demonstrator aircraft, the forward attachment connects directly with the forward pylon spar and then the forward bulkhead, which is located within the passenger cabin, and separates the seating area from the lavatory area (see Figures 2-3 and 2-5). Thus, this represents a major transmission path for UHB vibration energy into the cabin (on MD-80 aircraft, transmission through the aft pylon spar is significantly lower than through the forward spar). Although vibration propagation through the actual UHB pylon is not simulated, the test approach simulates vibration propagation from its point of entry into the fuselage structure.

For the measurements which do not utilize UHB vibration simulation (the structural mode surveys), the shaker was connected directly to selected fuselage frames. Details are described in Section 3.

## **2.3 Measurement and Processing Instrumentation**

A custom designed digital data acquisition and processing system (DDAPS) was used for all tests except the sound intensity and structural mode surveys. DDAPS consists of a special digitizer coupled to a DEC microVAX II computer, and is designed to permit rapid calculation and display of a variety of time-series functions from which frequency domain data can subsequently be obtained. The system is capable of simultaneous sampling of up to 32 channels of analog data at a rate of 12,600 samples/second/channel for up to 2 minutes, covering a frequency range of up to 4 kHz. User selectable anti-aliasing filters and sampling rates allow tradeoffs between the upper frequency range and the number of channels which can be sampled simultaneously; for the measurements reported here the frequency range of interest was limited to between 100 and 1000 Hz, so all 32 channels were available. The sampling duration for each measurement was 30 seconds, which was sufficient to provide the frequency resolution

(3.125 Hz) used in the analysis.

During the various tests, up to 50 exterior and interior microphones were utilized to monitor noise levels outside and inside the fuselage. The exterior microphones were mounted on a special framework constructed around the fuselage section (see Figure 2-9); the interior microphones were mounted on test stands. All exterior microphones were either 1/2 inch B & K model 4134 or 1/4 inch B & K model 4136, with B & K model 2639 preamplifiers. All interior microphones were 1/2 inch B & K model 4134 with Genrad model 1560-P42 preamplifiers. Figures 2-10 and 2-11 show typical interior microphone positions in the bare and furnished cabins, respectively.

Up to 40 accelerometers were utilized to monitor vibration levels at various pylon, frame, and longeron locations. These were Endevco model 2250A accelerometers with Endevco model 102 power supplies/preamplifiers and Ithaco model 452 signal conditioning amplifiers. Figure 2-12 shows tri-axial accelerometers mounted on the left pylon to monitor the shaker input acceleration levels.

Specific locations for all the transducers used during the various tests are listed in subsequent report sections.

Data were recorded on a Honeywell model 101 FM tape recorder, 26 channels at a time. Annotation information and a time code were recorded on the remaining two recorder channels. The data tapes were then processed on DDAPS. Special software operating on a DEC VAX 8300 coupled with a Numerix MARS 432 array processor was used to convert the digitized time series data into the frequency domain, and to produce tabular and graphic output for subsequent analysis and data presentation.

The microphone channels were calibrated periodically with a B & K model 4220 pistonphone, which produces a constant 250 Hz signal at 124 dB. The accelerometer channels were similarly calibrated with a B & K model 4294 calibrator exciter which produces a constant 159 Hz signal at 1 g (rms). The various amplifiers were set to provide a 1 volt input to the tape recorder corresponding to either 124 dB or 1 g, depending on transducer type. This same 1 volt signal level was then used as a surrogate calibration signal on subsequent data tapes.

All test operations (including generation and control of test signals; conditioning, monitoring, and recording of transducer signals; and control of fuselage pressurization) were conducted in a control room adjacent to the anechoic chamber. The control room also houses all the electronic instrumentation necessary for the tests except DDAPS, which is located in a separate building. Figure 2-13 shows the control room during testing.

Throughout the test program described in this report, some 30,000 individual measurements were acquired (not all of which were utilized for the analyses contained in

this document). To ensure the accuracy and validity of the measurement results, each data point was initially screened by comparing signal levels and noise floors with those of other points in the same test, and/or for the same transducer in subsequent tests. As necessary, test data were discarded if instrumentation malfunction occurred or was suspected. As a further means of data validation, the broadband measurements were used to check the consistency of the tonal measurements.

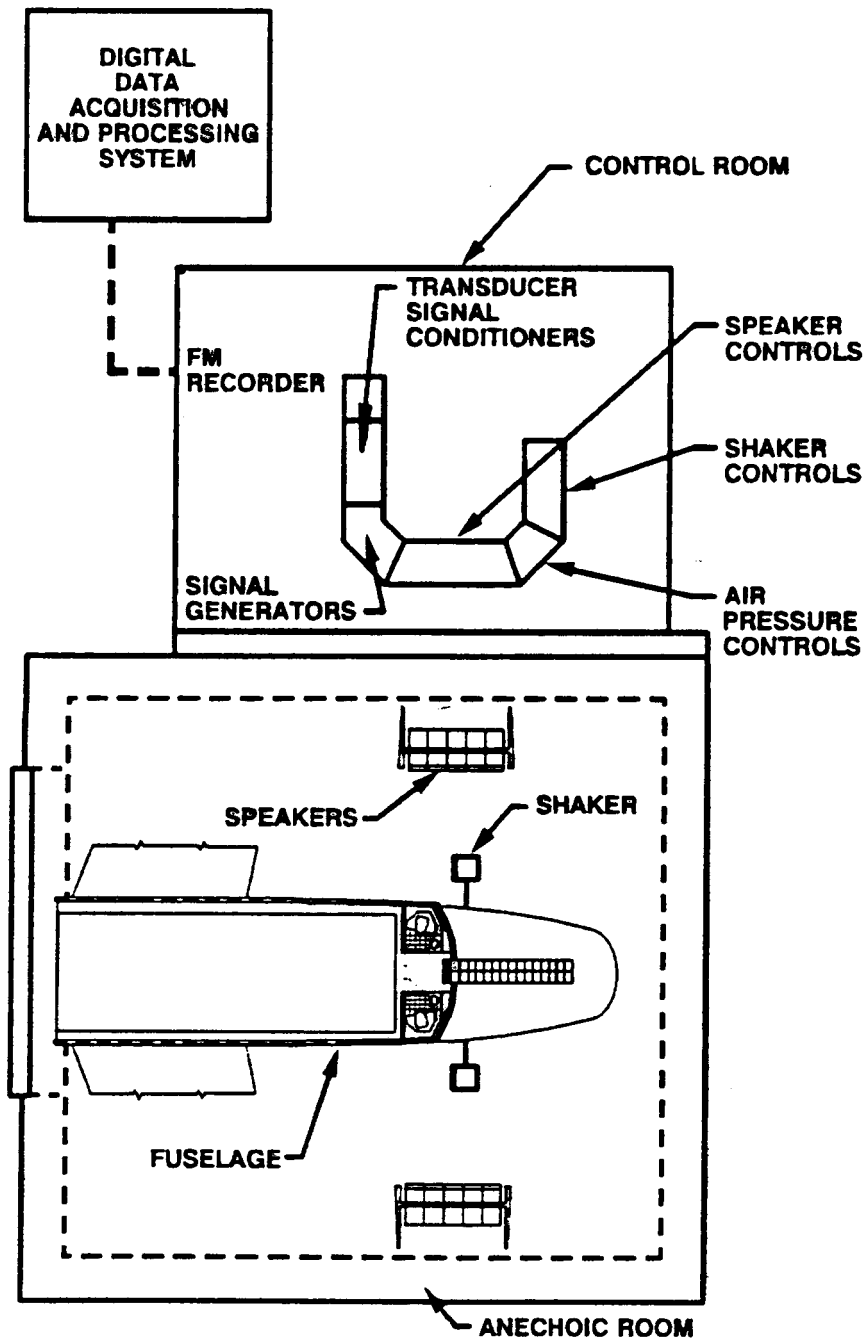


Figure 2-1 Schematic of the Fuselage Acoustic Research Facility (FARF)

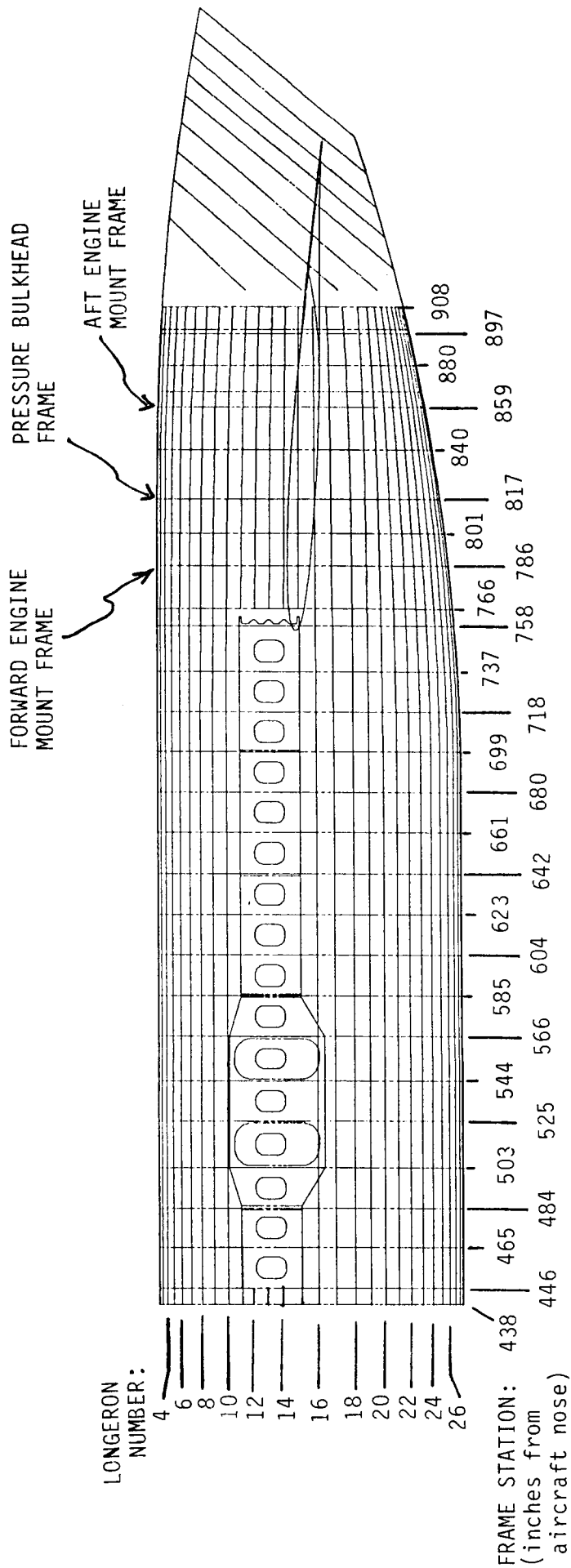


Figure 2-2 The DC-9 Aft Fuselage Section, Showing Frame and Longeron Numbering

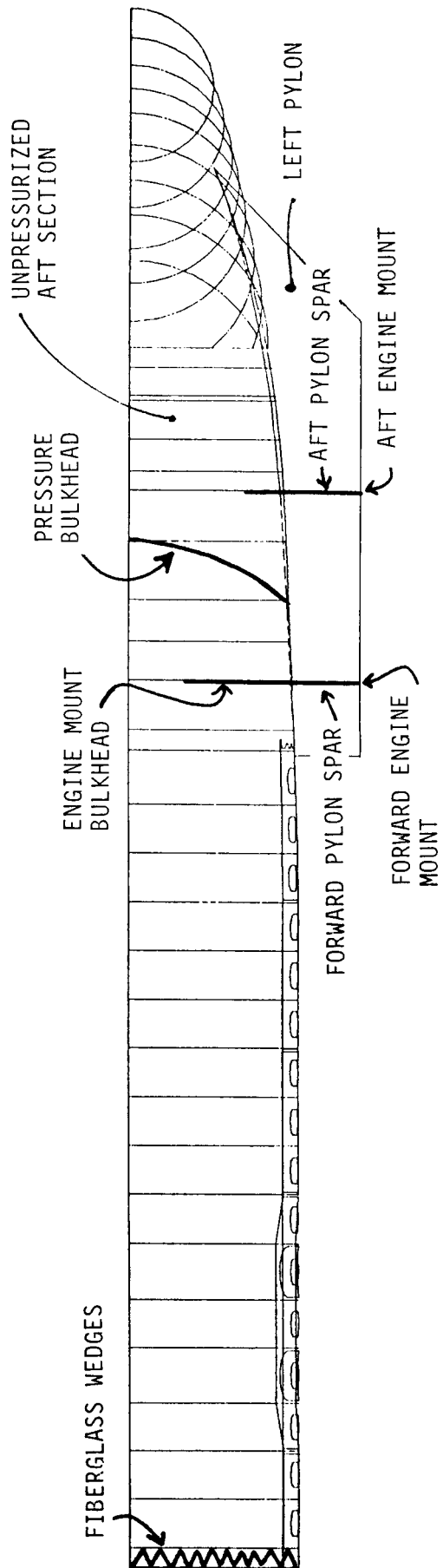


Figure 2-3 Plan View of the Bare Cabin

ORIGINAL PAGE  
BLACK AND WHITE PHOTOGRAPH

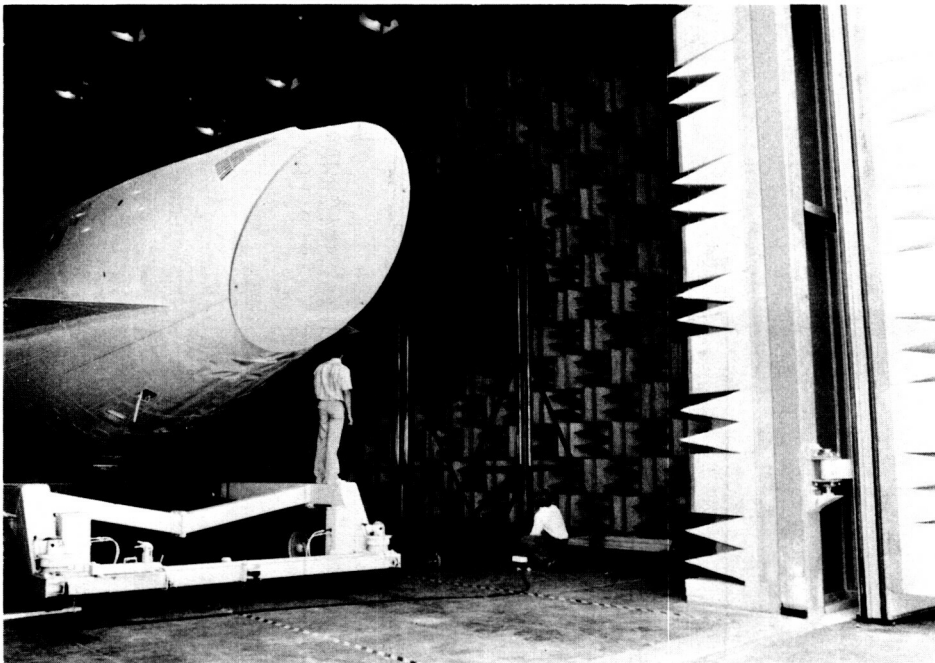
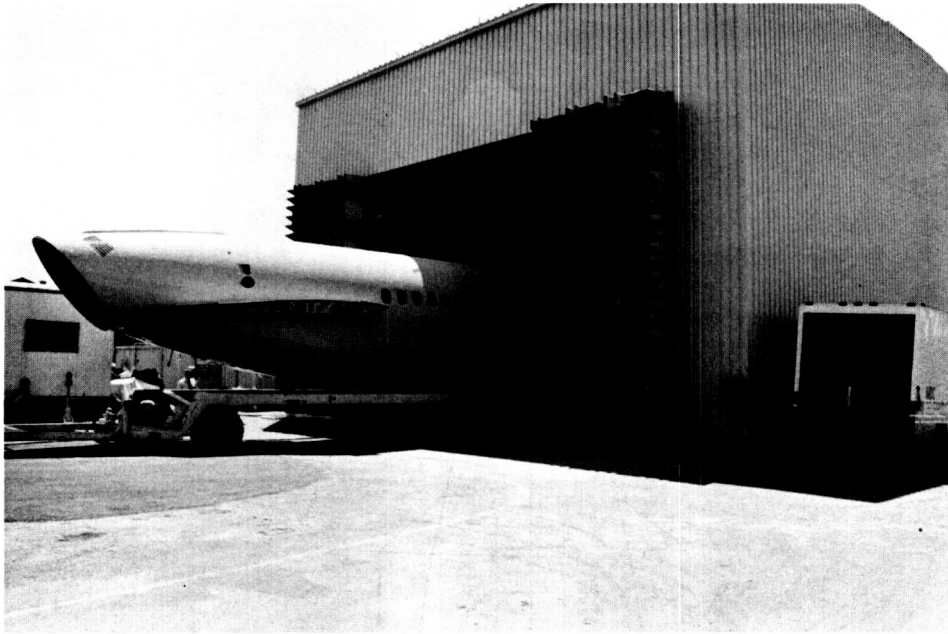


Figure 2-4 The Test Section on its Transporter,  
Entering the Anechoic Chamber

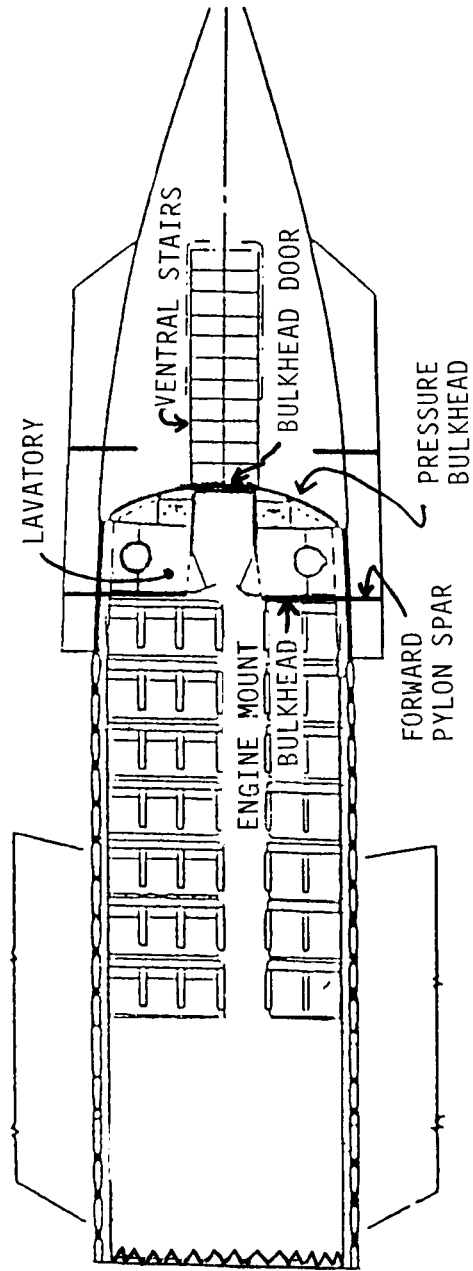


Figure 2-5 Plan View of the Furnished Cabin

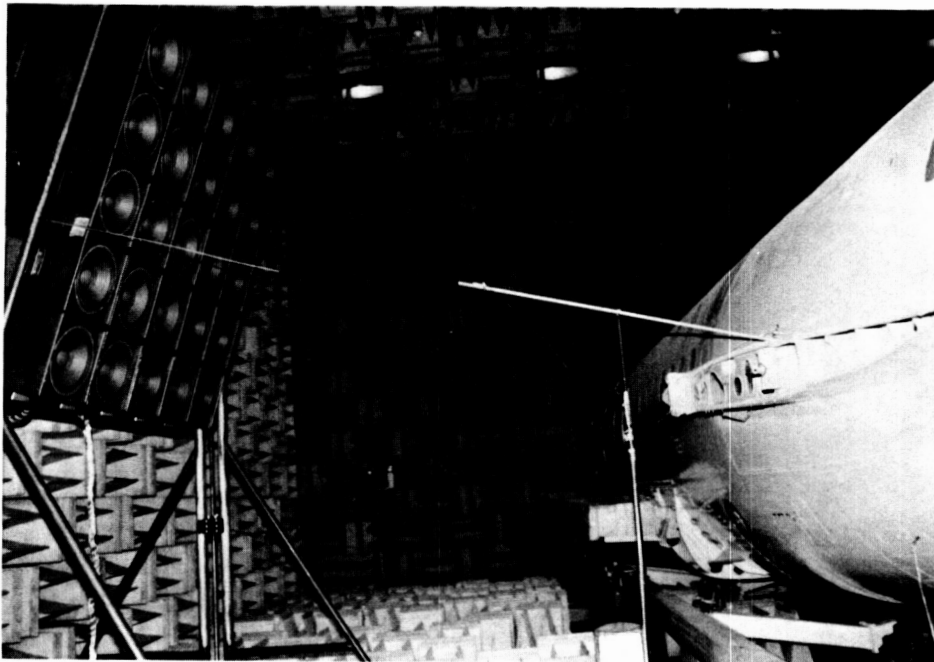


Figure 2-6 The Loudspeaker Array, Positioned at the UHB Prop Plane

ORIGINAL PAGE  
BLACK AND WHITE PHOTOGRAPH

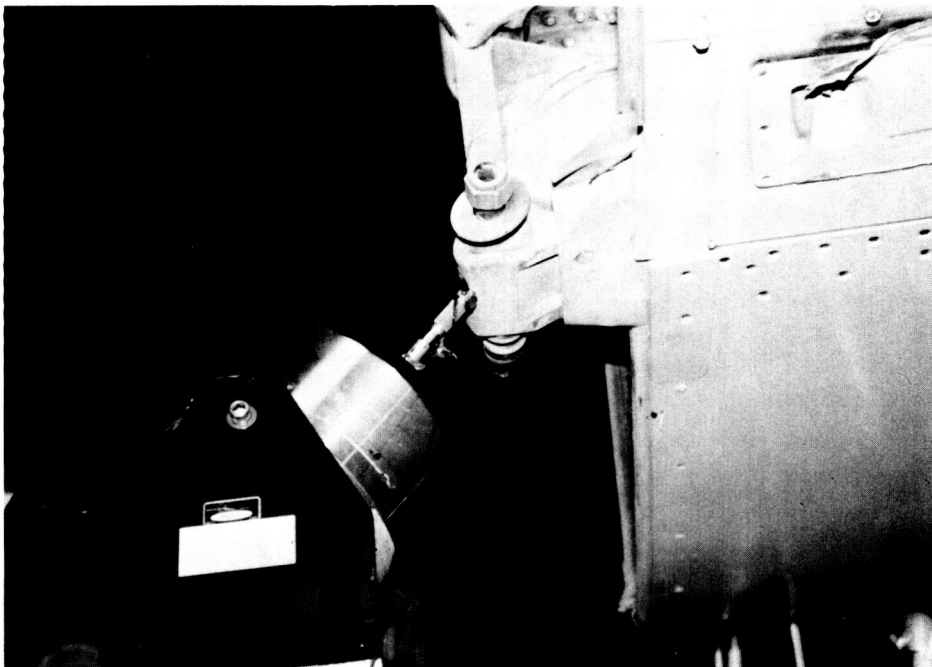
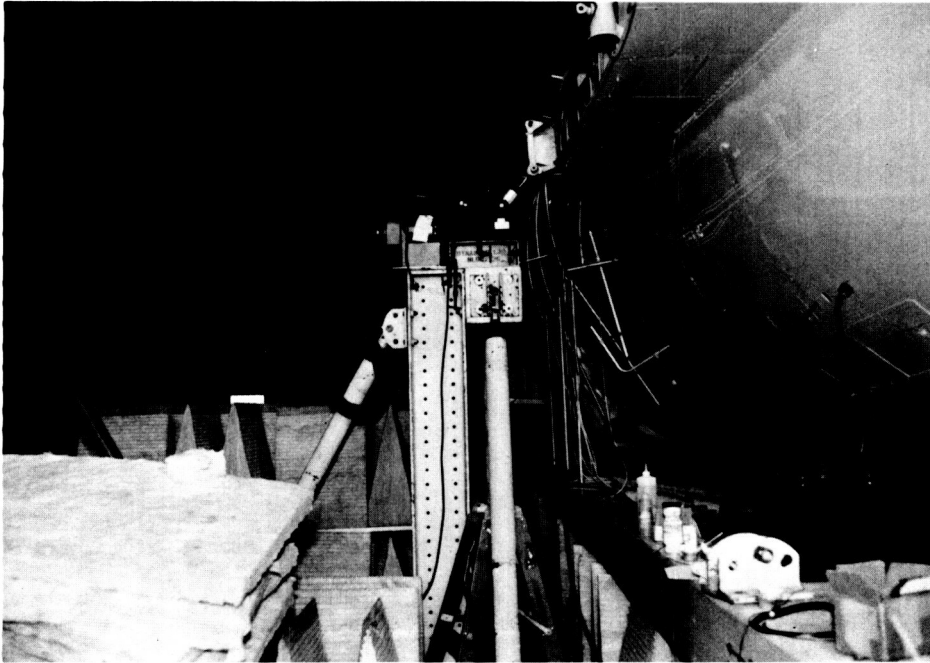


Figure 2-7 The Shaker Mounted to the Left Pylon  
at the Engine Attachment Point

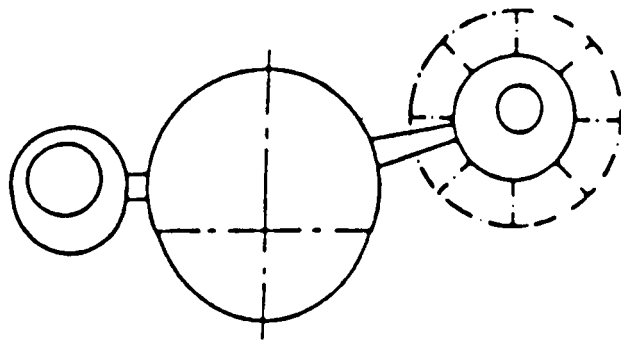
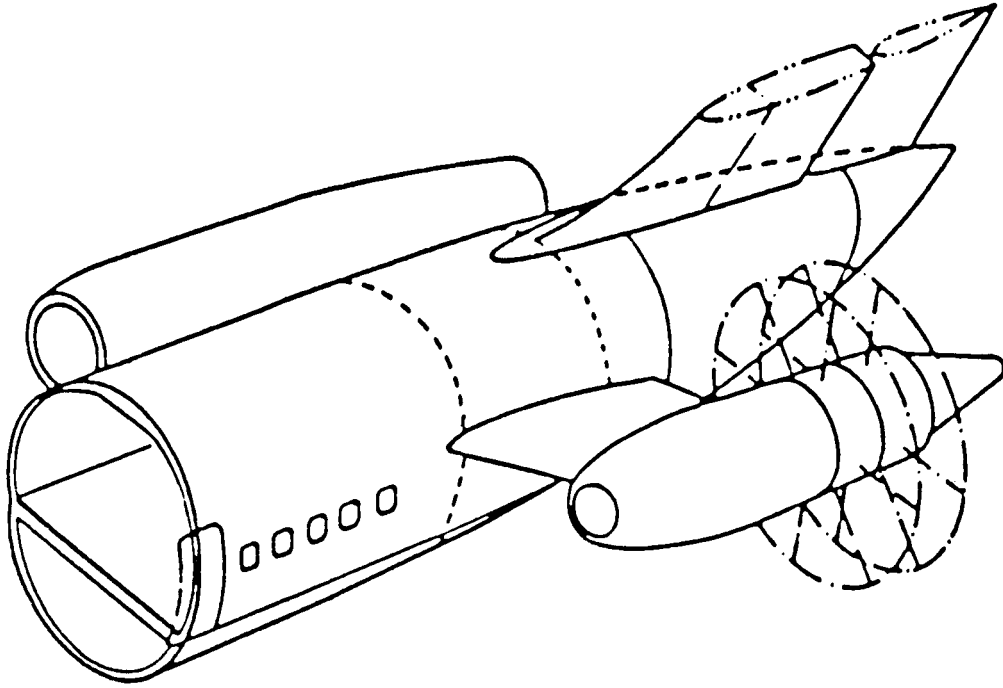


Figure 2-8 Comparison of the JT8D and UHB Pylons and Engine Installation

ORIGINAL PAGE  
BLACK AND WHITE PHOTOGRAPH

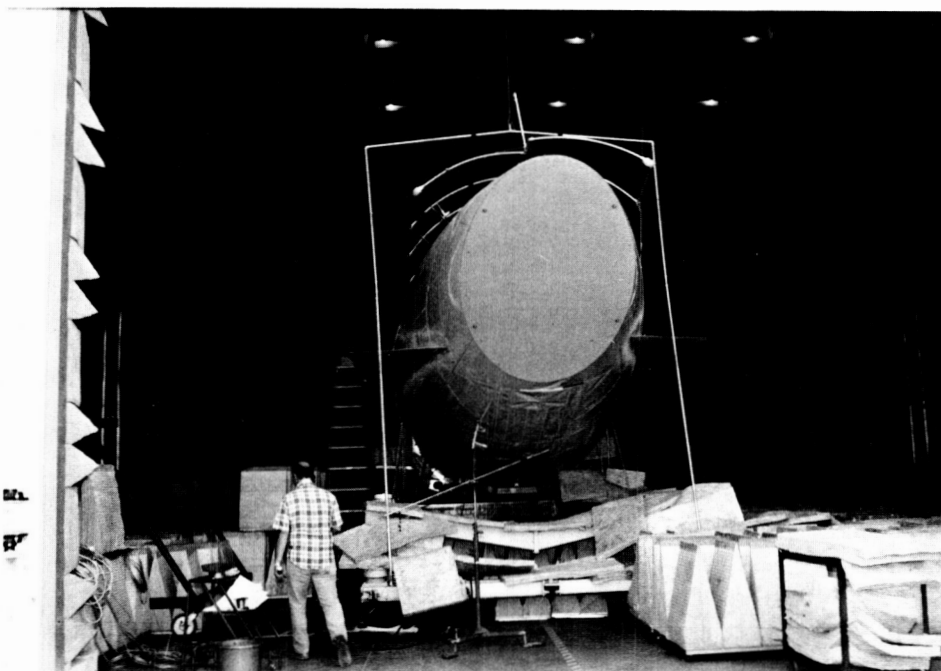


Figure 2-9 Exterior Microphones Mounted Around the Fuselage

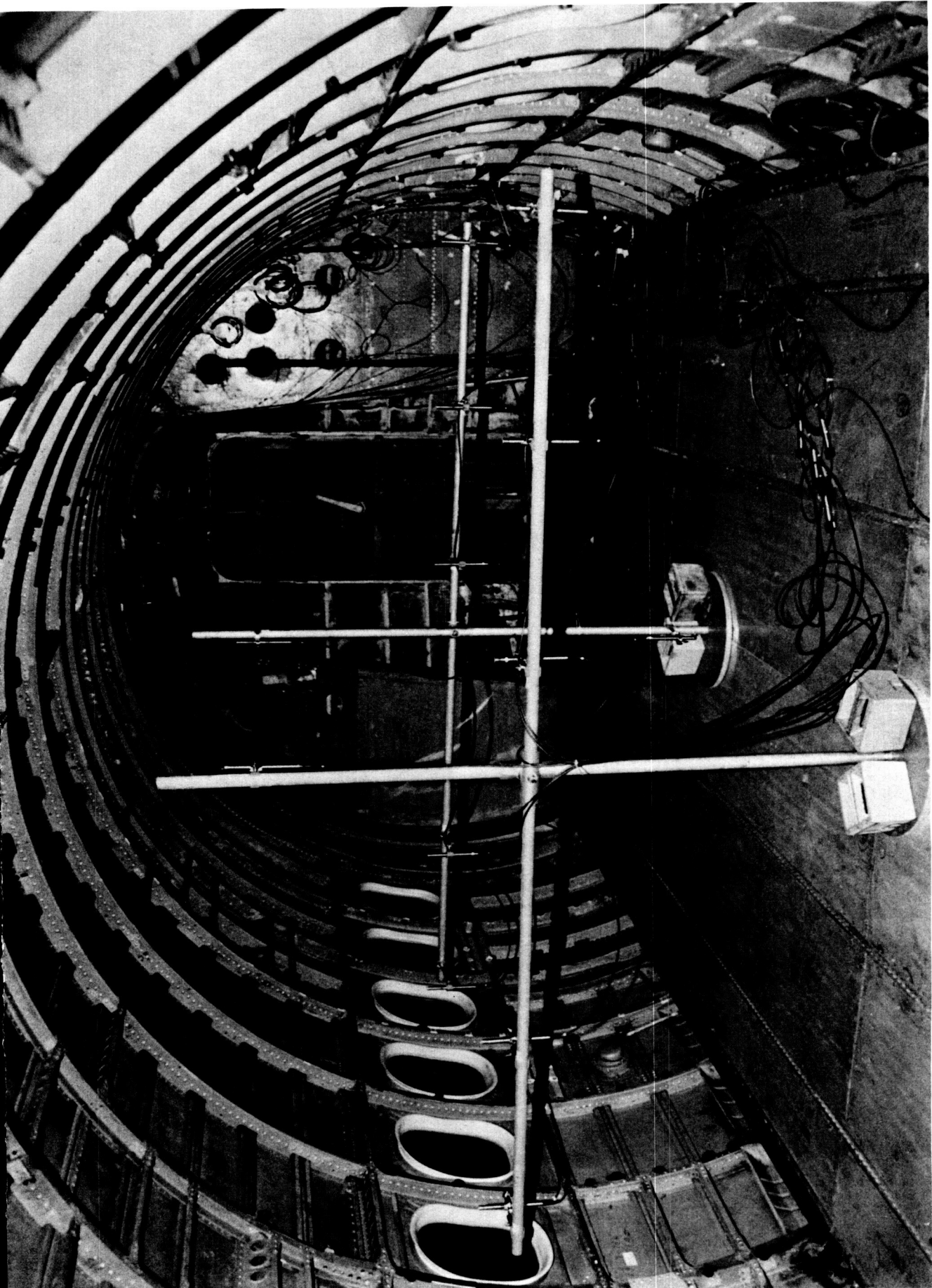


Figure 2-10 Interior Microphones in the Bare Cabin



Figure 4.1 - Interior Microphones in the

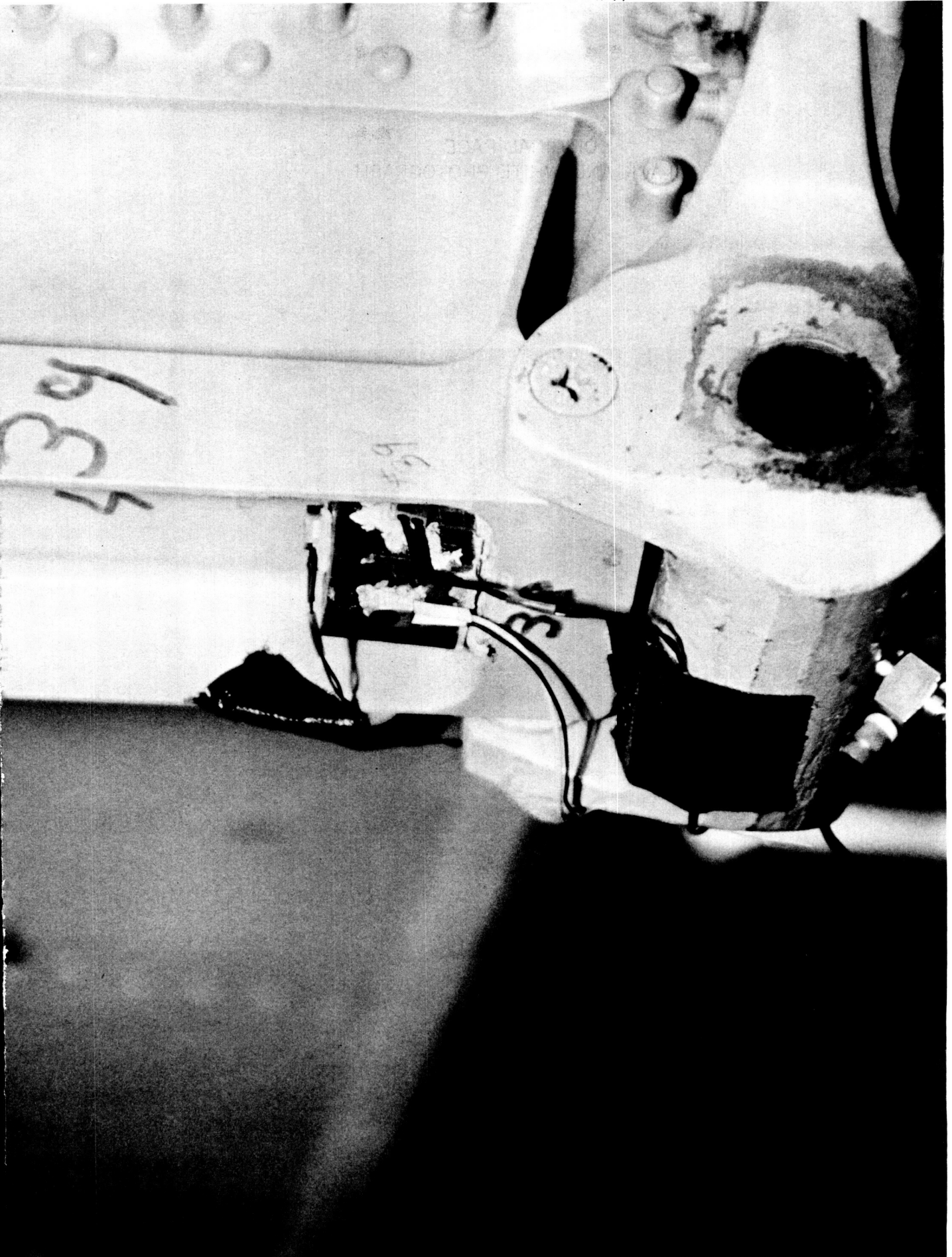


Figure 2-12 Tri-axial Accelerometers Mounted on the Pylon

ORIGINAL PAGE  
BLACK AND WHITE PHOTOGRAPH

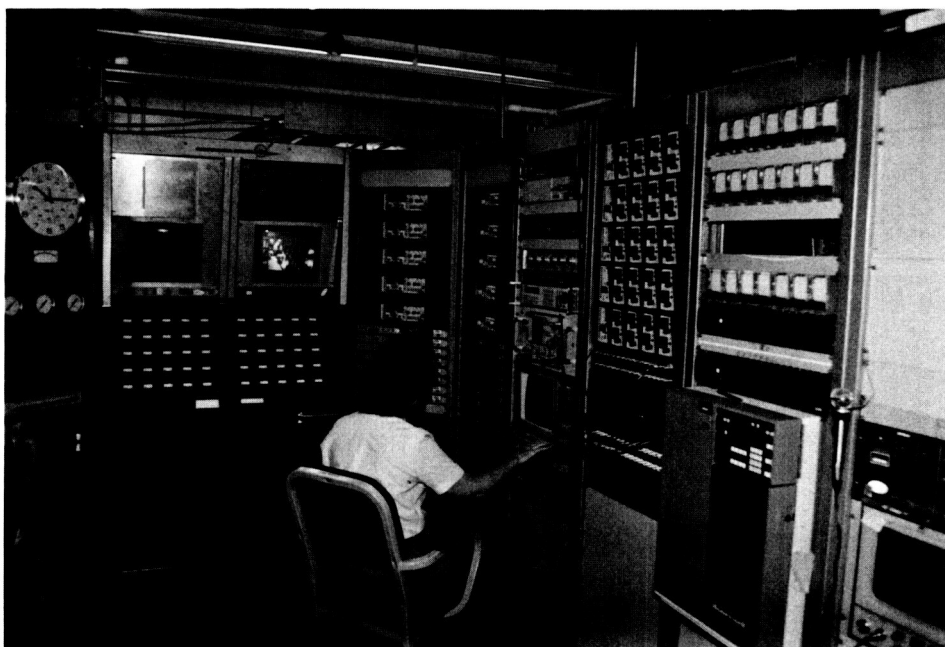


Figure 2-13 View of the Control Room During Testing

## 3 Fuselage Structural Mode Surveys

Vibration measurements were conducted to identify frame and shell modes in the aft cabin of the test fuselage. For these surveys of structural modes, the fuselage was in the Baseline (bare, untreated) configuration. The main purpose of the surveys was to supply modal information early in the fuselage test program as an aid in selecting treatments and in understanding subsequent experimental results; a second purpose was to support development of analytical models of the structural response of the fuselage test section.

### 3.1 Measurement and Analysis Procedures

As shown in Figure 3-1, the mode surveys were performed on three aft frames for ring mode measurements. For these frames, measurement locations were defined around the entire circumference of the frame. Partial shell modes were measured on the aft fuselage encompassing several frames and longerons using about one-fourth of the fuselage circumference.

The tests were performed using a single point shaker vibration input. The shaker was located in the fuselage interior along longeron 10, and provided a random vibration excitation at a force level of 10 lbs. The acceleration response was measured using a "roving" accelerometer measuring only perpendicular to the fuselage (radially). The shaker input force was measured with a B & K model 2800 force transducer.

The input force and output acceleration signals were processed by a Hewlett-Packard model 3562A analyzer to form a Frequency Response Function (FRF) for each measurement location. The set of all FRF's for each frame comprised the set of data from which the normal vibration modes were determined for that frame. Similarly, for the shell survey, the set of all FRF's for the frames and longerons that defined the shell test area comprised the set of data from which the shell modes were determined.

For a given set of FRF data, the normal modes were calculated using SMS Modal Analysis Software. This software is specially designed for modal testing, and extracts from the set of FRF's the modal frequency, damping and modal amplitude for any (or all) frequencies selected from the FRF set. The resultant mode represents the "global" mode at each modal frequency (i.e., all the data of the FRF set was used to determine the modal frequencies and amplitudes). For each modal frequency, the software produces a figure showing the mode shape superimposed on the undeformed structure. Figure 3-2 shows the undeformed frame and shell structures.

## 3.2 Measurement Results

Figure 3-3 shows a sample Frequency Response Function. In the two plots on this figure, the transfer accelerance measured at longeron 4 on the aft frame (at station 766) is plotted separately from 20 to 120 Hz and from 100 to 200 Hz. The transfer accelerance is the response acceleration (measured at longeron 4) divided by the applied force (measured at the input point, longeron 10). Peaks in the FRF indicate those frequencies at which modes may occur. Based on the FRF's shown in this figure, major modes occur at about 86, 107, 158 and 189 Hz.

Frame 766 was selected for detailed modal analysis. Table 3-1 lists the modal frequencies and the corresponding damping for this frame up to 400 Hz, determined from the measured data. The table also lists the major modal frequencies and damping measured for frames 699 and 737, and for the shell sidewall area. Sample frame and shell mode shapes are presented in Figures 3-4 and 3-5, respectively. In Figure 3-4 two plots of the same frame mode shape, 180 degrees out of phase, are shown; in Figure 3-5 different views of the same shell mode are shown.

From the tables, it can be seen that the fuselage test section has a high modal density, with many frame and shell modes occurring in the frequency region (150 to 250 Hz) where UHB blade passage frequencies are likely to occur.

A NASTRAN two-dimensional finite element model developed for frame 766 was used to predict modal frequencies and mode shapes. Figure 3-6 compares the predicted modes with the corresponding measured modes, and shows reasonably good agreement in both frequency and shape.

Table 3-1 Measured Frame and Shell Modes

FRAME 766 MODES		FRAME 737 MODES	
FREQUENCY, Hz	Damping, %	FREQUENCY, Hz	Damping, %
34.64	1.13	107.77	1.11
48.85	3.12	120.87	0.21
50.78	1.42	261.09	0.27
65.91	0.72	264.16	0.20
76.82	1.48	280.07	0.56
86.15	1.71		
106.96	3.19		
122.22	1.77		
130.61	2.12		
135.04	3.22		
153.10	0.57		
164.40	0.95		
165.92	1.90		
175.37	1.48		
184.60	0.43		
189.25	2.99		
206.32	1.23		
214.74	2.19		
231.43	1.91		
240.31	0.77		
250.99	0.63		
272.88	0.66		
312.87	1.06		
365.45	1.16		
387.89	0.69		
		FRAME 699 MODES	
		FREQUENCY, Hz	Damping, %
		110.90	1.64
		120.15	0.34
		131.86	0.66
		151.02	0.93
		178.02	0.64
		191.85	0.84
		269.65	0.07
		288.28	0.77
		296.71	0.35
		317.41	1.68
		328.98	2.40
		364.17	0.66
		383.04	0.35
SHELL MODES			
FREQUENCY, Hz	Damping, %		
63.87	1.22		
86.76	1.81		
107.93	4.71		
125.49	3.48		
208.61	0.98		
238.43	0.58		
259.64	0.35		
293.16	0.19		

- FRAME MEASUREMENT POINT  
FRAMES 766, 737, 699
- × SHELL MEASUREMENT POINT,  
SIDEWALL AREA BETWEEN  
FRAMES 661 and 766,  
LONGERONS 1 and 17
- ▲ SHAKER EXCIATION POINT  
(@ 737 FOR SHELL SURVEY)

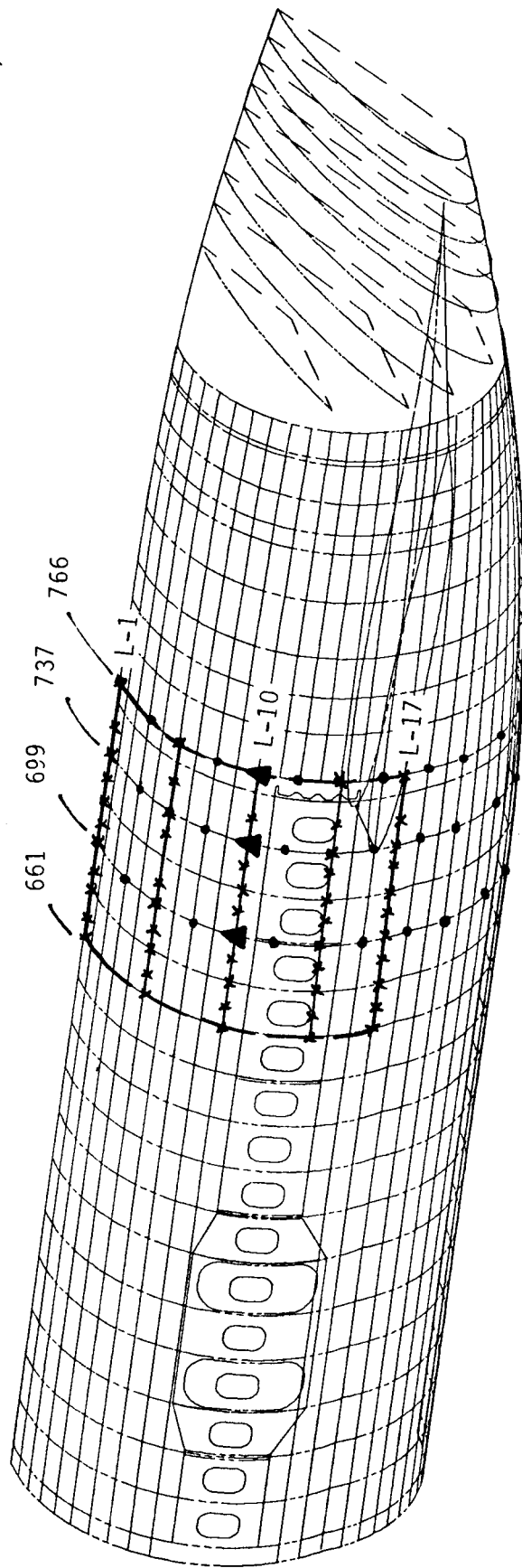


Figure 3-1 Structural Mode Survey Measurement Locations

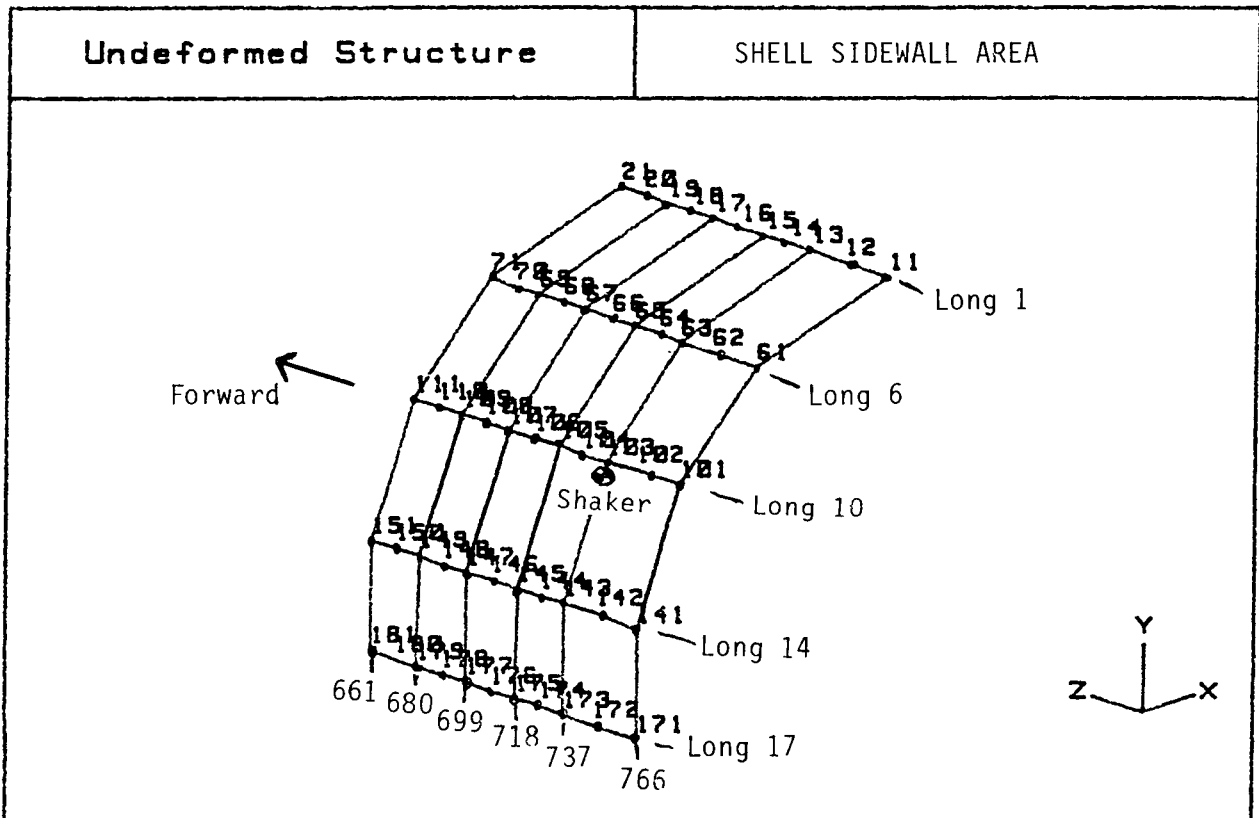
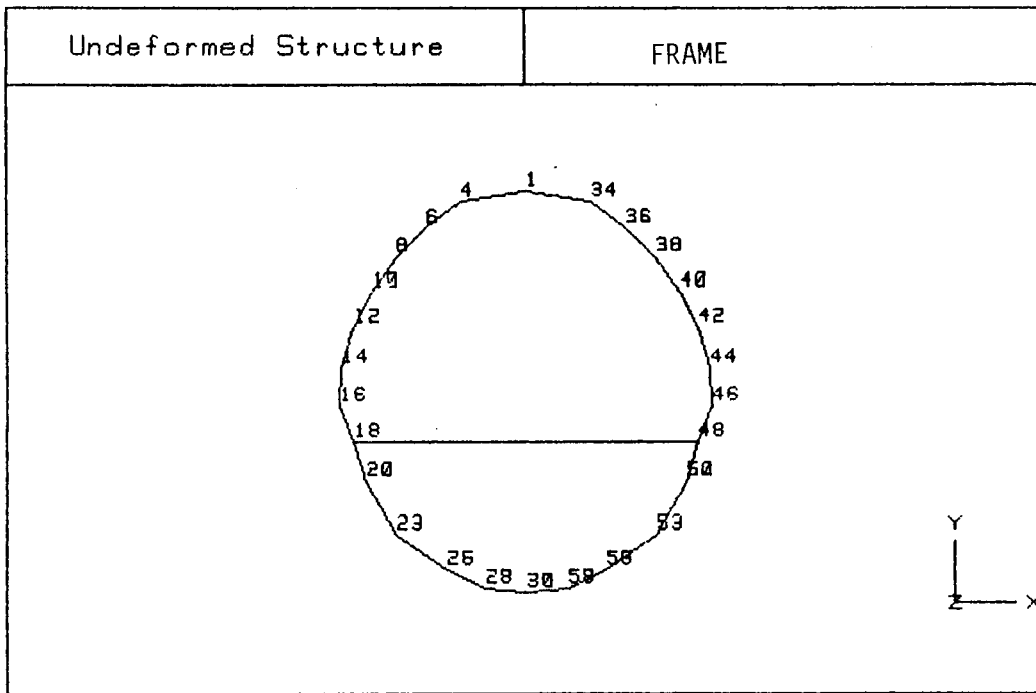


Figure 3-2 Frame and Shell Undeformed Structures

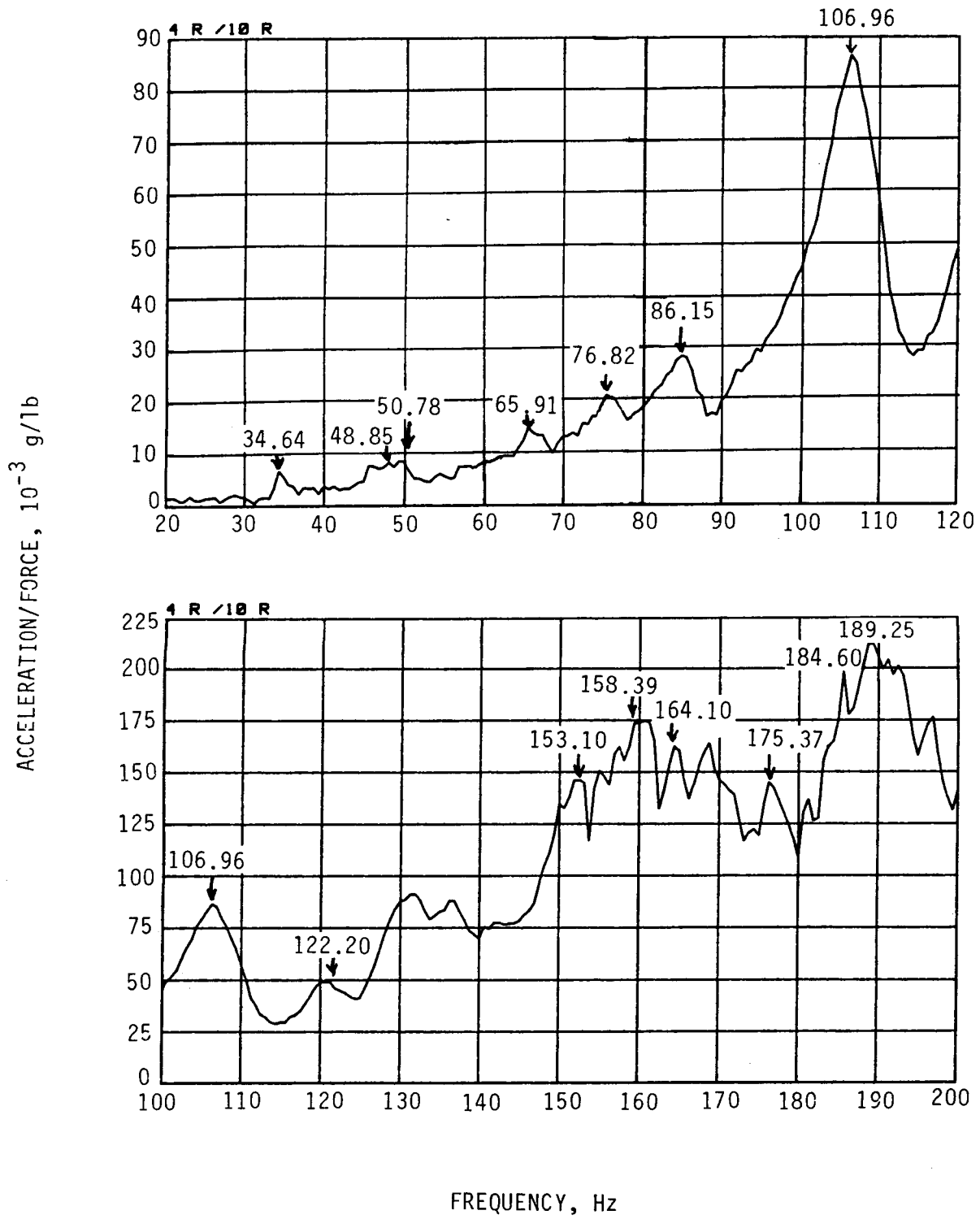


Figure 3-3 Frequency Response Function for Frame 766 at Longeron 4 (Input at Longeron 10)

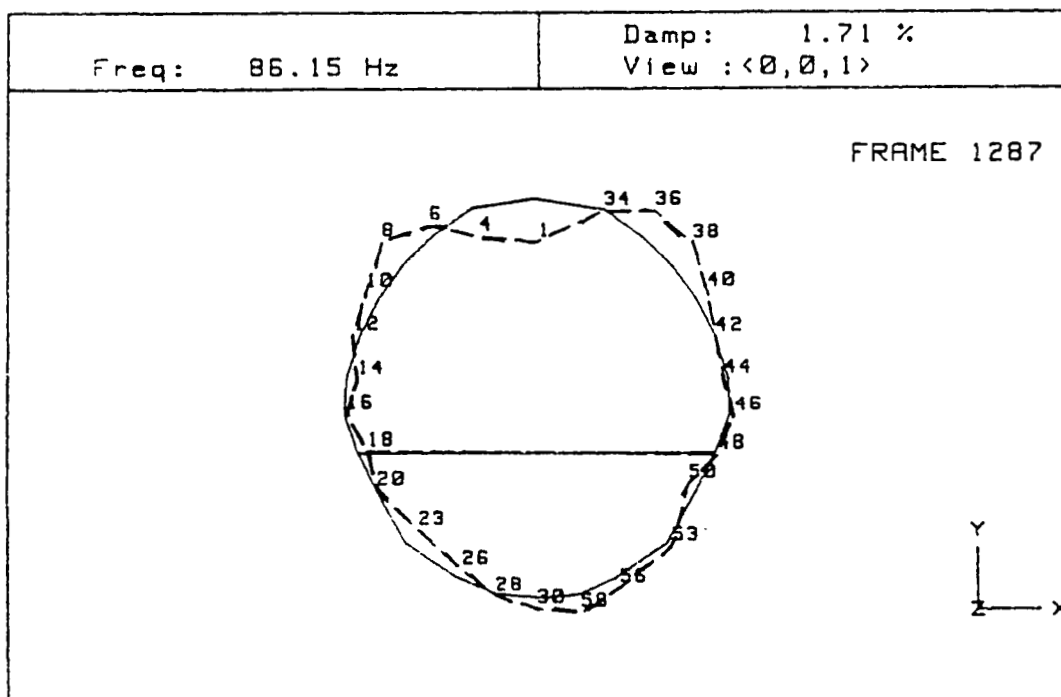
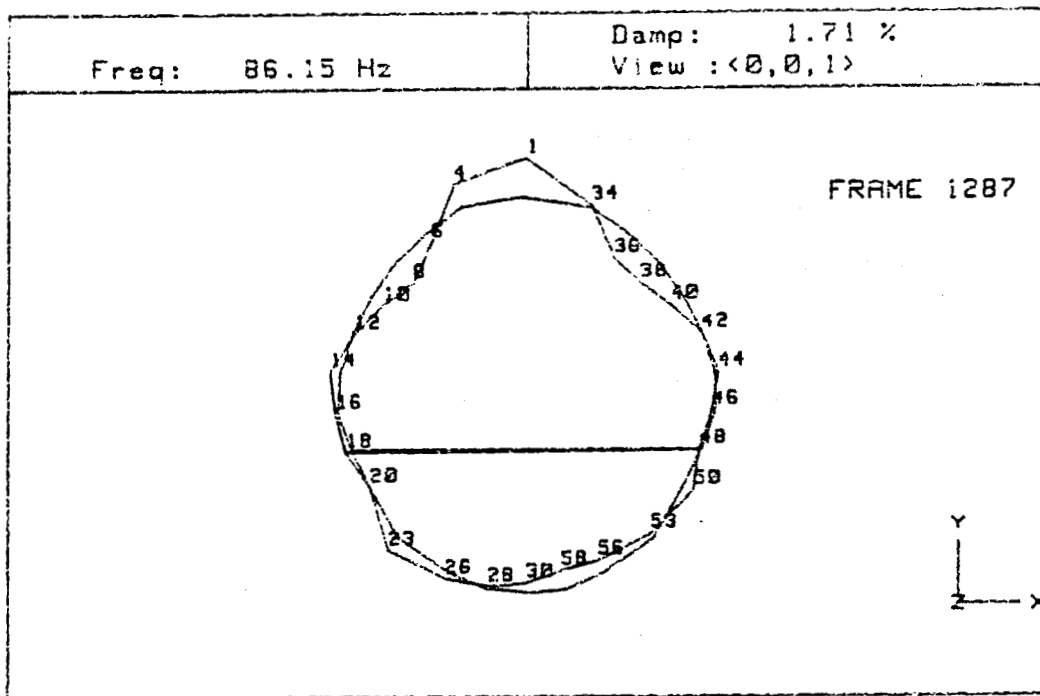


Figure 3-4 Sample Frame Mode, Station 766

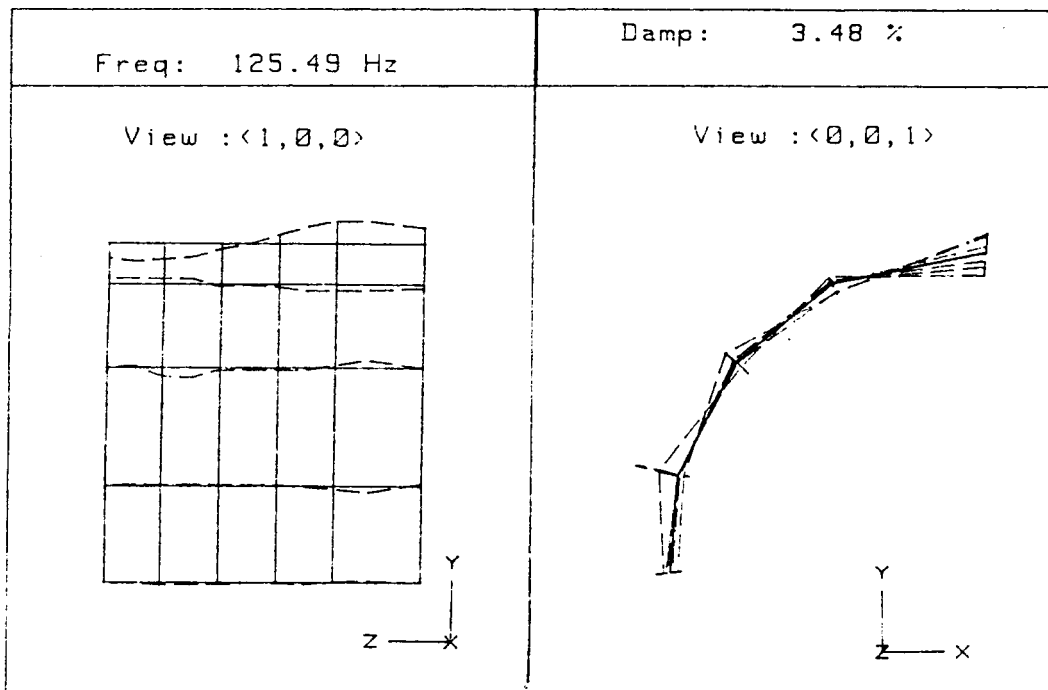
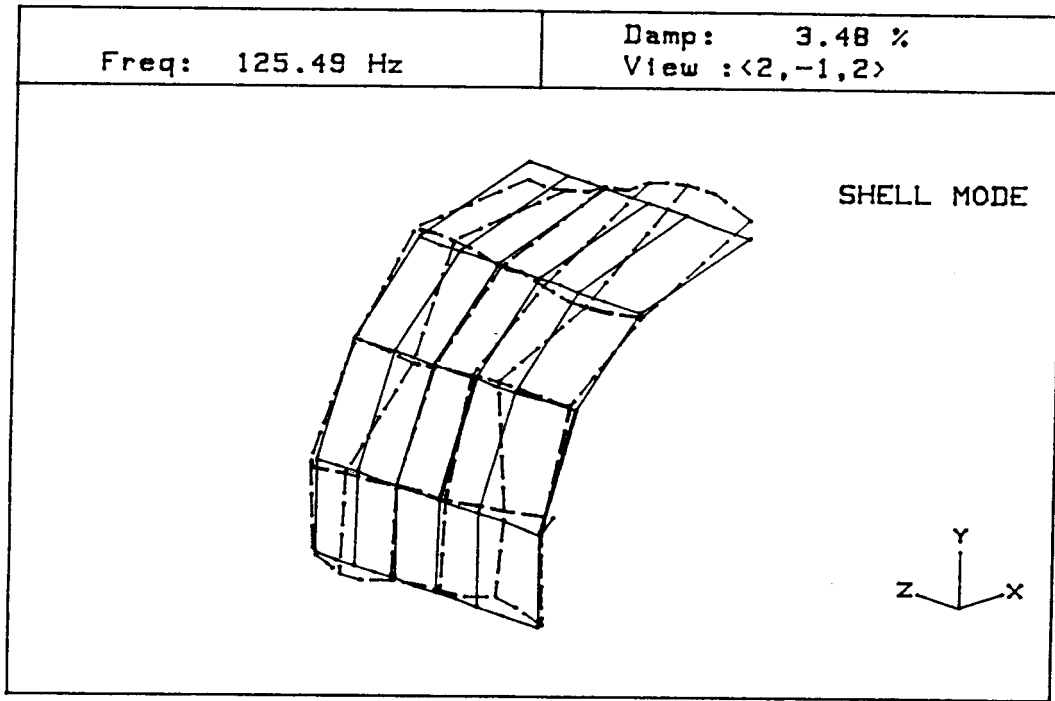


Figure 3-5 Sample Shell Mode

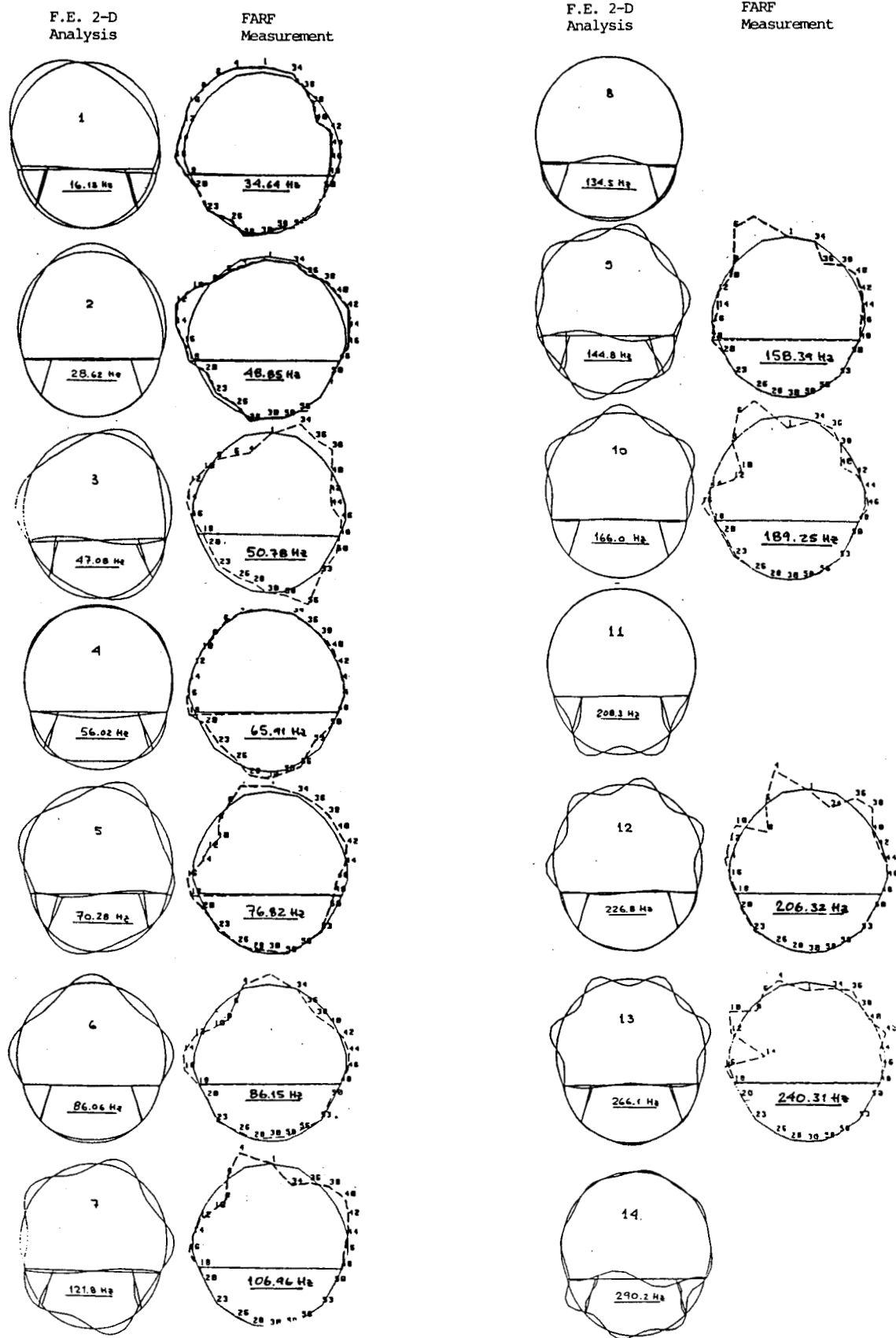


Figure 3-6 Comparison of Predicted and Measured Frame Modes at Station 766

## 4 Cabin Cavity Mode Surveys

Noise measurements were made to identify acoustic cavity modes in the cabin of the test fuselage. These cavity mode surveys were conducted for both bare and furnished cabin conditions. The objectives of the cavity mode surveys were similar to those of the structural mode surveys: to provide modal information to assist in understanding and interpreting the interior noise data to be collected later in the test program, and to support development of analytical models of the cabin acoustic environment.

### 4.1 Measurement and Analysis Procedures

For the bare cabin survey, cavity modes were measured in a vertical plane through the cabin at station 642 (transverse modes). For the furnished cabin survey, transverse modes were again measured at station 642, and also at stations 690, 748, and 772. In addition, cavity modes were measured in a vertical plane through the aircraft centerline (longitudinal modes). Figure 4-1 shows these measurement locations.

The tests were conducted using a single loudspeaker at the forward end of the cabin, through which a broadband random noise signal was played. As shown in the figure, the loudspeaker was oriented at a 45 degree angle relative to the cabin centerline (to create a more diffuse sound field), and a microphone one meter in front of the loudspeaker was used for reference purposes.

Response microphones were located on a test stand with a rotating arm. For the transverse mode measurements the arm was sequentially positioned at 30 degree increments (see Figure 4-2). For the longitudinal mode measurements, the arm was positioned vertically, and the entire stand was sequentially moved to the appropriate station locations. Measurements were always obtained at the reference microphone simultaneously with each set of measurements of the response microphones; response levels in the transverse or longitudinal planes were normalized to levels at the reference microphone. For all tests, the cabin was pressurized to pressure differential of 5 psi.

Transfer functions between the reference microphone and each response microphone were computed for each transverse or longitudinal plane. To identify the modal frequencies in each plane, the real and imaginary parts of these transfer functions were separately added together for all the response microphones in that plane. Plots of these summed real and imaginary values were examined to find frequencies at which the real value was zero (or near zero) and the imaginary value was at a peak in the spectrum. Figure 4-3 shows an example of this approach for measurements at station 772 during the furnished fuselage mode survey.

For each such frequency between 50 and 300 Hz, the sound pressure level distribution within the measurement plane was mapped from the normalized response microphone data.

## 4.2 Measurement Results

The cavity modal frequencies determined from measurements in the bare and furnished cabins are listed in Table 4-1. For selected modal frequencies, sample plots of the sound pressure level distribution are shown in Figures 4-4, 4-5 and 4-6. Note in Figure 4-5 the presence of the bag racks in the furnished cabin.

The plots depict, in color, the variation in level across the cabin. Note that the scale is arbitrary, and may differ from plot to plot. Areas of red indicate the highest measured levels and areas of dark blue indicate the lowest levels (the location of nodes in the sound field).

As for the structural modes, there is a high density of acoustic modes in the cabin, again with several modes in the frequency range of UHB tones. It should also be noted that for individual frequencies, there is often a large variation in sound pressure levels (20 dB or more) over relatively small distances within the cabin, particularly in the bare cabin. This variation was also observed in the bare cabin forced response tests (see section 5.2.1).

A comparison of measured bare cabin transverse cavity modes was made with modes predicted from a three dimensional finite element model of the cabin cavity. Figure 4-7 shows good agreement for the two frequencies presented. (Note that the predicted modes are plotted on a pressure scale with positive and negative values, while the measured modes are plotted on a sound pressure level scale; to facilitate comparisons, areas of maximum and minimum levels are labeled.) In general, however, agreement between the predicted and measured cavity modal frequencies was inconsistent. For certain frequencies, a clear modal pattern can readily be seen in the figures derived from the measurements. For many of the plots, however, there is not a well defined pattern. Additional testing and analysis are needed to resolve these discrepancies. Such activities are the subject of a future task assignment.

Table 4-1 Measured Transverse and Longitudinal Modes

-----  
 TRANSVERSE CAVITY MODES, Hz  
 -----

Bare Cabin Station 642	Furnished Cabin Stations 642, 690, 748, 772
102	78
114	102
124	132
138	168
140	194
160	237
178	256
206	279
236	290
270	
290	
328	
365	

-----  
 LONGITUDINAL CAVITY MODES, Hz  
 -----

Furnished Cabin, Centerline  
 -----

- 50
- 72
- 95
- 109
- 122
- 138
- 142
- 167
- 192
- 197
- 209
- 238
- 250
- 256
- 270
- 284
- 290

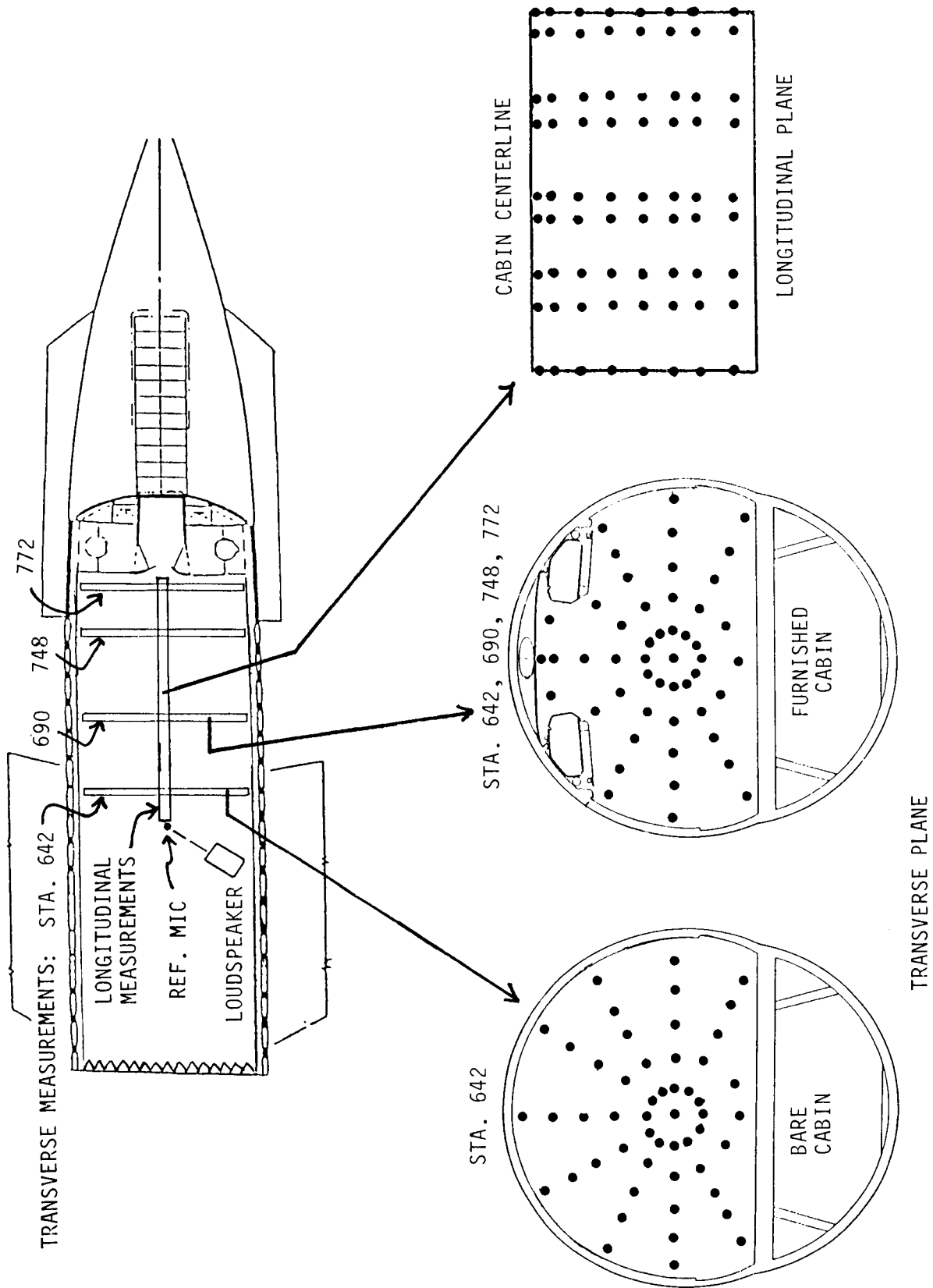


Figure 4-1 Cavity Mode Measurement Locations

ORIGINAL PAGE  
BLACK AND WHITE PHOTOGRAPH

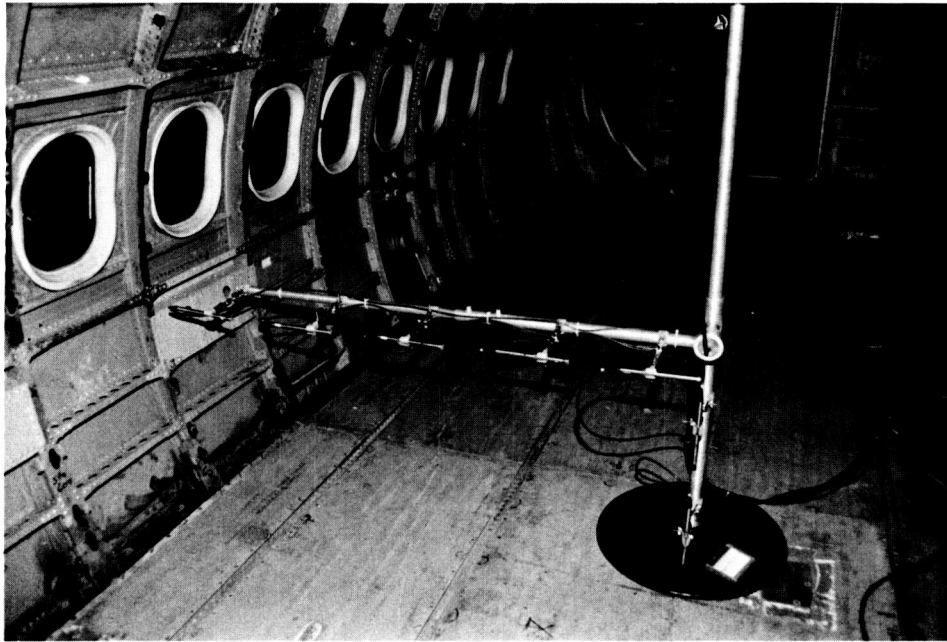
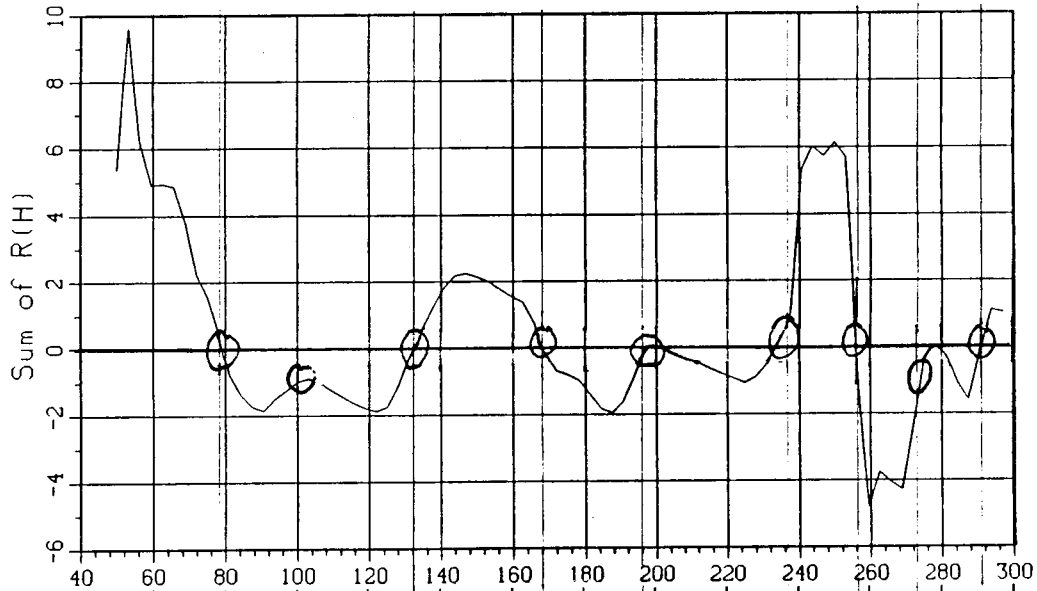


Figure 4-2 Cavity Mode Measurements in the Bare and Furnished Cabin

# TRANSFER FUNCTION: REAL PART

Summation: ref. mic: I-772-R



# TRANSFER FUNCTION: IMAGINARY PART

Summation: ref. mic: I-772-R

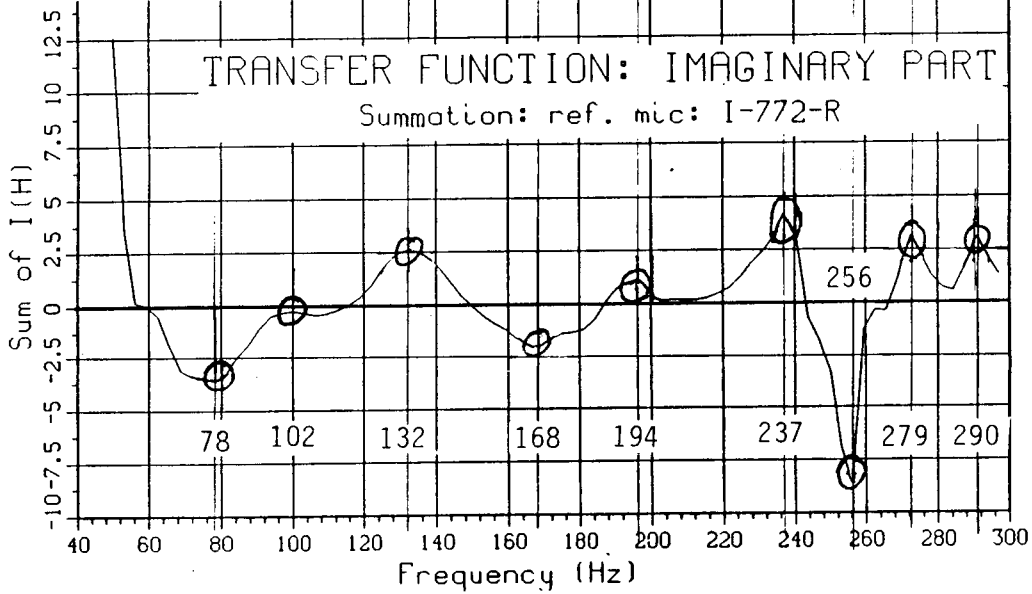


Figure 4-3 Identification of Modal Frequencies from Transfer Function Plots

ORIGINAL PAGE  
COLOR PHOTOGRAPH

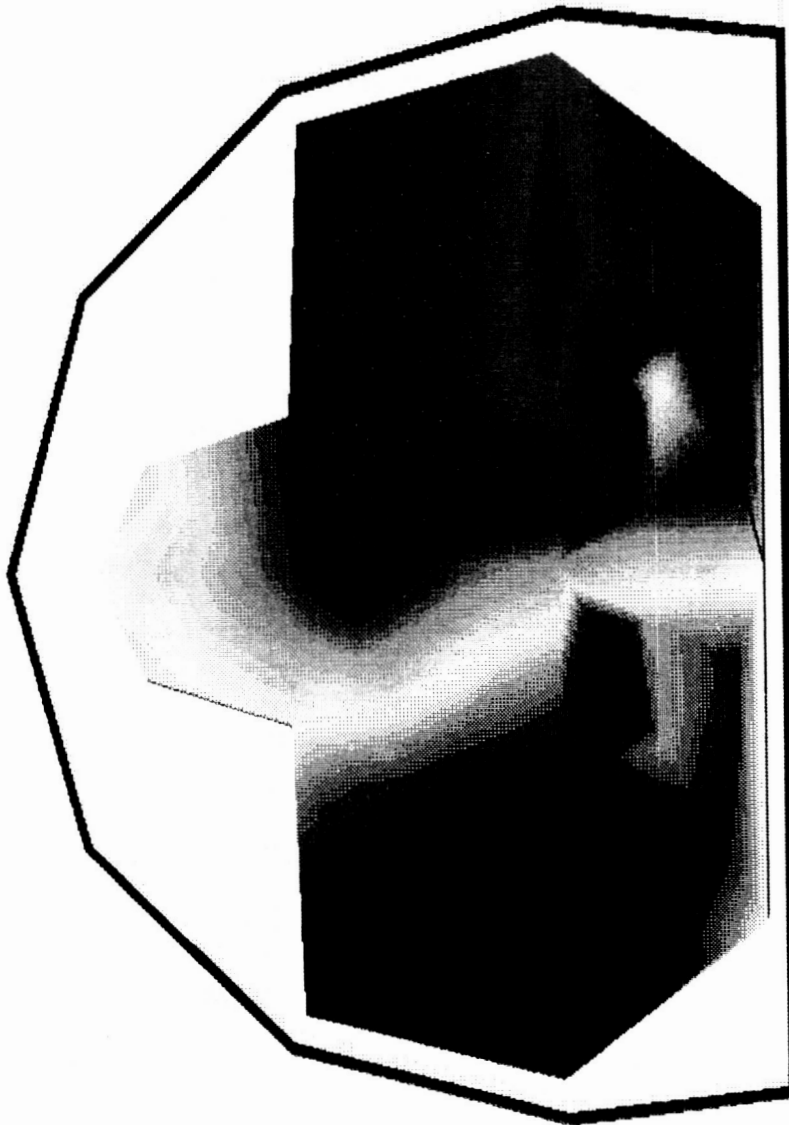


STATION 642  
140 HZ

Z  
X

Figure 4-4 Sample Transverse Cavity Mode in the Bare Cabin

ORIGINAL PAGE  
COLOR PHOTOGRAPH



STATION 642  
78 Hz



ORIGINAL PAGE  
COLOR PHOTOGRAPH

80.0  
82.0  
81.0  
80.0

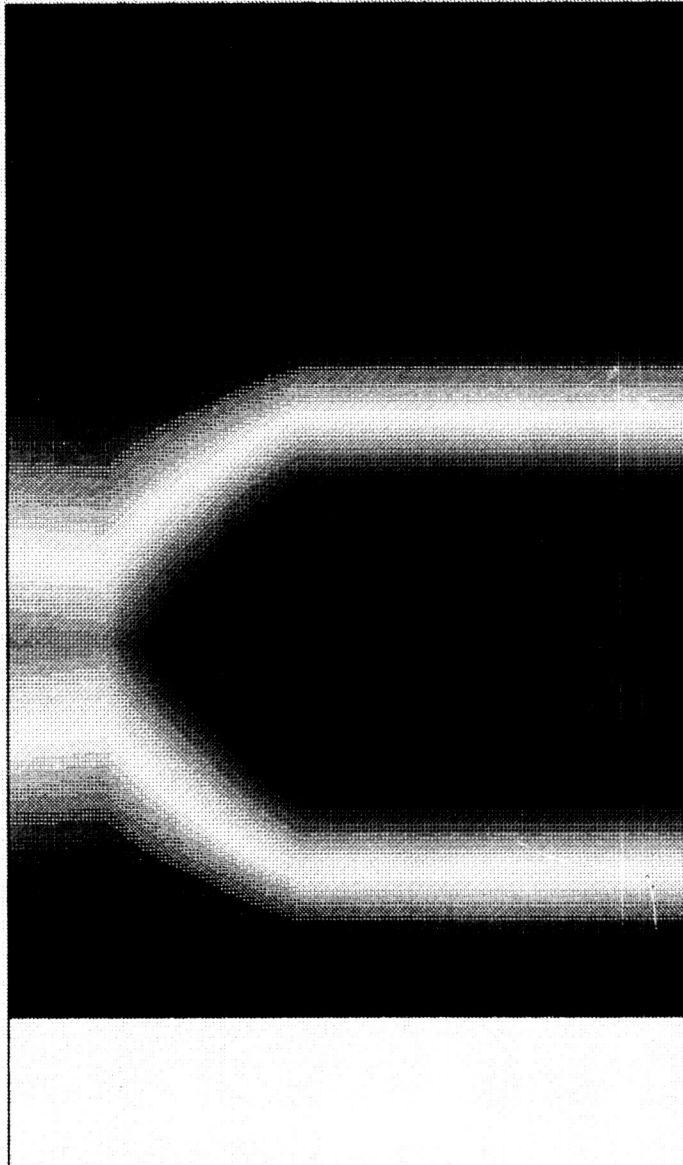
ARTIS: McDonnell Douglas Corp.

Figure 4-5 Sample Transverse Cavity Mode in the Furnished Cabin

78.5

78.0

ORIGINAL PAGE  
COLOR PHOTOGRAPH



78 Hz

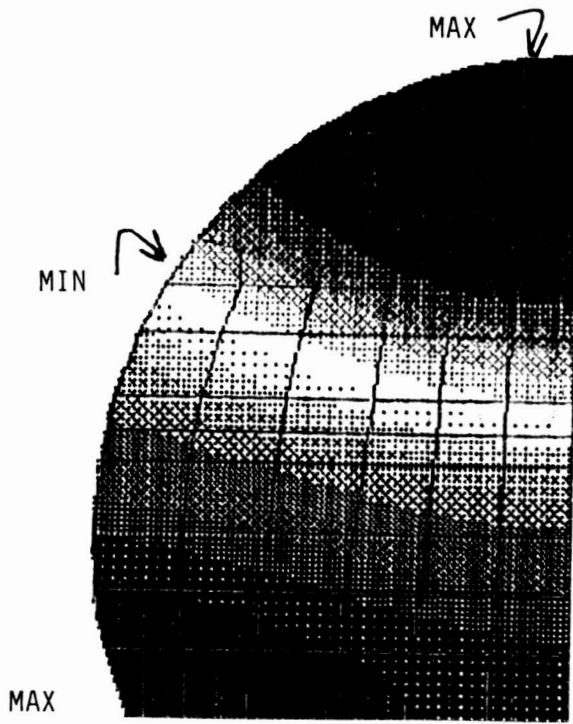


ARTIS: McDonnell Douglas Corp.

Figure 4-6 Sample Longitudinal Cavity Mode in the Furnished Cabin

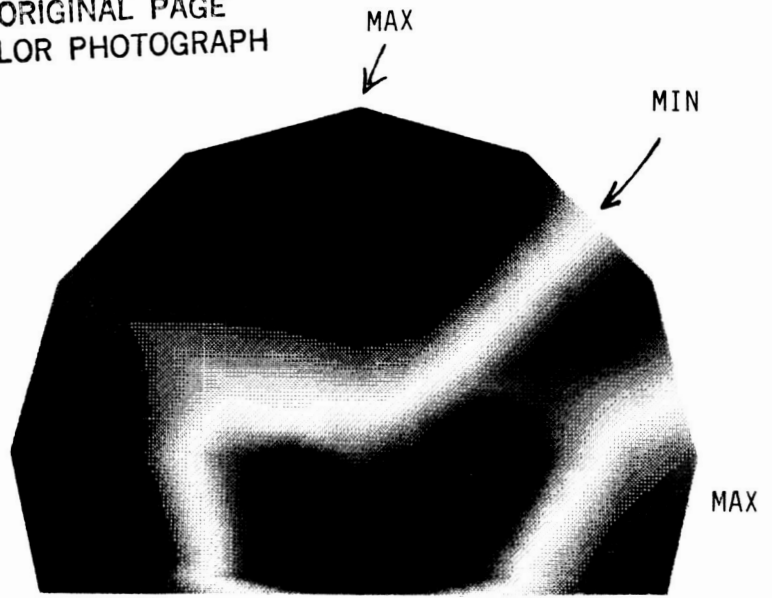
FE 3-D PREDICTED MODES\*

MEASURED CAVITY MODES

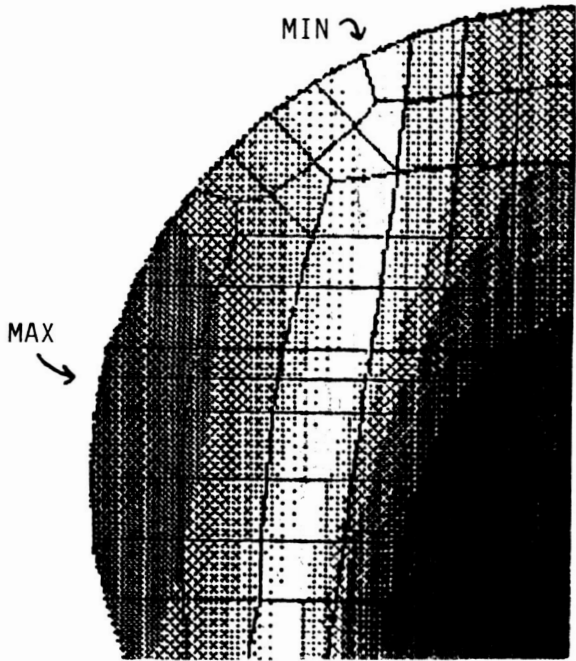


105.4 Hz

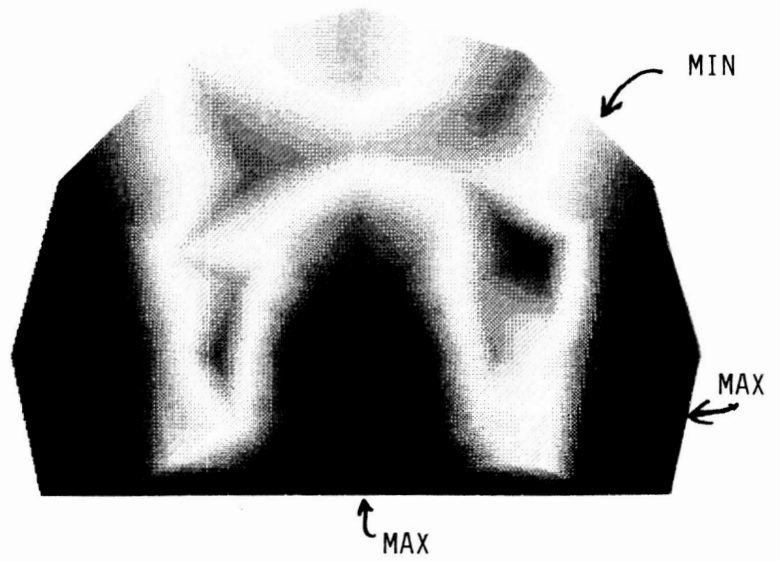
ORIGINAL PAGE  
COLOR PHOTOGRAPH



102 Hz



115.6 Hz



114 Hz

\*Ringstrom, Torsten, Saab-Scania, 1987  
(Unpublished analyses)

Figure 4-7 Comparison of Predicted and Measured Transverse Cavity Modes in the Bare Cabin

## 5 Baseline Forced Response Tests

The forced response tests described in this section and in section 6 involve the measurement of noise levels in and vibration levels on the test fuselage at numerous points, as it is exposed to acoustic and vibration excitation designed to simulate the actual excitation that would occur on an advanced turboprop aircraft with two aft-mount engines, and specifically on a UHB aircraft whose engines have a 10x8 propulsor configuration. These tests are divided into three phases: a Baseline phase described herein, and two modification phases described in the next section in which selected noise control treatments are evaluated. The primary purpose of the Baseline phase is to measure noise and vibration levels for an untreated fuselage, against which noise and vibration levels measured after installation of the various treatments can be compared. On the basis of these comparisons, an assessment of the effectiveness of each treatment can be made.

For these and later tests, the physical condition of the test fuselage is described in terms of specific configurations. The untreated fuselage used in the Baseline phase is described as follows:

**Configuration 1.** This is the "bare" fuselage configuration, with no interior furnishings or treatments; this is sometimes termed a "green" aircraft. In both the pressurized and unpressurized fuselage sections, the various skin and floor surfaces and frames and longerons are completely uncovered. The lavatories are removed, so that the engine mount bulkheads (which separate the lavatories from the passenger seating area) and the complete aft pressure bulkhead are also uncovered. The only exposed surface that is other than bare metal is the bulkhead plug at the forward end of the fuselage section, on which fiberglass wedges are attached. In the aft unpressurized section, all systems, ductwork and equipment are removed. The cargo compartment below the floor is also bare and empty. See Figure 2-10.

### 5.1 Measurement and Analysis Procedures

#### 5.1.1 Transducers

For the forced response tests, the transducers used to measure excitation and response levels included exterior microphones, interior microphones and accelerometers. To identify these various transducers, each was assigned a label consisting of a letter prefix indicating its type (E, I, or A for Exterior microphone, Interior microphone, or Accelerometer, respectively), the station number corresponding to its longitudinal location, and a letter suffix corresponding to its vertical or lateral location.

Microphone locations are shown in Figure 5-1. Exterior microphones were located on the aft fuselage and in an array outside of the passenger cabin. The labels for two exterior microphones, one at station 908 (which corresponds to the longitudinal location of the forward propeller for a UHB engine), and one at station 642 (at the forward end of the measurement area), are illustrated in the figure. Circumferentially, the microphones are distributed along three microphone rows, identified as B, C, and D on the left side of the fuselage and G, H, and I on the right side of the fuselage. (Exterior microphone rows A, E, and F were not used for these tests.)

Interior microphones were located at typical passenger positions. As shown in the figure, at each of four stations an array of six microphones was utilized. The microphones at lateral positions A, B, C, E, and F correspond to seated passenger head height (40 in above ground), and the microphone at lateral position D corresponds to a standing head height (65 in above ground) in the aisle on the cabin centerline.

Accelerometers were located on a frame in the mid-cabin area (at station 718), and along longeron 10 from station 859 forward to station 718 (see Figure 5-2). In addition, accelerometers were mounted on the pylon at the shaker attachment point to measure the lateral, longitudinal and horizontal components of the input acceleration.

Since the number of transducers exceeded the number of available data channels (26) on the recorder, it was not possible to measure noise and vibration levels at all transducers simultaneously. Accordingly, multiple measurements were made with constant (or near constant) acoustic or vibration excitation. During these multiple measurements, several transducers were always utilized in order to monitor input levels, and to provide a basis for normalization if any variation in these levels were to occur. These include microphones E-908-B and E-908-G for acoustic excitation tests, and the three pylon input accelerometers for vibration excitation tests.

### 5.1.2 Acoustic Excitation Sources

To simulate the acoustic excitation of a UHB 10x8 engine, the first step was to estimate the acoustic loads expected on the fuselage for the operating conditions of interest (high speed, high altitude cruise). These estimates, based on scale model data, indicated that the maximum overall sound pressure level on the fuselage is on the order of 150 dB. The acoustic field is composed of several tones, corresponding to the blade passage frequency (BPF) of each rotor and associated harmonics. For a 10x8 engine operating in the 1260 to 1280 rpm range, the BPF and first two harmonics for the rear 8-bladed rotor are nominally 169, 338 and 507 Hz, respectively, and for the forward 10-bladed rotor are nominally 213, 426 and 639 Hz, respectively. For each of these tones, the maximum fuselage level occurs in the plane of the rotor producing the tone, and the levels decrease quickly with distance forward and aft of this plane.

Within 6 to 10 feet, the tonal levels are lower by some 50 dB. In addition to these six tonal components, other components are also present at lower levels, including tones at subsequent harmonic frequencies and interaction tones (which occur at frequencies corresponding to the sums and differences of the various harmonic frequencies).

For the forced response tests, the estimated UHB acoustic loads were simulated using the two loudspeaker arrays described in Section 2.2. The approach adopted was to attempt to simulate the relative distribution of levels on the fuselage surface, since it is not necessary to utilize the correct absolute exterior levels in order to measure the noise reduction into the passenger cabin or to compare the effectiveness of different treatments. Simulating the source directionality characteristics (that is, generating the expected fuselage level distribution) was believed to be important so that the various transmission paths into the cabin on the test fuselage would correspond to those on the actual aircraft as closely as possible. It was also believed to be desirable to simulate the various phase relationships between the levels at different fuselage locations, since these phase relationships, along with the source directivity, will affect the transmission of sound through the fuselage structure.

Conceptually, the directionality of an array of sources can be controlled by adjusting the relative level and phase of the component sources and the spacing between the sources. To help determine the appropriate array characteristics that would produce the desired directionality patterns for each tone, a computer program was written to predict the level and phase at any point on the fuselage surface as a function of loudspeaker array location and orientation, and the source level and phase of each of the 25 available loudspeakers in the array. After exercising this program numerous times, it was found that for a given frequency in the range of interest, control over directionality was limited by constraints on the location of the loudspeaker array within the dimensions of the anechoic chamber, and by the fixed loudspeaker-to-loudspeaker spacing within the support rack. It was also found that large, abrupt variations in level occurred over small distances on the fuselage surface when there were large phase differences among the various loudspeakers. Nevertheless, reasonable directionality characteristics were obtained for each of the six frequencies mentioned above, using three different patterns of loudspeakers. (It should be noted that attempts to simulate UHB phase relationships were halted when the effects of forward motion on phase were considered. For an aircraft at a speed of Mach 0.76, the phase changes through 360 degrees several times along the fuselage length of interest. Time constraints in initiating the measurement program prevented a more thorough analysis; this will be the subject of further investigation and possible testing in FARF in a subsequent task assignment.)

Figure 5-3 compares the projected and measured decrease in levels along the fuselage from station 908 forward, for the tones at the first four frequencies. Station 908 represents the longitudinal location of the forward UHB rotor. In the Figure 5-3a, the

expected fuselage level distribution is shown. In the Figure 5-3b, the fuselage level distribution measured along microphone row C is shown, for each loudspeaker pattern indicated. (During the forced response tests, each test was conducted in three sequential "passes", one for each loudspeaker pattern, in order to expose the fuselage to acoustic excitation at all six frequencies: pass 1 was used for 169 Hz, pass 2 for 213 Hz, and pass 3 for 338, 426, 507 and 639 Hz. Because of this procedure, the three loudspeaker patterns shown in the figure are identified by a "pass number".)

In Figure 5-3b, the noise levels are seen to decrease by about 20 to 35 dB, depending on frequency, from the maximum levels at station 908 (aft of the pressure bulkhead). Although this is less than the 50 dB or more estimated for the actual aircraft, this distribution was judged to be acceptable for the purposes of comparing treatment effectiveness. One major reason for this is that in FARF the aft, unpressurized section behind the pressure bulkhead is devoid of the various systems and equipment found on a real aircraft; it is also lacking the additional structural members needed to support the UHB engine and its pylon. Thus, the transmission loss through the aft fuselage in FARF is much lower than the actual transmission loss through the aft fuselage on a UHB aircraft. This difference in transmission loss was expected to be at least 20 dB, over the frequency range of interest (later measurements on the UHB demo aircraft confirmed this expectation). To illustrate the effect of this transmission loss difference, in Figure 5-3c the measured level distribution has been adjusted by this assumed 20 dB, for the region exterior to the aft, unpressurized section (aft of station 820). This "adjusted" level distribution agrees much more closely with the projected distribution, indicating that the relative strengths of the two expected airborne paths (through the aft fuselage and then through the pressure bulkhead versus directly through the cabin sidewall) are reasonably well simulated in FARF.

In addition to tonal acoustic excitation using the three loudspeaker patterns shown in Figure 5-3, all of the forced response tests also included random, broadband excitation from 100 to 1000 Hz. For this type of excitation, Pass 2 loudspeakers were utilized. On a one-third octave band basis, the loudspeaker pattern for Pass 2 provided the largest and most uniform decrease in level with distance along the fuselage for the various frequency bands.

### 5.1.3 Vibration Excitation Sources

Structureborne noise expected on the UHB aircraft arises from engine vibrations which propagate through the pylon (and particularly along the pylon spars) into the fuselage structure, and then along frames and longerons to the cabin area. However, the planned UHB pylon is significantly different than the existing DC-9 pylon on the test fuselage in FARF. In order to support the UHB engine and provide sufficient clearance

for the propeller tips, the UHB pylon is much wider and higher than the short, stubby DC-9 pylon, resulting in significantly different vibration propagation characteristics. Because of these differences and the limited information on the vibration magnitudes expected from the UHB engines, the approach used to simulate UHB vibration excitation was to induce structural vibration at the point where UHB vibrational energy is expected to enter the fuselage, that is, at the forward pylon spar. Accordingly, a shaker was attached to the left pylon at the forward engine mount point, which connects directly to the forward pylon spar. The shaker was mounted at a 45 degree angle (see Figure 2-7), in order to generate vibration in both the lateral and vertical directions.

Since the major purpose of the forced response tests is to compare the effectiveness of various treatments, simulation of the correct absolute vibration level is unnecessary. Input vibration forces of approximately 40 lbs were used (as measured with a force transducer on the stinger between the shaker and the pylon). The vibration excitation tests consisted of tone signals (at 169 and 213 Hz) and random, broadband signals (100 to 1000 Hz).

#### 5.1.4 Data Analysis and Normalization

As discussed in the preceding section, the forced response tests involved separate acoustic and vibration excitation of the fuselage. For both types of excitation, tones of various frequencies as well as random, broadband signals were utilized.

The purpose of using tone excitation was to study the cabin noise environment resulting from acoustic and vibration loads that simulate a UHB 10x8 engine; thus the six tonal frequencies of 169, 213, 338, 426, 507 and 639 were included in the tests. The purpose of conducting random, broadband excitation tests was to provide data at other frequencies, and thereby permit evaluations of treatment effectiveness for additional advanced turboprop engine designs. In this report, analysis of the forced response data is limited to the tonal excitation measurements.

For presentation of the baseline levels in this section, and to properly compare levels measured after various treatments are installed (presented in section 6), all of the measured data have been normalized based on the sound pressure levels and acceleration levels measured at specific reference transducers. Different normalizations were utilized for the different types of data. For the noise data acquired during the acoustic excitation tests, measured levels were normalized to an average level at microphones E-908-B and E-908-G of 120 dB. For the acceleration data acquired during the vibration excitation tests, measured levels were normalized to an acceleration level of 1 g at the pylon vertical input accelerometer. For the corresponding noise data acquired during these vibration excitation tests, measured levels were normalized to the same 1 g pylon input level. (Measurements in FARF showed a linear relationship between

vertical input acceleration levels in dB and interior noise levels in dB, thereby allowing the normalization of noise data based on pylon vibration data.)

## **5.2 Measurement Results**

For the acoustic and vibration excitation tests, this section documents the measured response levels for the Baseline configuration. The corresponding measured response levels for each treatment configuration are presented in section 6, relative to the response levels provided here.

### **5.2.1 Baseline Response Levels, Acoustic Excitation**

Figures 5-4 through 5-7 show the baseline tone noise levels measured at the four interior microphone stations (see Figure 5-1). In each figure, the normalized level measured at each microphone is shown for each of the six excitation frequencies.

It is clear from these figures that there is a large variability in the level of each tone among the six microphones at each station. This is not surprising given the highly reverberant nature of the unfurnished fuselage. In order to reduce the measurement scatter, and as a basis for subsequent comparisons, the six levels at each station were arithmetically averaged. Figure 5-8 shows these averaged levels for each frequency and each measurement station.

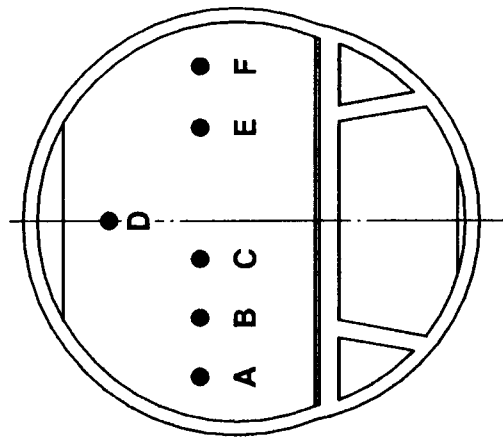
### **5.2.2 Baseline Response Levels, Vibration Excitation**

Figures 5-9 and 5-10 present the baseline tone vibration levels for accelerometers along longeron 10 and on frame station 718, respectively. On each figure, the normalized levels at 169 and 213 Hz are shown.

During the vibration excitation tests, noise levels were monitored by the interior microphones at the aft two microphone stations (748 and 772). Figure 5-11 presents the normalized measured noise levels for these two stations, showing the 169 and 213 Hz levels for the individual microphones. As for the noise levels measured during acoustic excitation, the noise levels due to vibration excitation show large variability among the various microphones.

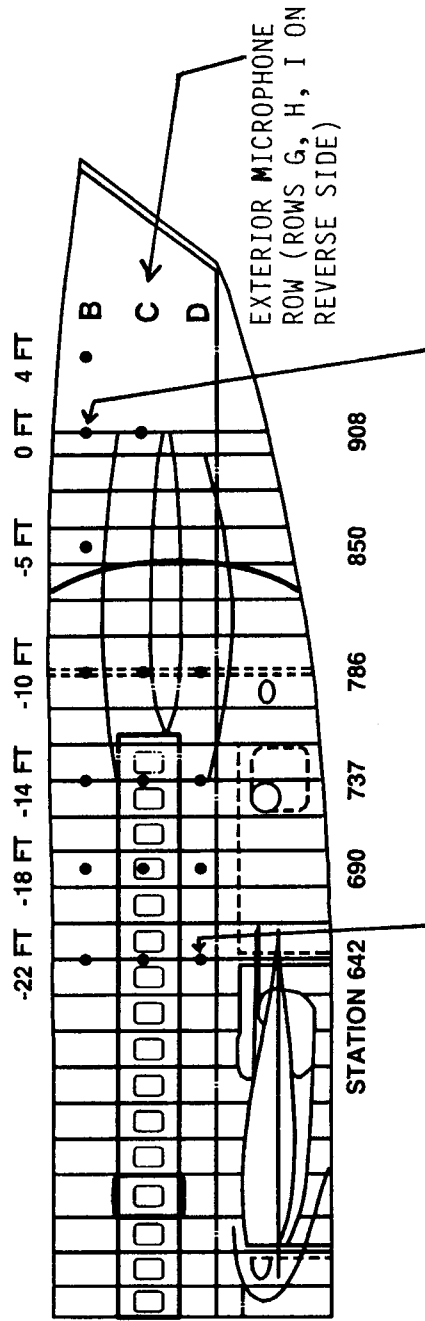
Noise levels averaged over the microphones at each microphone station are shown in Figure 5-12 for both frequencies.

**INTERIOR MICROPHONE CONFIGURATION**



**AT STATIONS  
642, 690, 748, AND 772**

**EXTERIOR MICROPHONE CONFIGURATION**

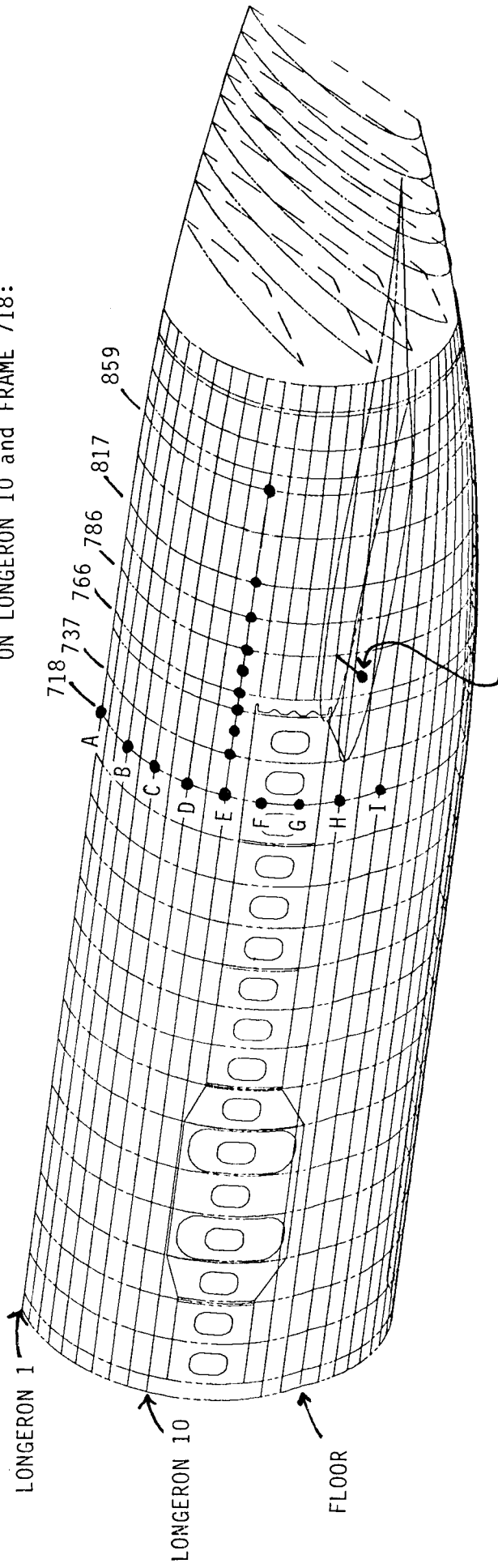


MICROPHONE LABEL: E-642-D

MICROPHONE LABEL: E-908-B

**Figure 5-1 Location of Microphones**

RESPONSE ACCELEROMETERS  
ON LONGERON 10 and FRAME 718:



INPUT ACCELEROMETERS (TRI-AXIAL) -  
ADJACENT TO STA 786 and LONGERON 15,  
ON ENGINE MOUNT

Figure 5-2 Location of Accelerometers

**Figure 5-3a**

UHB LEVELS PROJECTED FOR  
A 10x8 ENGINE CONFIGURATION

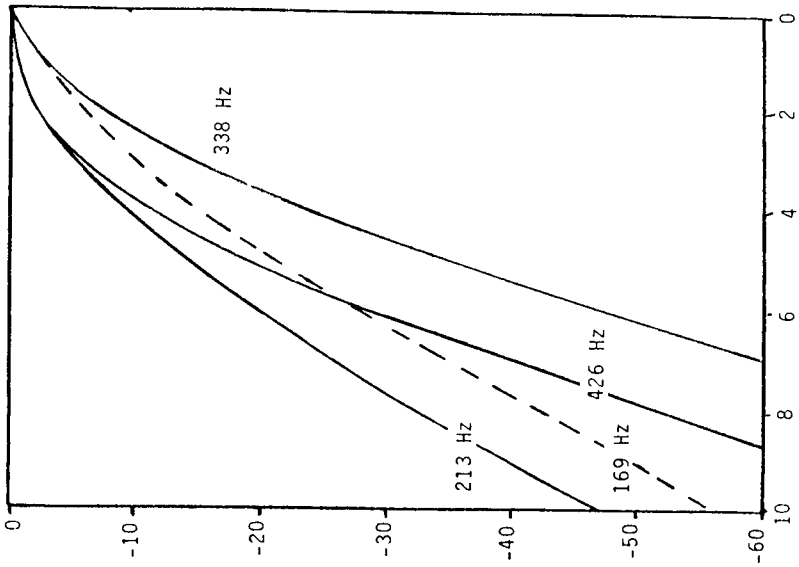


**Figure 5-3b**

UHB LEVELS SIMULATED BY THE  
INDICATED SPEAKER ARRAYS

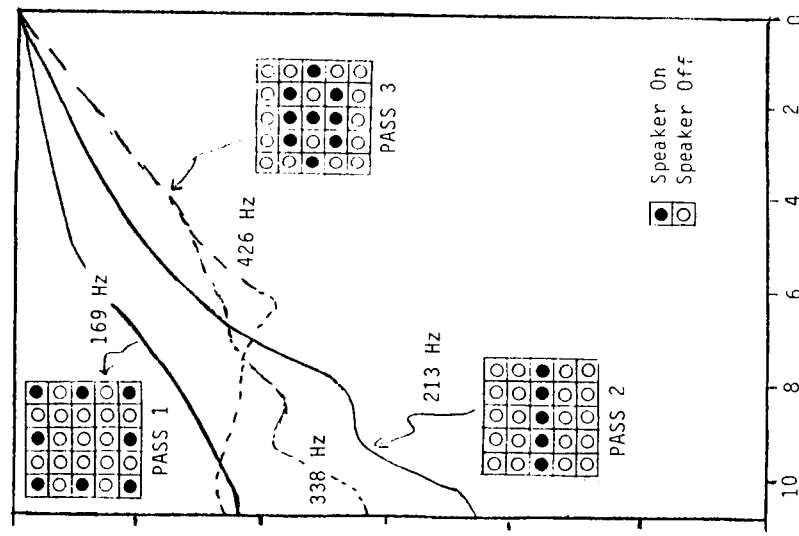
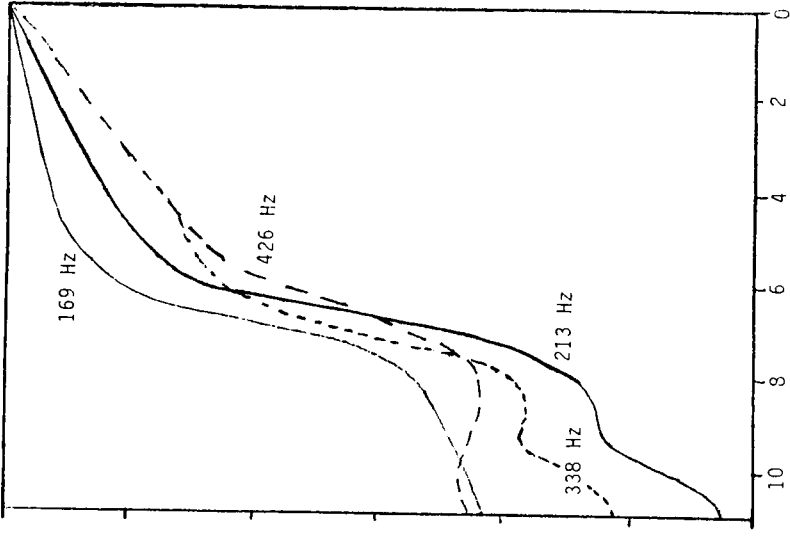


**Figure 5-3c**

"ADJUSTED" SIMULATED UHB LEVELS (TO  
ACCOUNT FOR AFT FUSELAGE T.L. DIFFERENCES)



DISTANCE ALONG FUSELAGE FROM FORWARD PROP PLANE (STATION 908), FT  
(At 75° from the fuselage vertical axis)

**Figure 5-3 Comparison of Predicted and Simulated UHB Level Distributions**

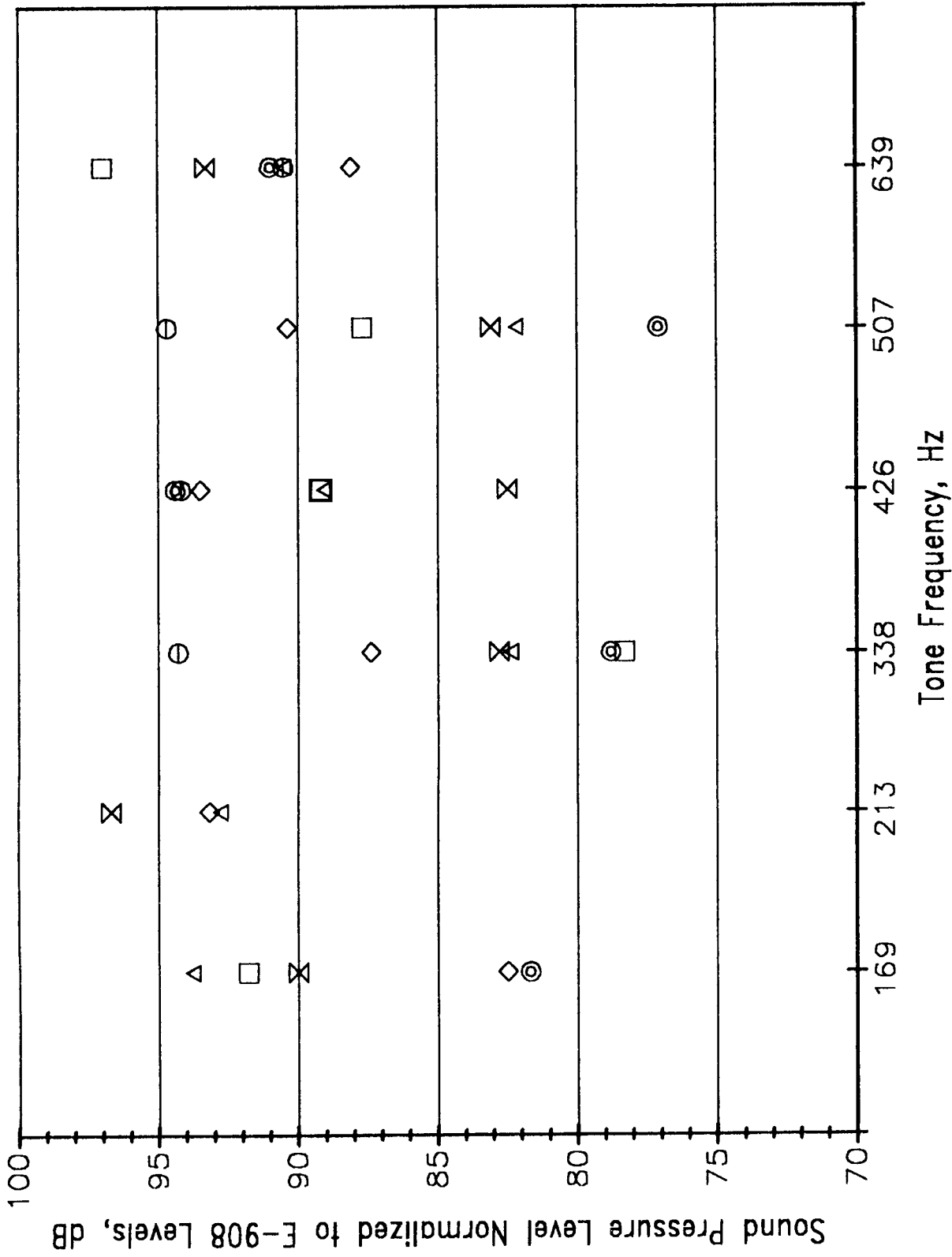
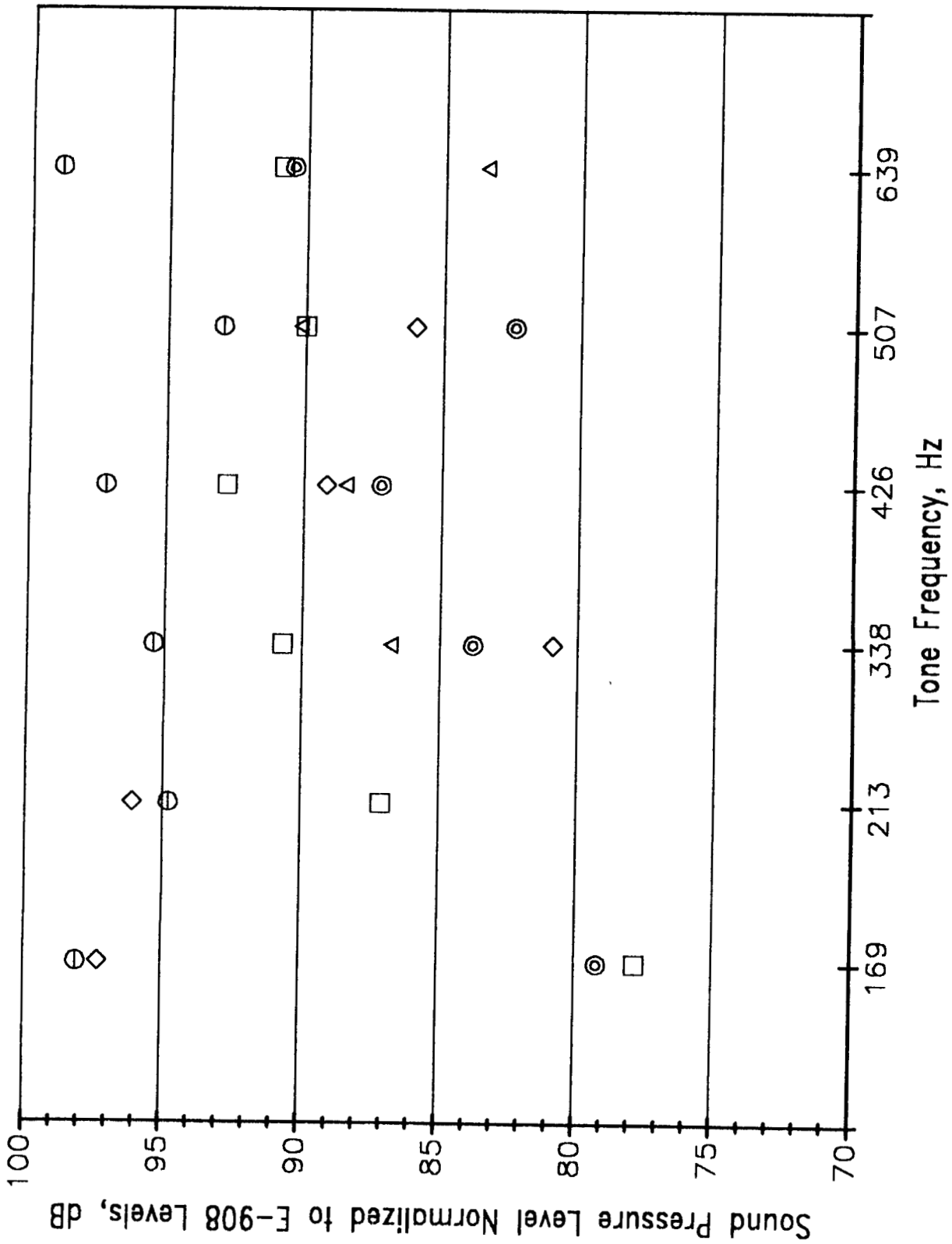
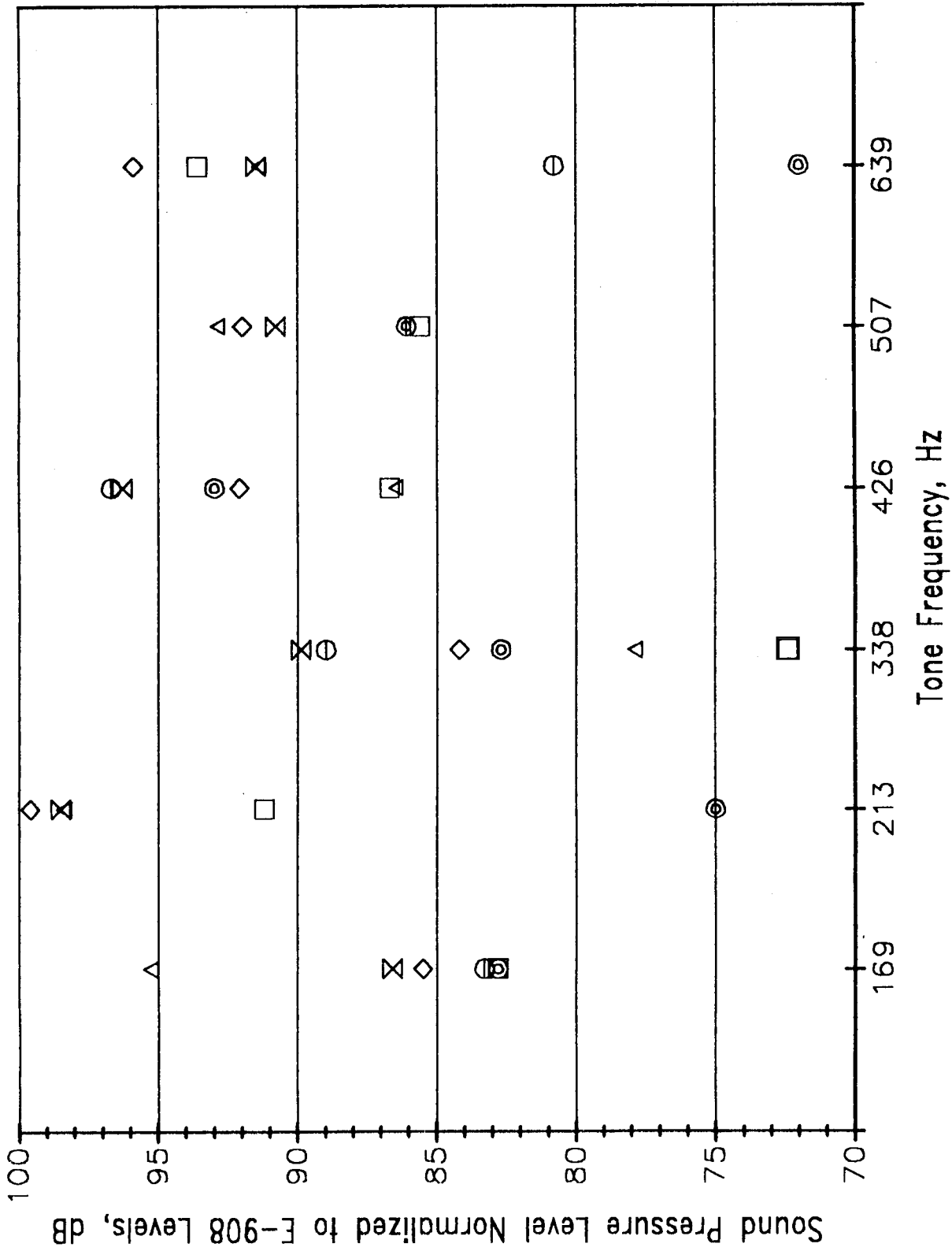


Figure 5-4 Measured Sound Pressure Levels for Tonal Acoustic Excitation, Baseline Phase, Sta. 642



Mic No.
◇ A
□ B
△ C
⊖ D
⊙ E
⊗ F

Figure 5-5 Measured Sound Pressure Levels for Tonal Acoustic Excitation, Baseline Phase, Sta. 690



Sound Pressure Level Normalized to E-908 Levels, dB

Tone Frequency, Hz

Mic No.
◇ A
□ B
△ C
⊖ D
⊙ E
⊗ F

Figure 5-6 Measured Sound Pressure Levels for Tonal Acoustic Excitation, Baseline Phase, Sta. 748

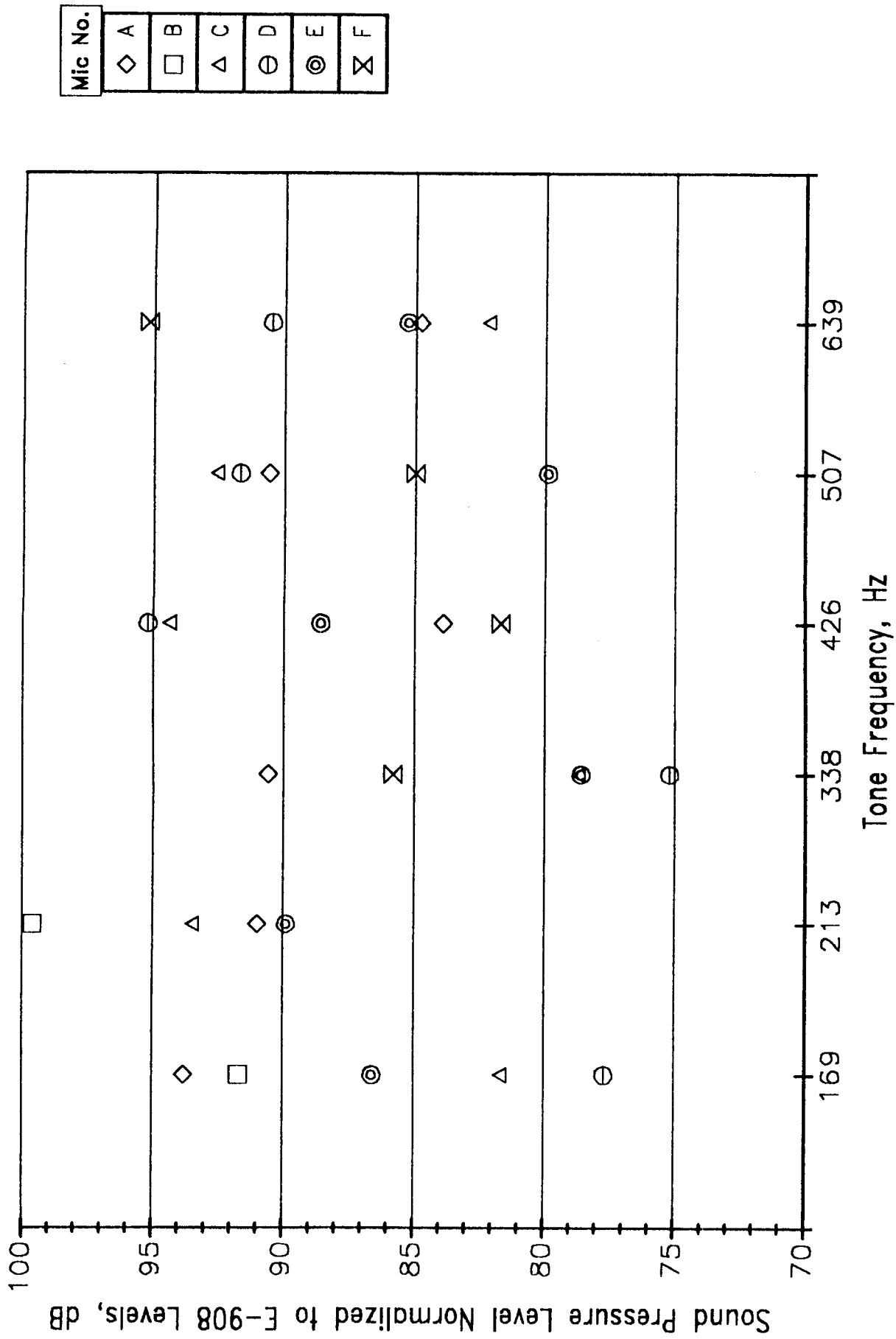
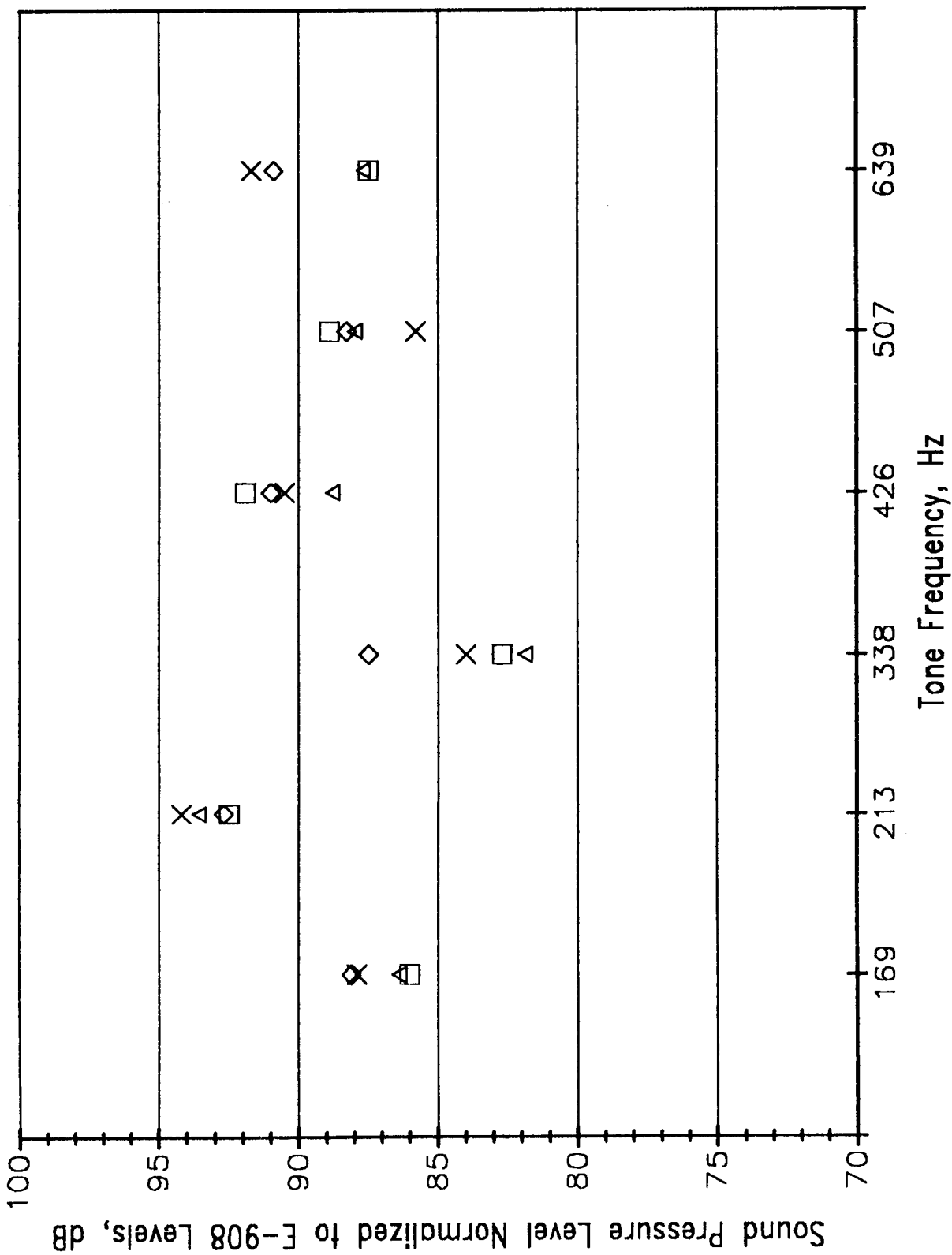


Figure 5-7 Measured Sound Pressure Levels for Tonal Acoustic Excitation, Baseline Phase, Sta. 772



Station No.
X 642
◇ 690
□ 748
△ 772

Figure 5-8 Measured Sound Pressure Levels for Tonal Acoustic Excitation, Baseline Phase, Station Averages

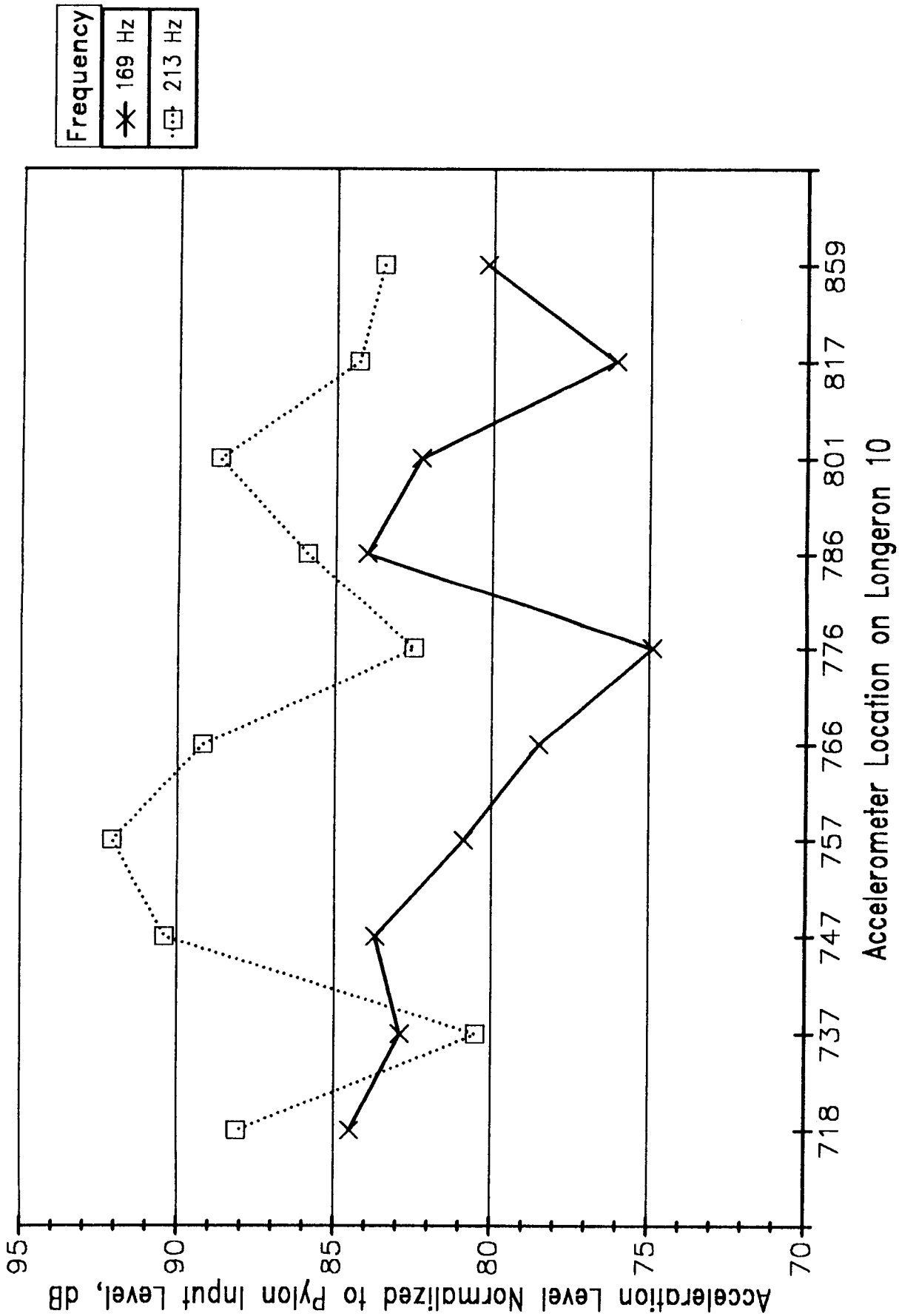
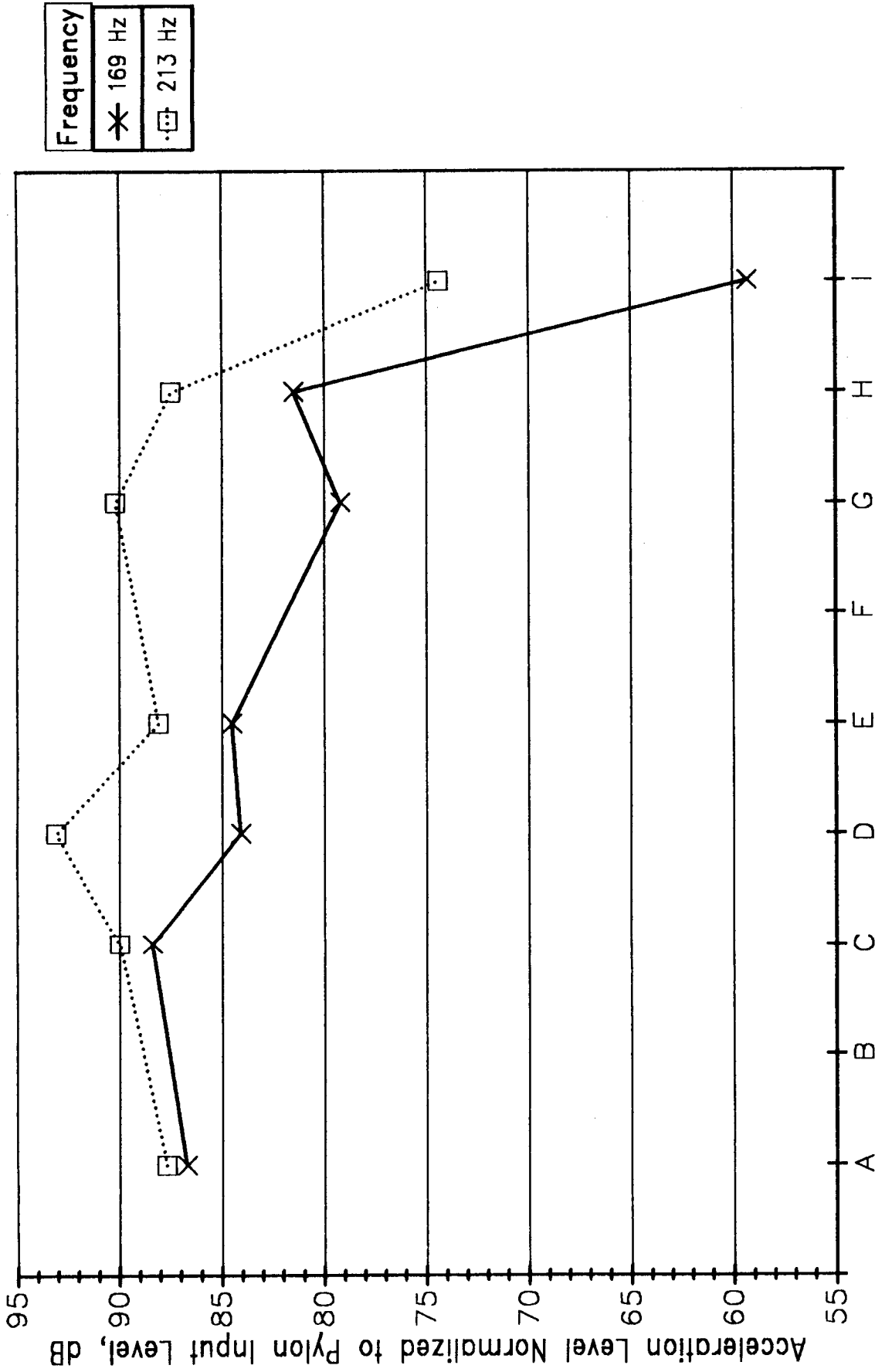


Figure 5-9 Measured Acceleration Levels for Tonal Vibration Excitation, Baseline Phase, Longeron 10



Accelerometer Location at Station 718

Figure 5-10 Measured Acceleration Levels for Tonal Vibration Excitation, Baseline Phase, Station 718

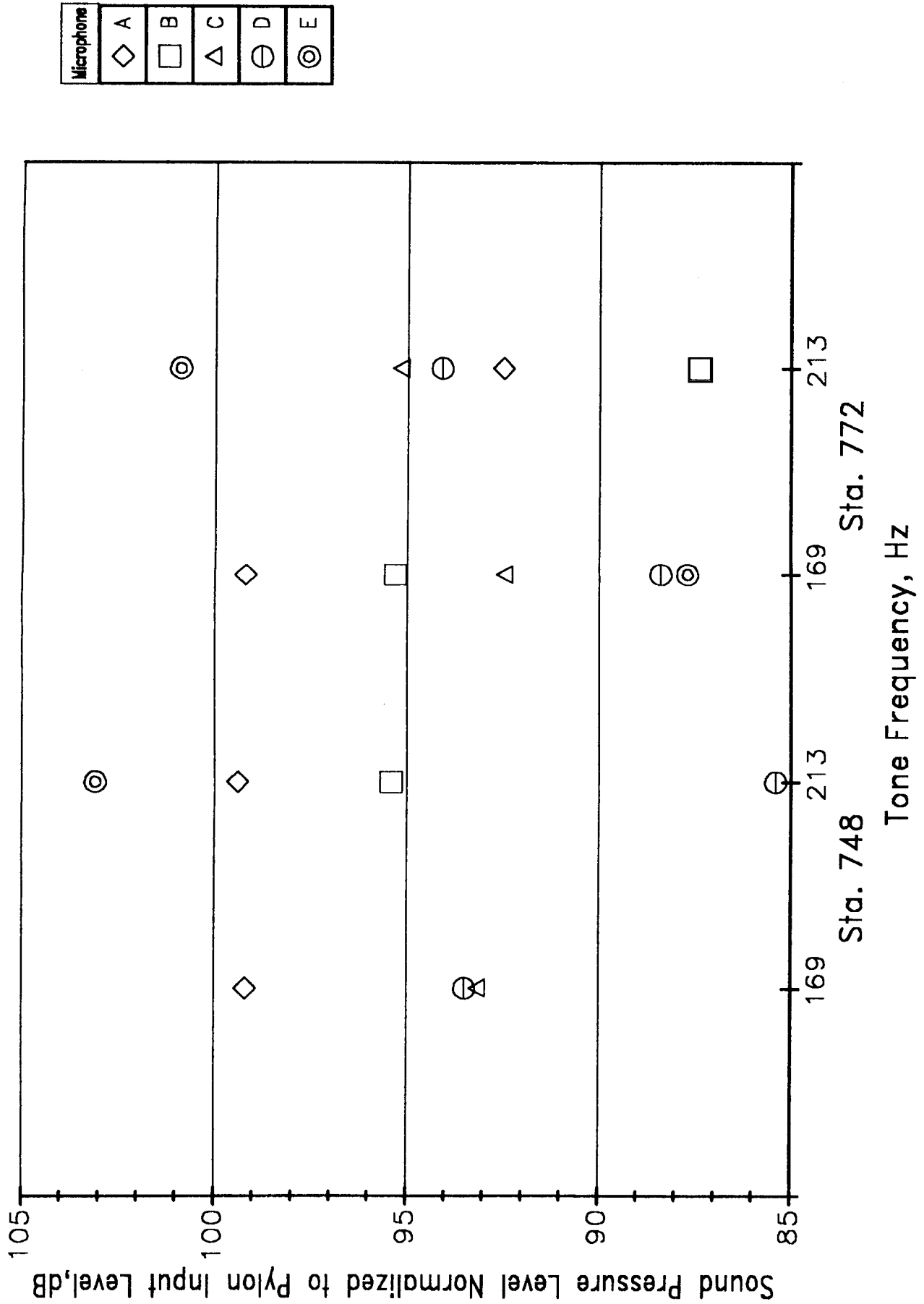


Figure 5-11 Measured Sound Pressure Levels for Tonal Vibration Excitation, Baseline Phase, Stations 748, 772

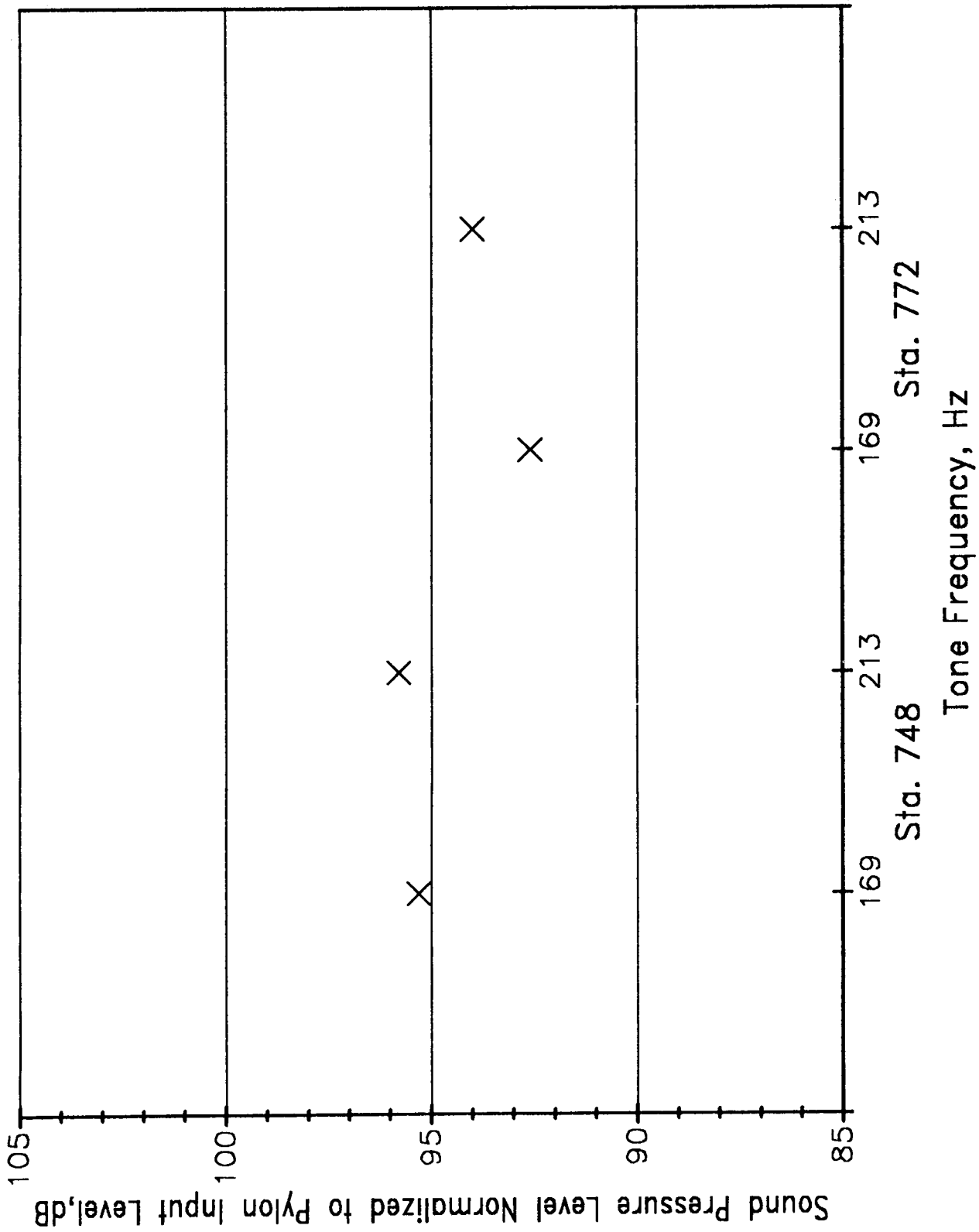


Figure 5-12 Measured Sound Pressure Levels for Tonal Vibration Excitation, Baseline Phase, Station Averages

## 6 Noise Control Treatment Forced Response Tests

Following the Baseline phase, several noise control treatments were installed in the test fuselage in two modification phases. In the Structural Modifications phase, selected structural treatments related to increasing the mass, stiffness, damping or isolation characteristics of the fuselage were applied and studied. In the Furnished Fuselage phase, further treatments and configurations related to increasing mass, damping and isolation in the furnished cabin were added and evaluated. The purpose of these forced response tests, then, was to assess the relative effectiveness of the individual treatments in reducing interior noise levels under simulated advanced turboprop excitation.

### 6.1 Description of Treatments

Treatments were selected to control propagation along three potential paths on a UHB aircraft (see Figure 6-1): an airborne path through the cabin sidewall, an airborne path into the aft unpressurized section and then through the pressure bulkhead, and a structural path through the engine pylon and into the fuselage structure. The treatment configurations used in the Structural Modifications phase, in sequential order, are as follows:

**Configuration 2.** A "torque box" was installed in the aft cabin area. This is a patented device designed to greatly increase the stiffness of an existing frame, particularly to torsional motion. The torque box consists of a new frame installed approximately 4 in from an existing frame (located at station 766), with a cover plate over both frames (see Figure 6-2).

**Configuration 3.** Two additional frames were installed in the aft cabin area, just forward of the engine mount bulkhead. These frames, identical to current production frames, were added midway between existing frames. Figure 6-3 shows the locations and station numbers. The purpose of these frames is to provide additional sidewall stiffness.

**Configuration 4.** A second set of two additional frames was installed in the aft cabin area, forward of the frames added in configuration 3. See Figure 6-3 for location details.

**Configuration 5.** Damping material was applied to the four new frames, and to several existing frames in the aft cabin area. This material (EAR type C-1002-12) was used to reduce structural vibration, particularly at the frame modal frequencies. Figure 6-3 shows the method of installation and the locations of the treated frames.

**Configuration 6.** Damping material was applied to the cover plate of the torque box, to reduce structural vibration from this device. The same damping material was used as in configuration 5, and the method of application was identical to that used on the top of the frames in that configuration.

**Configuration 7.** The torque box was "disabled", by drilling out the rivets connecting the cover plate to frame 762, and inserting damping material (the same as above) between the cover plate and the frame to prevent rattling. This configuration was prompted by test results which indicated that the torque box was causing increased, rather than decreased, cabin noise levels (see section 6.3 below).

**Configuration 8.** A "pressure bulkhead double wall" was installed approximately 3 in forward of the pressure bulkhead to reduce sound transmission from the aft unpressurized section into the cabin. The double wall was constructed of 0.063 in aluminum in three sections, one over the bulkhead door and the other two over the side sections of the bulkhead, where the lavatories are located. This configuration also includes damping material (EAR type SD-40AL/3203-50PSA) applied to the side sections of the pressure bulkhead, and isolator mounts to attach the double wall to the fuselage structure. See Figure 6-4 for details.

**Configuration 9.** Dynamic tuned absorbers were mounted on 9 frames between stations 672 and 801. Tuned to 169 Hz, these absorbers were used to reduce frame vibration at the BPF excitation frequency. The absorbers were installed at three locations per frame, near longerons L6, L10, and L14. Figure 6-5 shows one of the absorbers mounted on a frame.

**Configuration 10.** Absorption blankets were installed in the aft unpressurized section to absorb acoustic energy in this area and thereby decrease transmission through the pressure bulkhead. The blankets, made of 2 in thick fiberglass insulation with a quilted facing, were installed over the pressure bulkhead and over portions of the ventral stairs.

**Configuration 11.** Damping material was applied to the fuselage skin throughout the passenger cabin area and the aft unpressurized section. The material, Soundcoat type 10MS/10LT12, is being considered as a potential measure for reducing sonic fatigue of the fuselage skin in the vicinity of the UHB propeller planes, where high acoustic loads are expected. Since this treatment will also affect noise transmission into the aft section and structureborne propagation through the fuselage, it was tested in FARF and included here as a separate configuration. The damping material was installed on the skin in the rectangular areas formed by the frames and longerons.

**Configuration 12.** A second damping treatment was applied to the fuselage skin, specifically for acoustic purposes. The damping material, EAR type SD-40AL/3202-50PSA, was installed directly over the sonic fatigue damping material on all skin panels

throughout the passenger cabin.

The Structural Modifications phase concluded with configuration 12. Four additional configurations were studied in the Furnished Fuselage phase:

**Configuration 13.** The basic cabin furnishings were installed in this configuration. This included carpeting on the floor, on the sidewall kick panels and on the engine mount bulkhead walls; trim panels; two thermal insulation blankets in the sidewall; baggage racks; ceiling panels; and seats. Prior to installing these furnishings, the pressure bulkhead double wall, the aft absorption blankets and the dynamic tuned absorbers were removed. Also, lavatories were not installed for this configuration.

**Configuration 14.** The pressure bulkhead double wall was reinstalled. All other aspects are identical to configuration 13.

**Configuration 15.** The double wall bulkhead was again removed, and the lavatories were installed. Also, damping material (EAR type SD-40ALPSA) was added to all the trim panels throughout the cabin, on the side facing the sidewall cavity.

**Configuration 16.** The double wall bulkhead was again installed. This configuration represents the fully treated cabin.

Figures 6-6 through 6-8 show photographs of selected treatments. Table 6-1 summarizes all 16 configurations studied in the forced response tests. The table lists the configuration number, the test phase, a brief description of the treatment, the propagation path(s) on which the treatment is designed to be effective, and the type of data that was measured during the tests.

## 6.2 Measurement and Analysis Procedures

After each configuration was implemented on the fuselage, acoustic and vibration excitation tests were conducted, and noise and vibration levels were measured. The test conditions (source levels, transducer locations, etc.) were identical to those in the Baseline phase, described in section 5, except for minor differences in microphone positions to accommodate the presence of the passenger seats.

Noise and vibration levels measured for each configuration were normalized in the same manner as for the Baseline tests. Then, differences between the normalized levels for each treatment configuration and the normalized levels for the Baseline configuration were computed, for all the acoustic and vibration data. Evaluation of the effectiveness of each treatment was thus based on incremental differences in levels (noise and vibration) from Baseline levels, for acoustic and vibration excitations that are normalized to identical levels among all tests.

## 6.3 Measurement Results

As discussed in section 5, three types of data were collected in the various forced response tests: noise data during acoustic excitation tests, acceleration data during vibration excitation tests, and noise data during vibration excitation tests. Table 6-1 identifies the type of data obtained for each treatment configuration. In this section, results of the tonal excitation measurements for these three data types are presented.

### 6.3.1 Treatment Response Levels, Acoustic Excitation

In order to evaluate the effectiveness of the various treatments in reducing interior noise levels resulting from tonal acoustic excitation at simulated UHB frequencies, sound pressure levels for each treatment relative to baseline levels were determined from the measured data. Figures 6-9 and 6-10 show sample results, using the noise data (average microphone levels) obtained at the aft-most measurement location, station 772.

In the figures, the levels at each frequency relative to baseline levels (see Figure 5-8) are plotted for the individual Structural Modifications (Figure 6-9) and Furnished Fuselage (Figure 6-10) configurations. Several gross trends can be observed. First, it is interesting to note that noise levels increased above baseline levels after installation of the first few treatments at all frequencies. Second, configuration 2 (the torque box) generally causes the highest levels; levels decreased after installation of successive treatments. Third, the two skin damping treatments (configurations 11 and 12) generally result in observable reductions in level, and cause the lowest levels among the Structural Modifications treatments. Finally, the Furnished Fuselage configurations reduce levels substantially from the Structural Modifications configurations.

In order to deduce more detailed trends, the relative levels determined at each station were determined individually for each configuration. Figures 6-11 through 6-16 were generated from these data. Each figure applies to a single tone frequency. The relative noise levels are shown as a function of configuration, and are presented as the range and average value of the levels at the four measurement stations. (Note: given the relatively large ranges on the various figures, differences in average levels from one configuration to the next of one to two dB are not significant.)

For 169 Hz, Figure 6-11 shows that the torque box does result in interior levels that are higher than baseline levels. Adding two and then four frames (configurations 3 and 4) reduces the level back to baseline, but subsequent configurations in the Structural Modifications phase have negligible effect. Installing the fuselage interior (configuration 13) reduces levels, and a further reduction of 6 dB occurs when the trim panels are damped (configuration 15).

Figure 6-12 shows nearly identical trends for 213 Hz. Addition of the fuselage interior yields a greater benefit at this frequency than at 169 Hz.

For 338 Hz, it can be seen in Figure 6-13 that the torque box further increases levels relative to baseline, and again two additional frames counteracts this effect. The double wall pressure bulkhead (configuration 8) is seen to provide significant benefit, but is compromised somewhat by the next configuration (tuned absorbers). The four Furnished Fuselage configurations provide increasingly greater reductions.

The data in Figure 6-14 for 426 Hz differ from the data for the prior frequencies in that levels decrease by some 15 dB after installation of the two frames (configuration 3), and then remain nominally 5 dB below baseline levels (rather than at baseline levels) for the next few configurations. Addition of the double wall bulkhead (configuration 8) reduces levels, but not to the extent observed at 338 Hz. The tuned absorbers (configuration 9) appear to provide a benefit (which is surprising since the absorbers are tuned to 169 Hz!). Levels decrease further (by 4 dB) after installation of the sonic fatigue damping (configuration 11). The four furnished configurations provide significant reductions which increase with each subsequent configuration.

For 507 Hz (Figure 6-15), the torque box increases levels above baseline by 3 dB, and four added frames are required to reduce this effect. The double wall pressure bulkhead yields some benefit. For this frequency, the skin acoustic damping (configuration 12) shows an 8 dB improvement in levels, followed by a large decrease in levels when the furnishings are added. Here, additional configurations do not greatly reduce levels as they did for 338 and 426 Hz, although the net effect is a 5 dB reduction from configuration 13 to configuration 16.

Finally, the data for 639 Hz are presented in Figure 6-16. As seen for other frequencies, the torque box causes levels to increase above baseline levels, but two and then four frames reduce levels to near baseline. The double wall bulkhead yields a 4 dB improvement in levels. The sonic fatigue damping (configuration 11) then results in 4 dB lower levels, and the skin acoustic damping (configuration 12) drops levels further. The first Furnished Fuselage configuration then decreases levels by 15 to 20 dB, with an additional 5 dB occurring for the final configuration.

### **6.3.2 Treatment Response Levels, Vibration Excitation**

The approach taken for analysis of the vibration excitation data is similar to that for the acoustic excitation data. For the vibration tests, however, only two tonal frequencies were studied (169 and 213 Hz), and not all of the configurations were evaluated.

Figures 6-17 and 6-18 present Structural Modifications and Furnished Fuselage treatment levels, respectively, as measured at several accelerometer locations on frame

station 718 at 169 Hz. As for the preliminary noise plots, some gross trends can be observed in these two figures. First, the various configuration levels are generally below the baseline levels, indicating that all of the treatments (including the torque box) are providing some benefit. Second, the two damping treatments (configurations 11 and 12) show large reductions in level from the preceding treatments. Finally, the various Furnished Fuselage configurations do not provide significantly lower levels than many of the structural treatments, in contrast to the trends seen in the acoustic excitation data.

For a more detailed analysis of treatment effectiveness, Figures 6-19 through 6-22 show the acceleration levels relative to baseline levels for each configuration. Figures 6-19 and 6-20 present data measured on station 718 and longeron 10, respectively, at 169 Hz. Similarly, Figures 6-21 and 6-22 present 213 Hz data measured on station 718 and longeron 10, respectively. The station 718 data are based on the range and average values of relative acceleration levels measured at locations A, C, D, E, and H, and the longeron 10 data are based on the range and average values of relative acceleration levels measured at locations 718, 737, 747, 757, 766, and 776.

One immediately striking trend that can be observed on these four figures is that for both frequencies, the station 718 relative levels are consistently 5 dB lower than the longeron 10 relative levels, for nearly every configuration. One possible explanation for this observation is that each treatment yields benefits (in terms of reducing acceleration levels) that increase with distance along the fuselage from the vibration source. This explanation is supported by review of the normalized acceleration data measured along longeron 10, which shows relatively constant levels for the baseline configuration, but levels which generally decrease with distance from the vibration input point for the various treatments. This is not surprising for some treatments, such as the damping materials, for which there is a greater extent of treatment application with increasing distance. However, for other treatments which are localized, such as the torque box, this increasing benefit with distance was not anticipated.

Figures 6-19 and 6-20 both show that for 169 Hz, the torque box does not increase (average) vibration levels. Figure 6-19 shows a relatively steady decrease in vibration levels for station 718 with successive treatments from configuration 4 through configuration 12. (This trend is less pronounced in the longeron 10 data.) In particular, the station 718 data show that the tuned absorbers (configuration 9), sonic fatigue damping (configuration 11) and skin acoustic damping (configuration 12) each reduce acceleration levels significantly. For the Furnished Fuselage configurations, acceleration levels rise; this may be due to structural energy propagating through the frames into the trim panels and then radiating as acoustic energy through the sidewall air gap back to the fuselage skin and structural members where increased vibration levels result.

For 213 Hz, Figures 6-21 and 6-22 show that the torque box and four added frames

both reduce levels, but there is an increase in levels with frame damping (configuration 5). Disabling the torque box (configuration 7) appears to increase levels on station 718 but decrease levels on longeron 10. For station 718, the tuned absorbers and the sonic fatigue damping again show good reductions in acceleration levels, but the skin acoustic damping does not have the same benefit at this frequency as it did for 169 Hz. There is a reduction in level when the fuselage furnishings are added, but this benefit disappears for configuration 15.

Only a limited amount of noise data were collected during the vibration excitation tests. Figure 6-23 shows the 169 Hz and 213 Hz levels measured at stations 748 and 772, relative to baseline levels, for all the configurations for which data are available. This figure shows that there are relatively minor differences in levels between the baseline and each of the four structural configurations for both frequencies, which is in agreement with the longeron 10 acceleration data. Unfortunately no noise data were collected near station 718, which showed the higher reductions in acceleration levels than the longeron 10 data.

Figure 6-23 also shows, however, that the Furnished Fuselage noise levels are relatively lower than baseline levels, in contrast to the Furnished Fuselage acceleration data. This may be due to the additional absorption in the cabin for these configurations, relative to the Structural Modifications configurations.

Table 6-1 Forced Response Test Configurations

CONFIGURATION	PHASE	DESCRIPTION	PATH*	ACOUSTIC EXCITATION		VIBRATION EXCITATION	
				NOISE DATA	VIBRATION DATA	NOISE DATA**	VIBRATION DATA
1	BASE.	BARE CABIN	-	X	X		X
2	STRUCT.	TORQUE BOX	1,3	X**	X		X
3	STRUCT.	2 FRAMES	1,3	X			
4	STRUCT.	4 FRAMES	1,3	X			X
5	STRUCT.	FRAME DAMPING	1,3	X			X
6	STRUCT.	DAMPED TORQUE BOX	1,3	X			
7	STRUCT.	DISABLED TORQUE BOX	1,3	X			X
8	STRUCT.	DOUBLE WALL BULKHEAD	2	X			
9	STRUCT.	TUNED ABSORBERS	1,3	X			X
10	STRUCT.	ABSORPTION BLANKET	2	X			
11	STRUCT.	SONIC FATIGUE DAMPING	1,3	X			X
12	STRUCT.	SKIN ACOUSTIC DAMPING	1,3	X			X
13	FURN.	FURNISHED, NO LAV, NO DOUBLE WALL BULKHEAD	1,3	X			X
14	FURN.	DOUBLE WALL BLKHD ADDED	2	X			X
15	FURN.	TRIM DAMPING, LAV ADDED NO DOUBLE WALL BLKHD	1,3	X			X
16	FURN.	FULLY FURNISHED	1,2,3	X			

\*PATH: 1 = AIRBORNE THROUGH SIDEWALL  
 2 = AIRBORNE THROUGH AFT SECTION & PRESSURE BULKHEAD  
 3 = STRUCTUREBORNE

\*\*DATA AT STATIONS 748 AND 772 ONLY

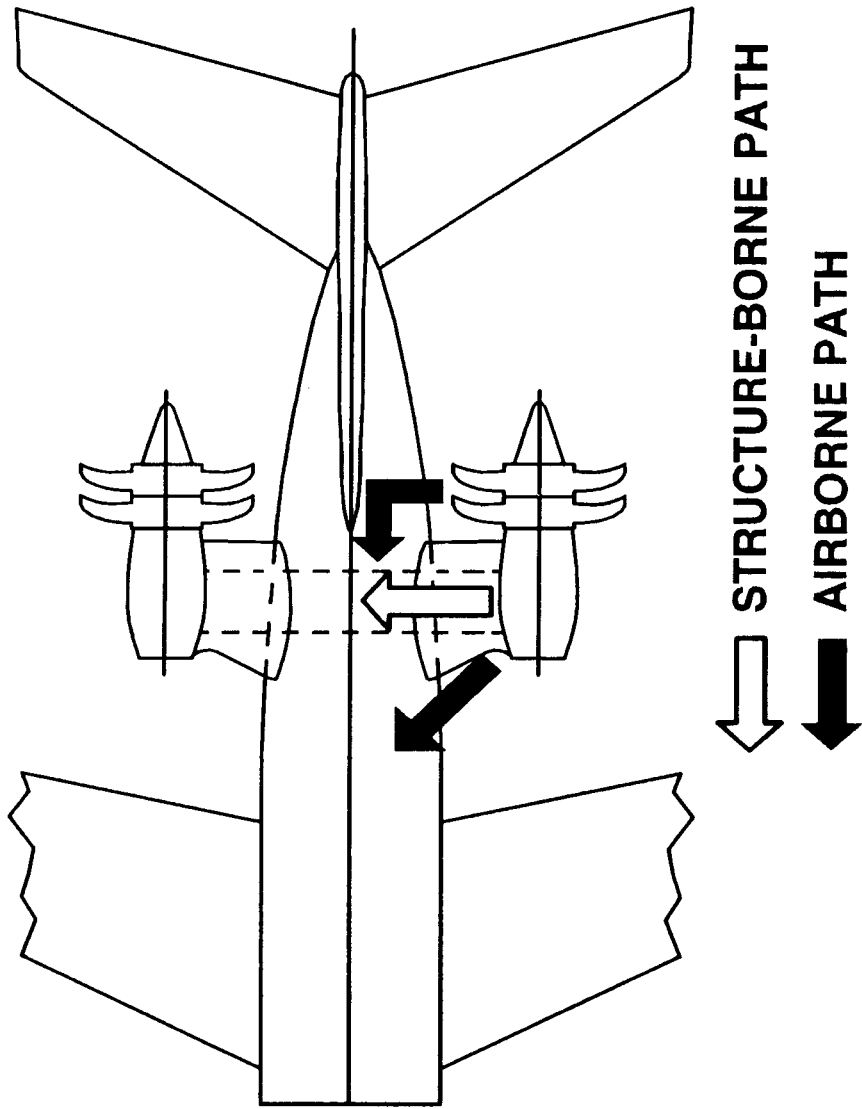
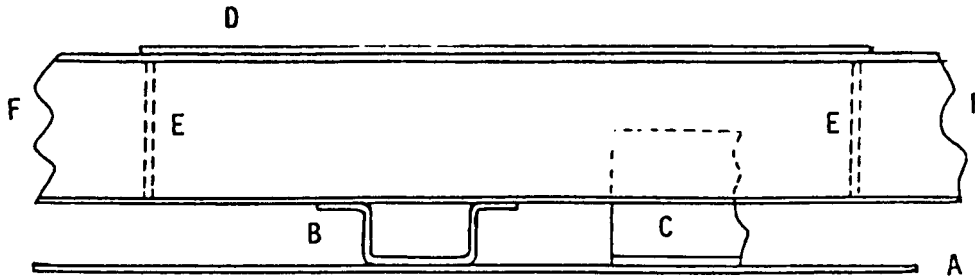
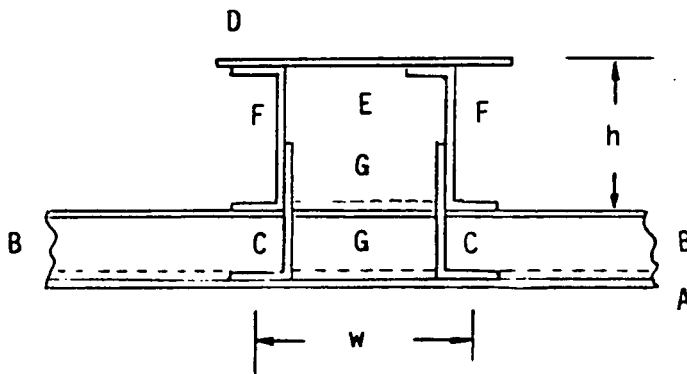


Figure 6-1 Predicted Transmission Paths for UHB Aircraft



LONGERON CROSS-SECTION



FRAME CROSS-SECTION

- A - SKIN
- B - LONGERON
- C - CLIP ANGLES OF TORSIONAL RING FRAME TO SKIN BETWEEN LONGERONS
- D - COVER PLATE OF TORQUE BOX (LIGHTENING HOLES CIRCUMFERENTIALLY)
- E - WEB STIFFENERS TO PREVENT BUCKLING
- F - FRAME CHANNELS
- G - DAMPING MATERIAL - ON SKIN BETWEEN LONGERONS  
- ON LONGERONS BETWEEN RING CHANNEL

Figure 6-2 Torque Box Design

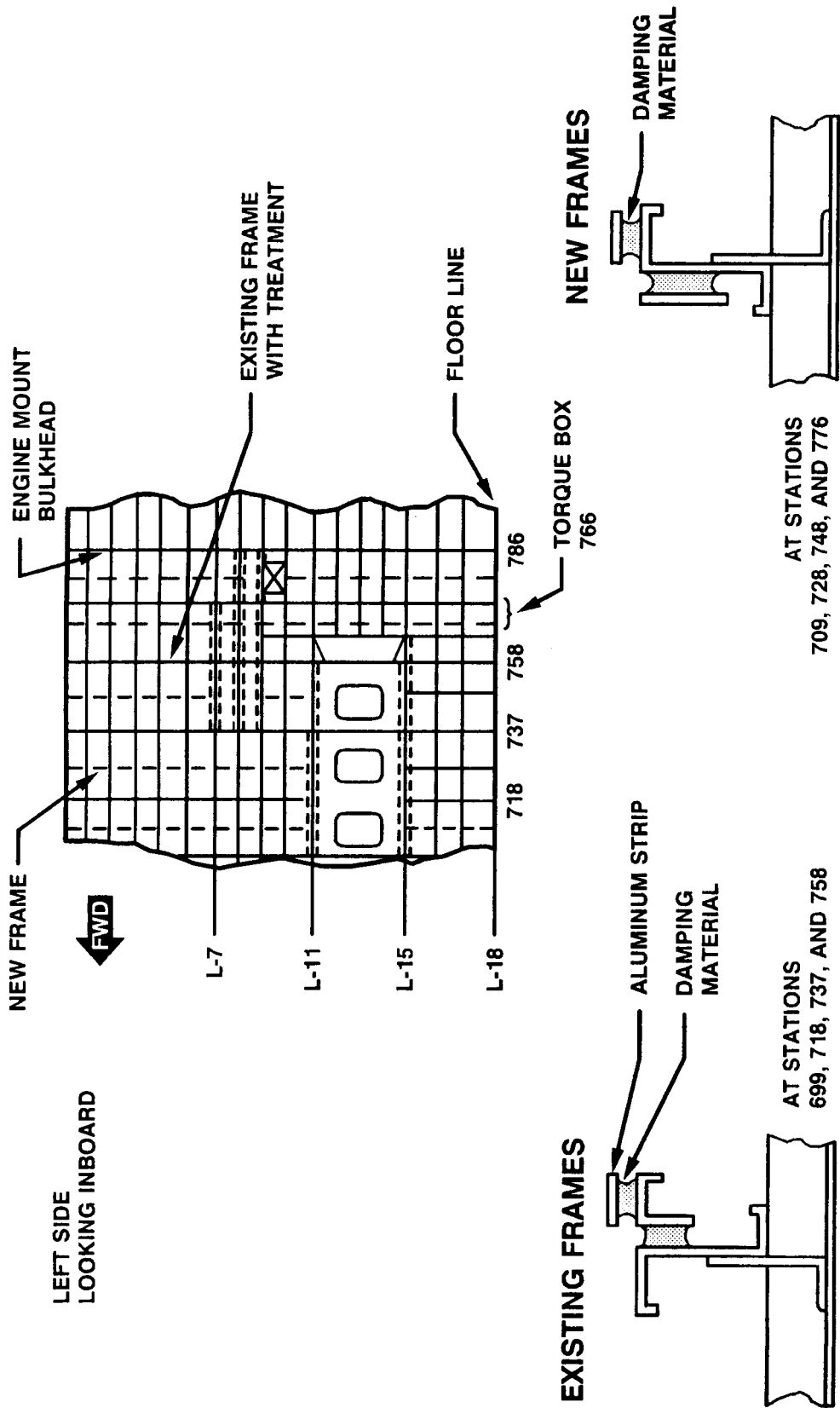


Figure 6-3 Frame Modification Details

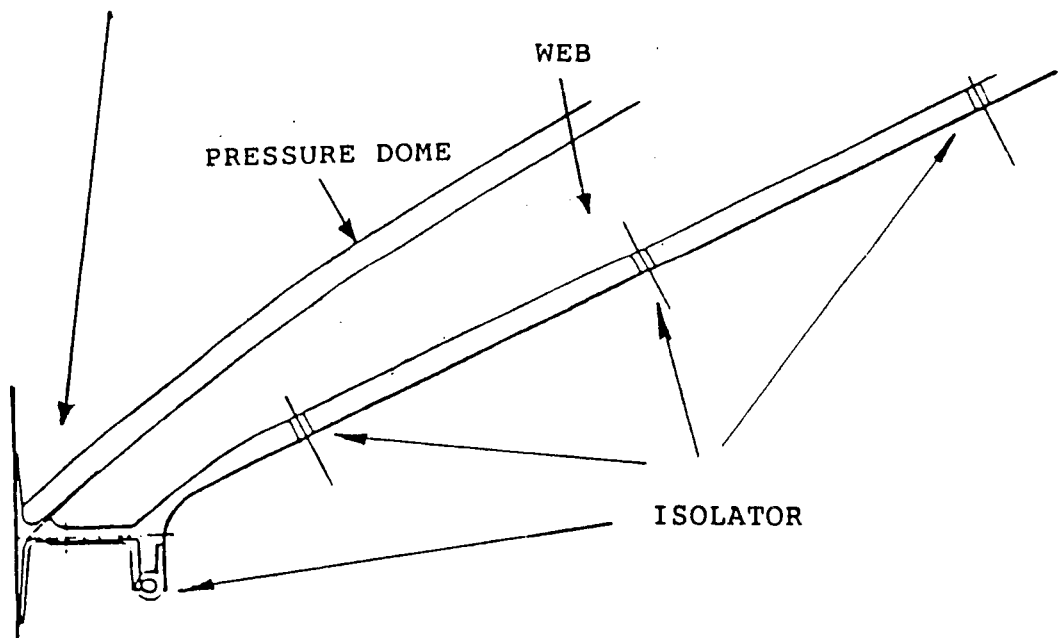
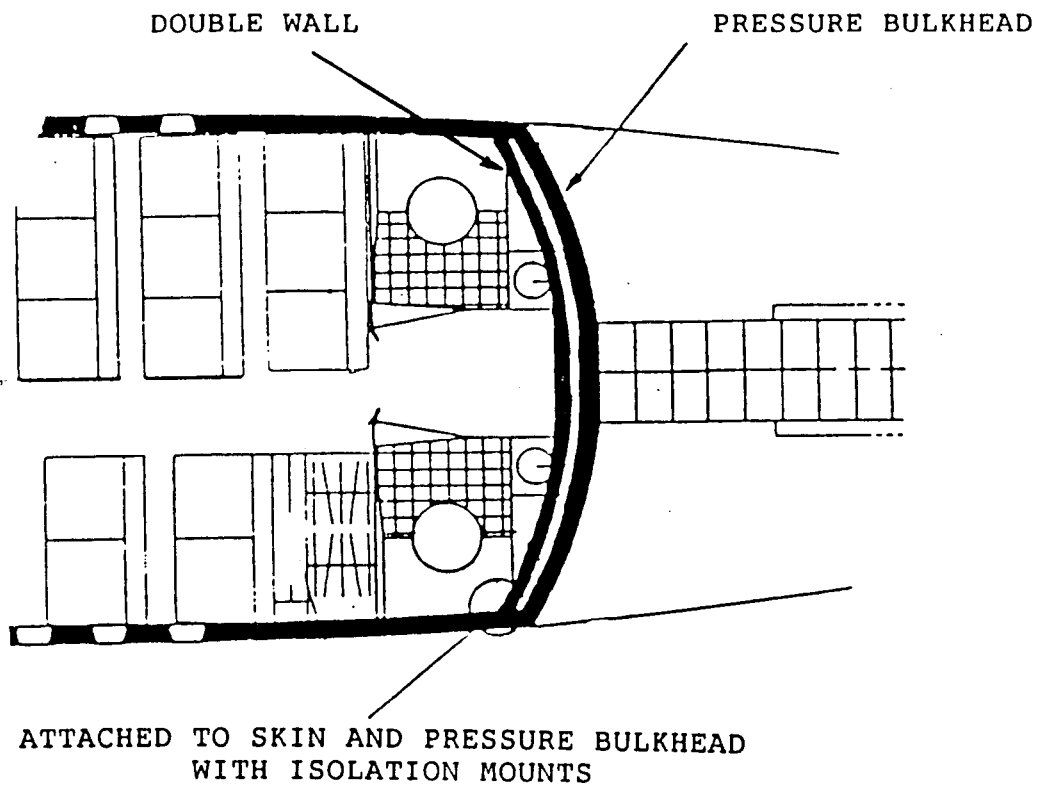


Figure 6-4 Double Wall Pressure Bulkhead Design

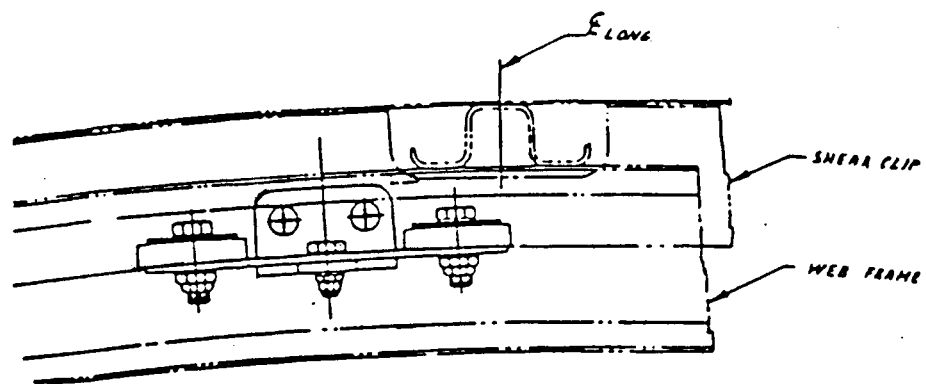


Figure 6-5 Dynamic Tuned Absorber Installed on Frame

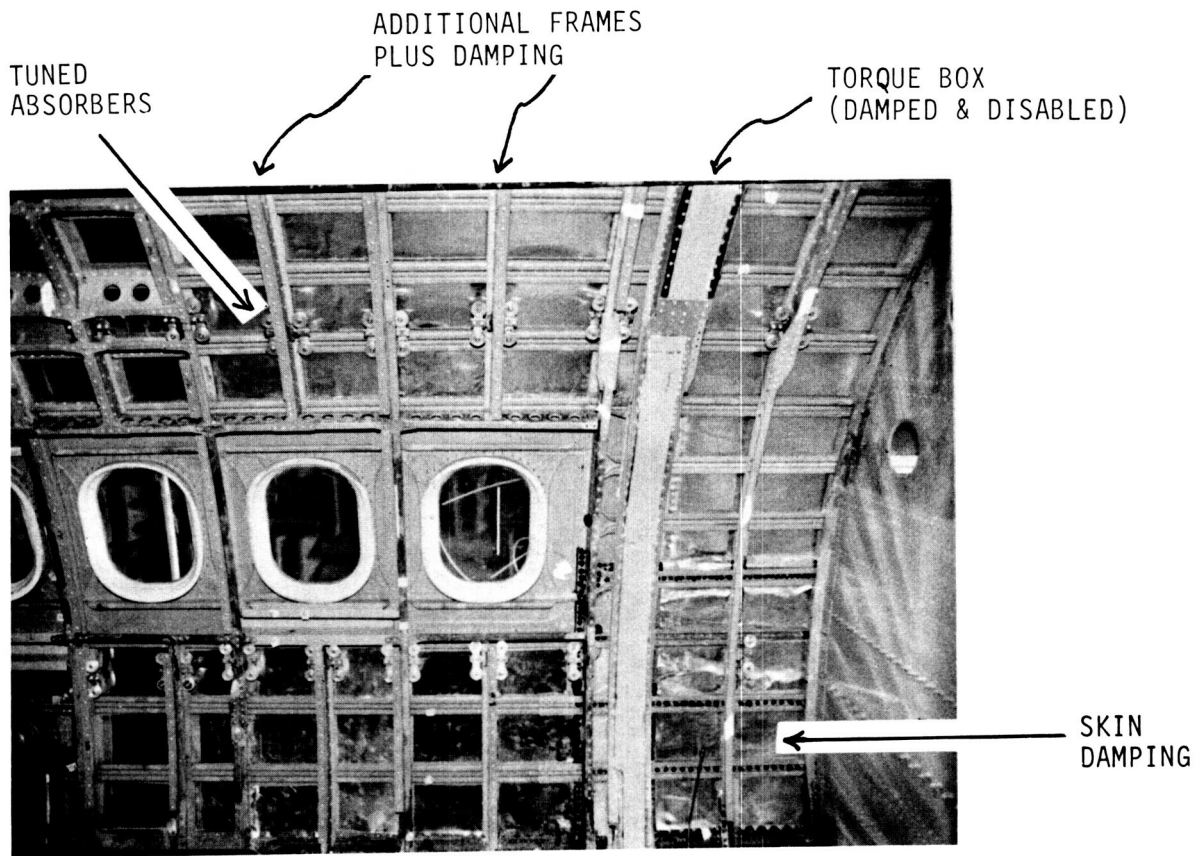


Figure 6-6 Selected Treatments Installed on the Fuselage Sidewall

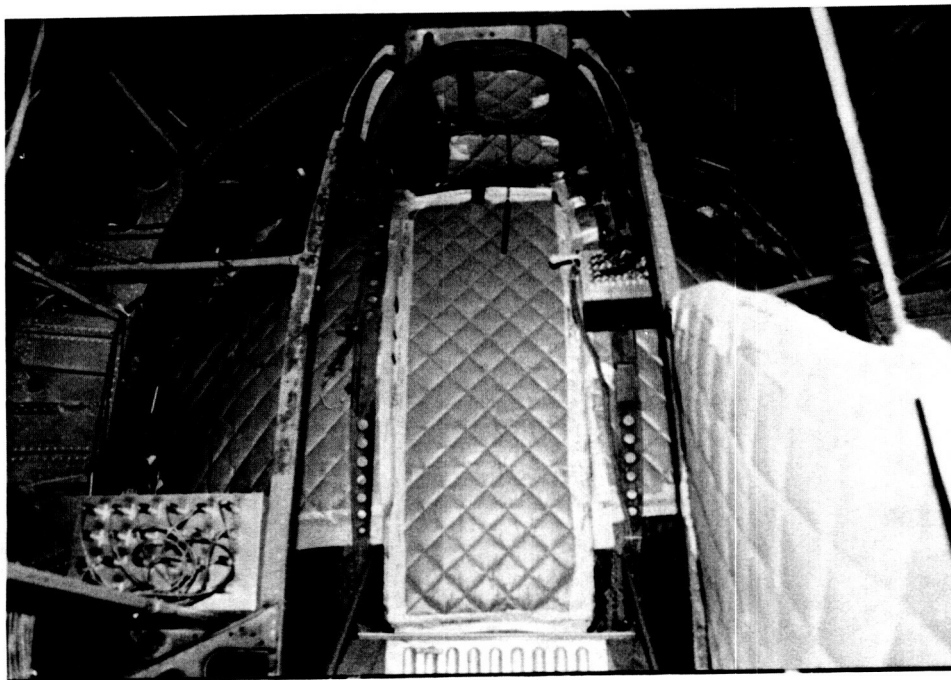


Figure 6-7 Absorption Blanket Installed in Aft Section



Figure 6-8 The Fully Furnished Cabin

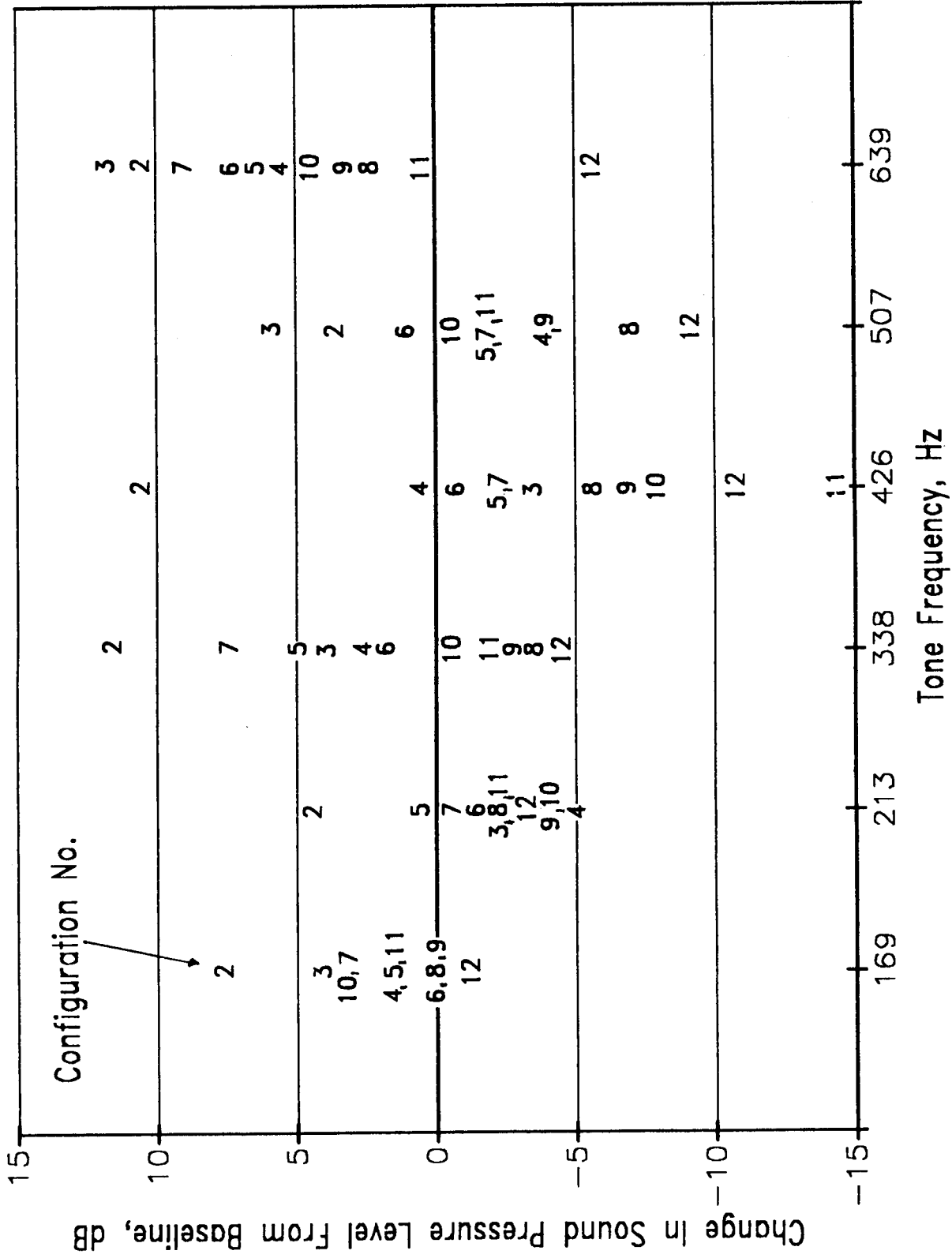


Figure 6-9 Measured Sound Pressure Levels for Tonal Acoustic Excitation, Structural Modifications Phase, Station 772

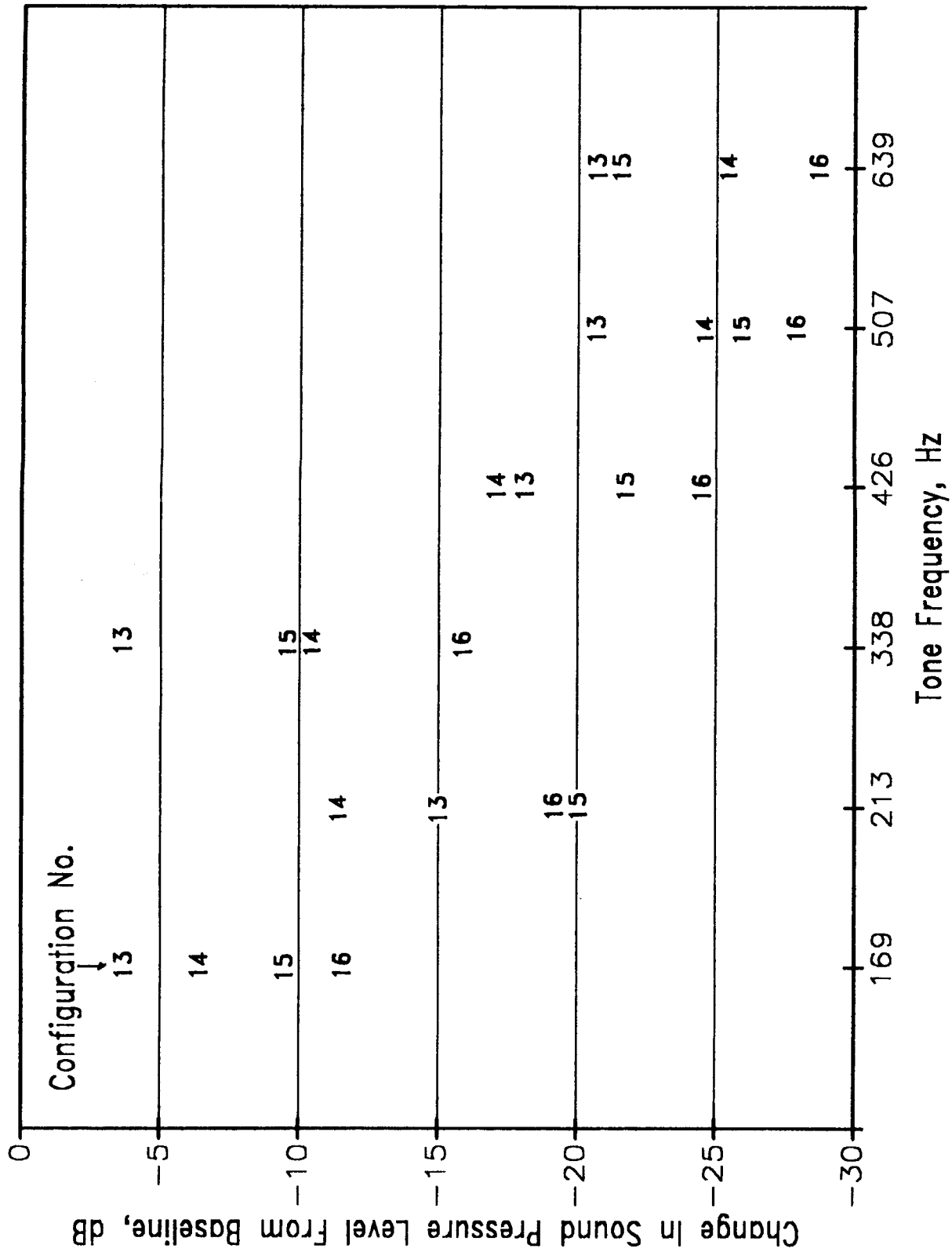


Figure 6-10 Measured Sound Pressure Levels for Tonal Acoustic Excitation, Furnished Fuselage Phase, Station 772

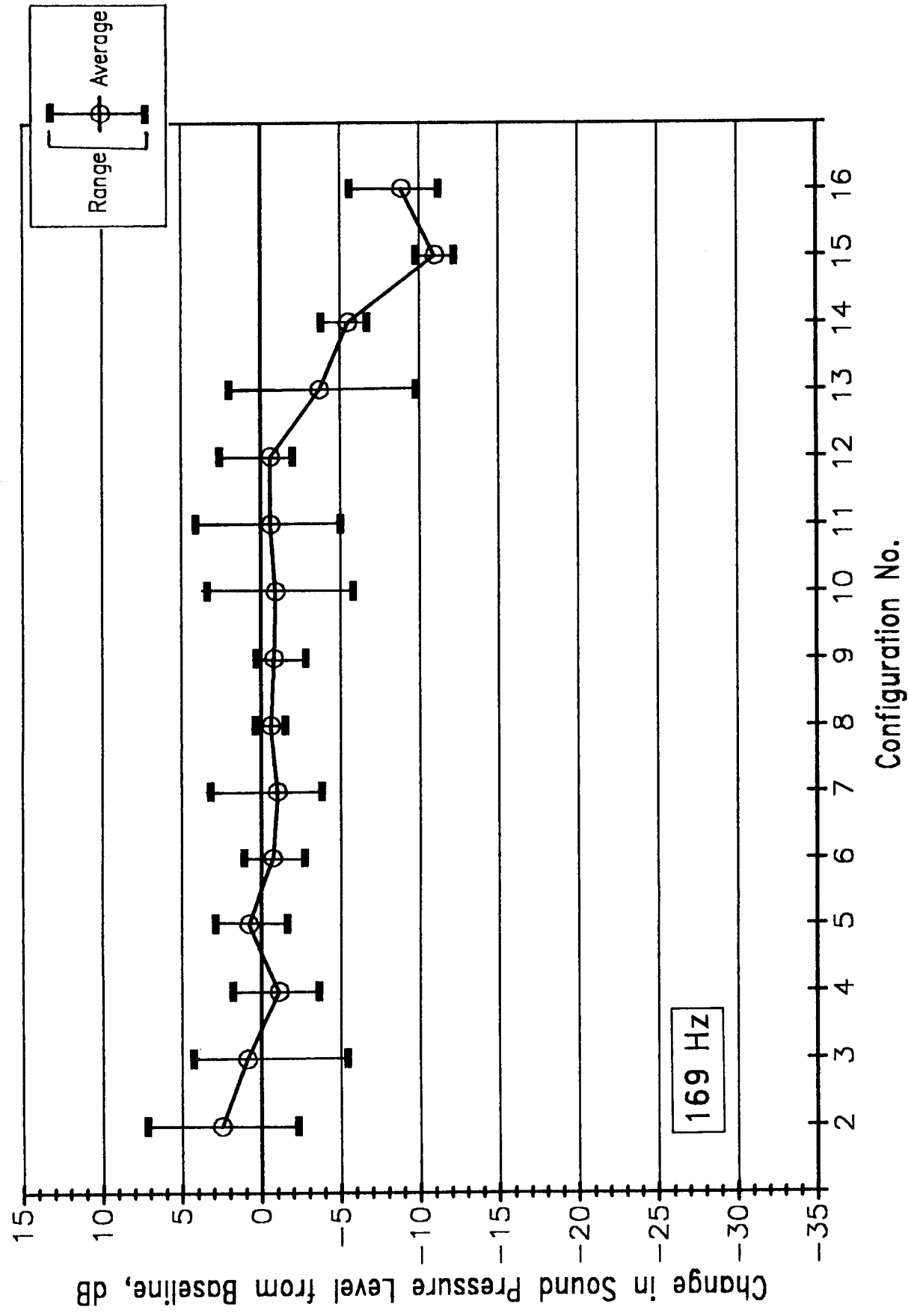


Figure 6-11 Comparison of Average Sound Pressure Levels for All Treatment Configurations, Tonal Acoustic Excitation, 169 Hz

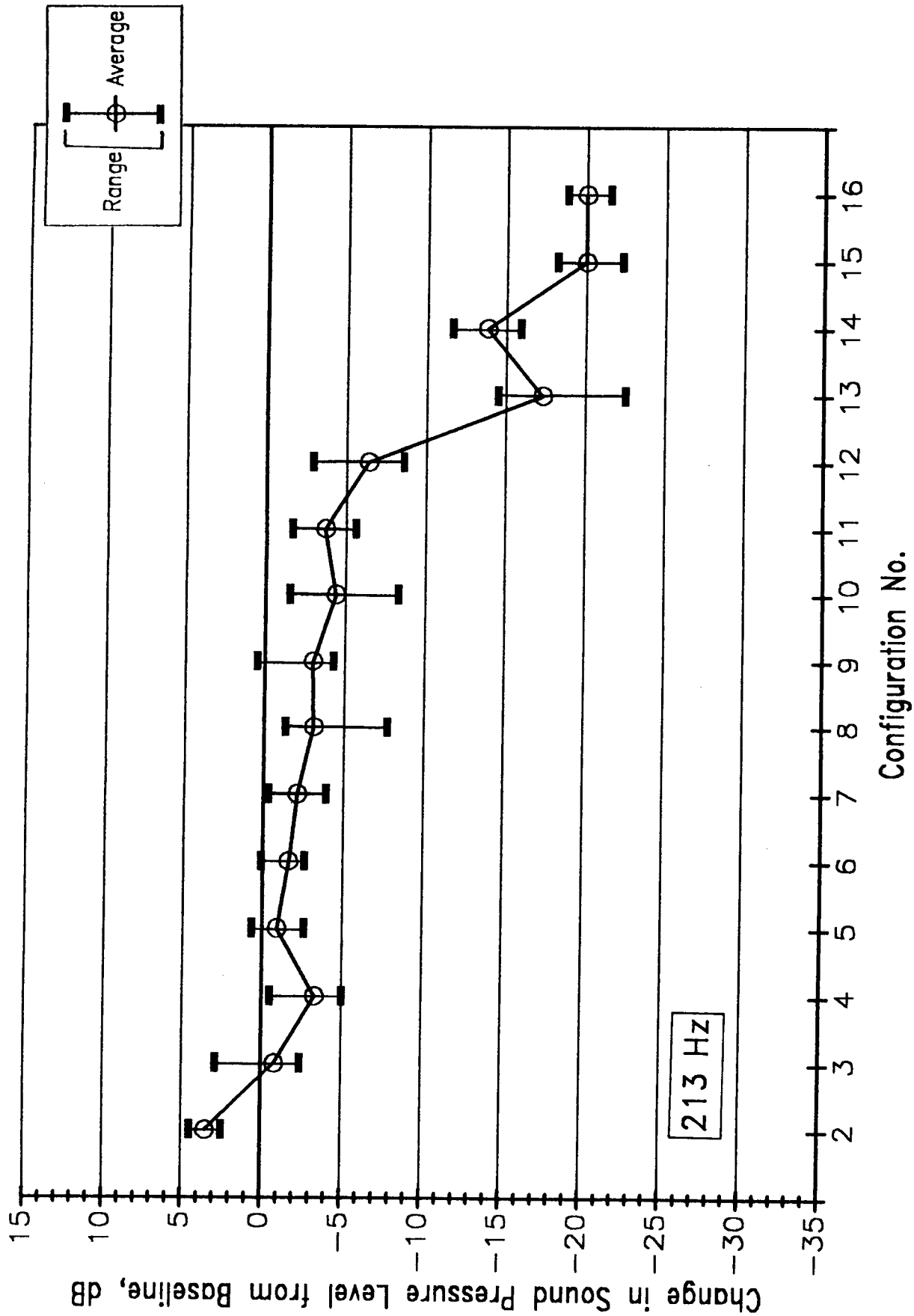


Figure 6-12 Comparison of Average Sound Pressure Levels for All Treatment Configurations, Tonal Acoustic Excitation, 213 Hz

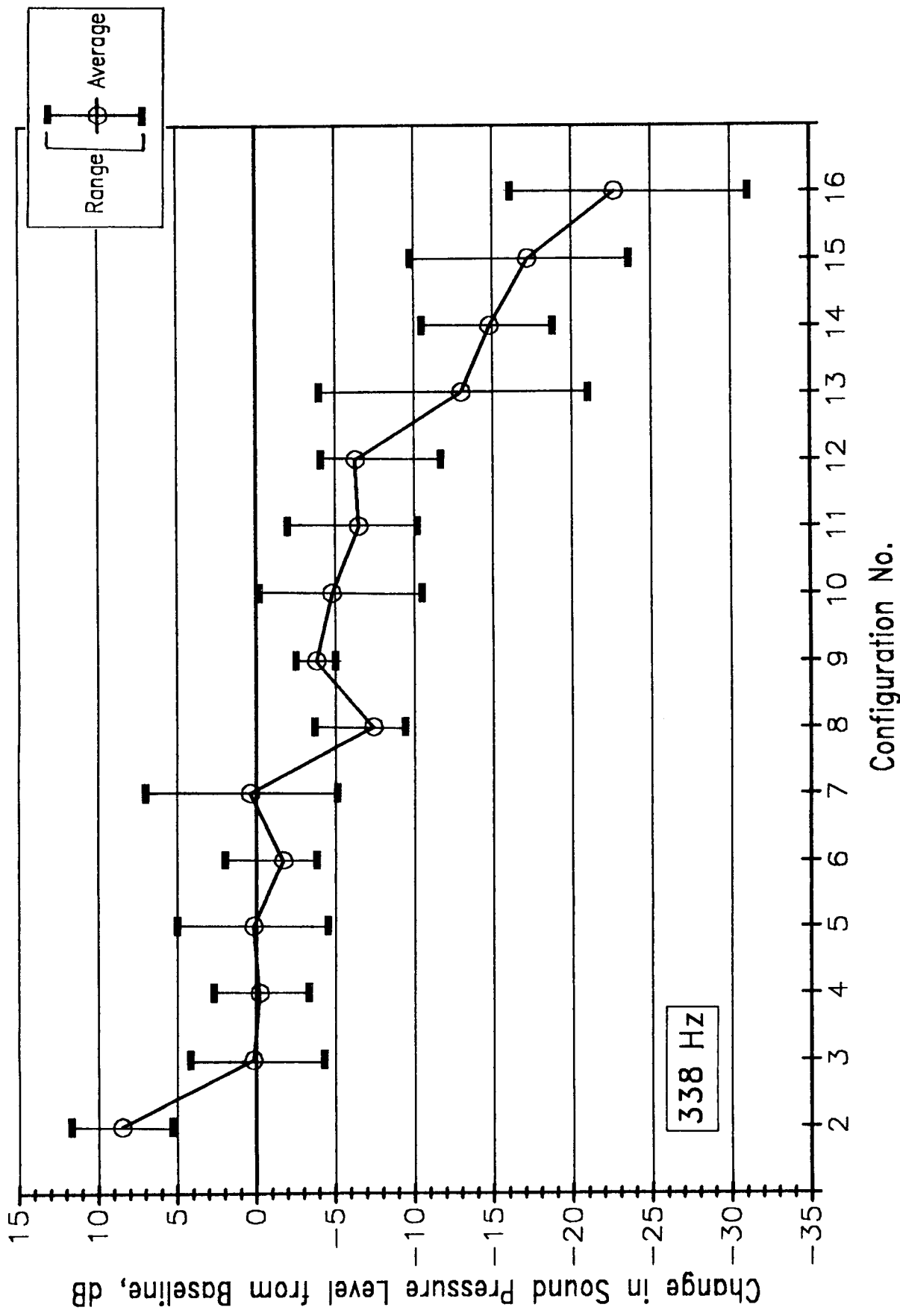


Figure 6-13 Comparison of Average Sound Pressure Levels for All Treatment Configurations, Tonal Acoustic Excitation, 338 Hz

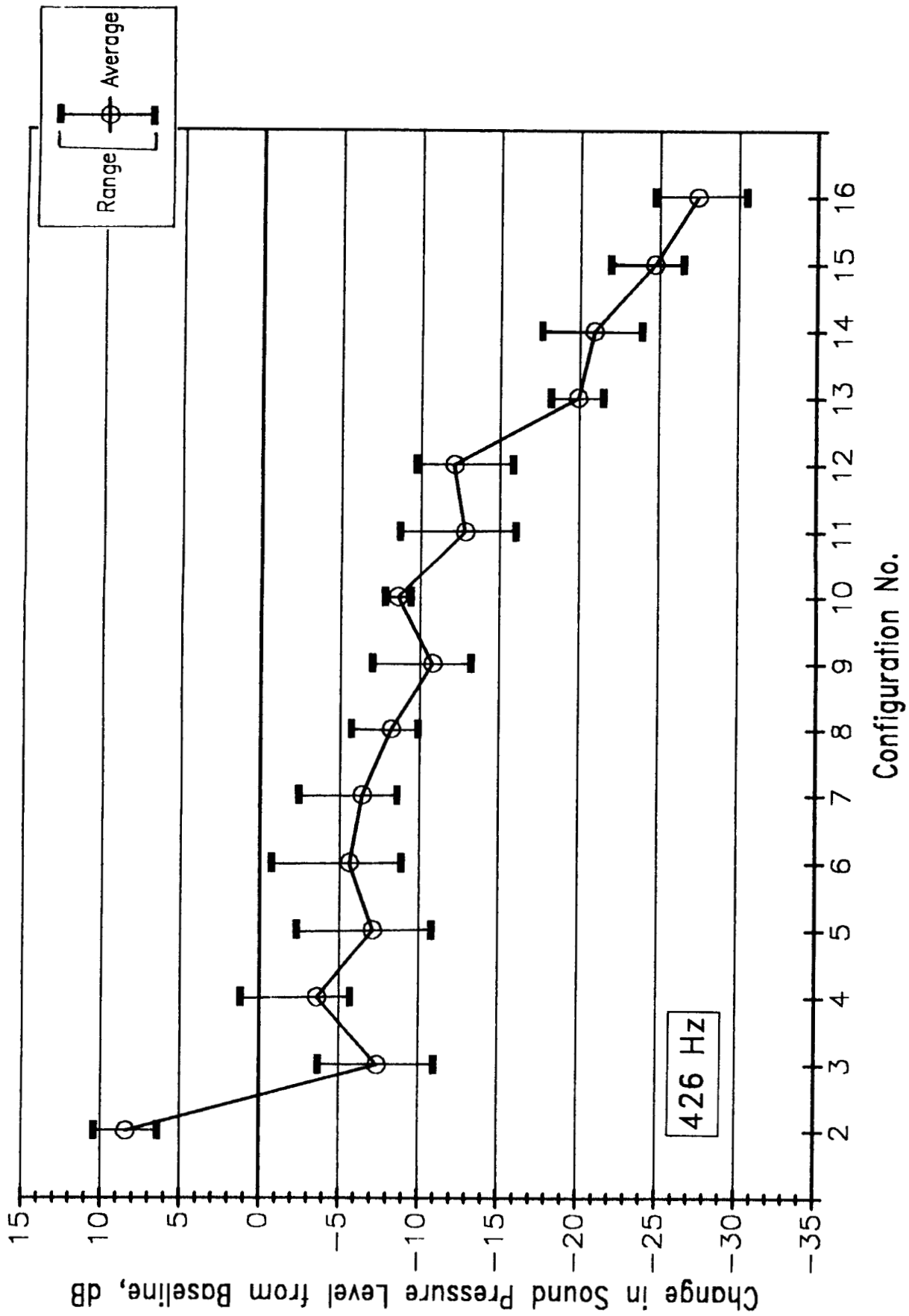


Figure 6-14 Comparison of Average Sound Pressure Levels for All Treatment Configurations, Tonal Acoustic Excitation, 426 Hz

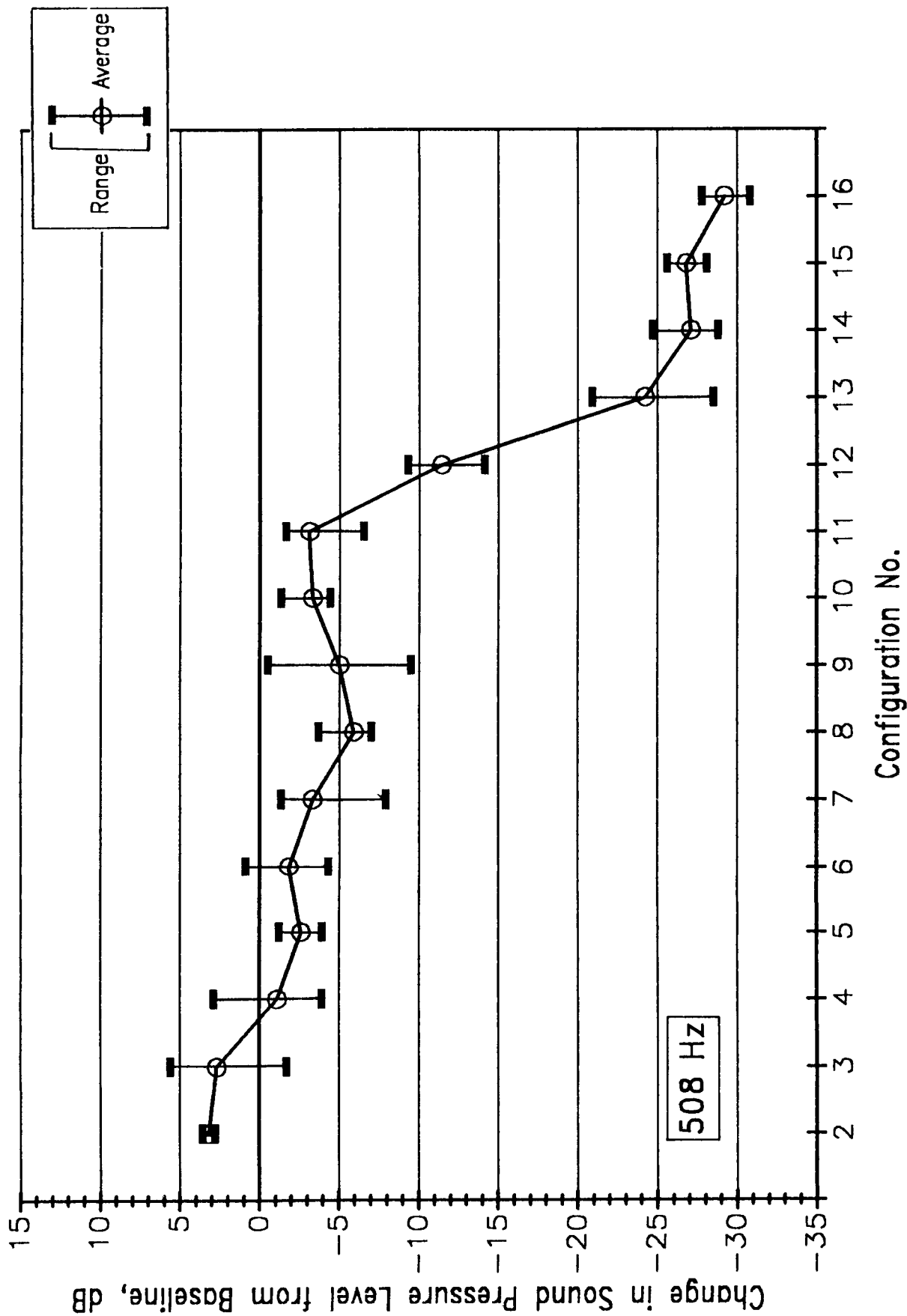


Figure 6-15 Comparison of Average Sound Pressure Levels for All Treatment Configurations, Tonal Acoustic Excitation, 507 Hz

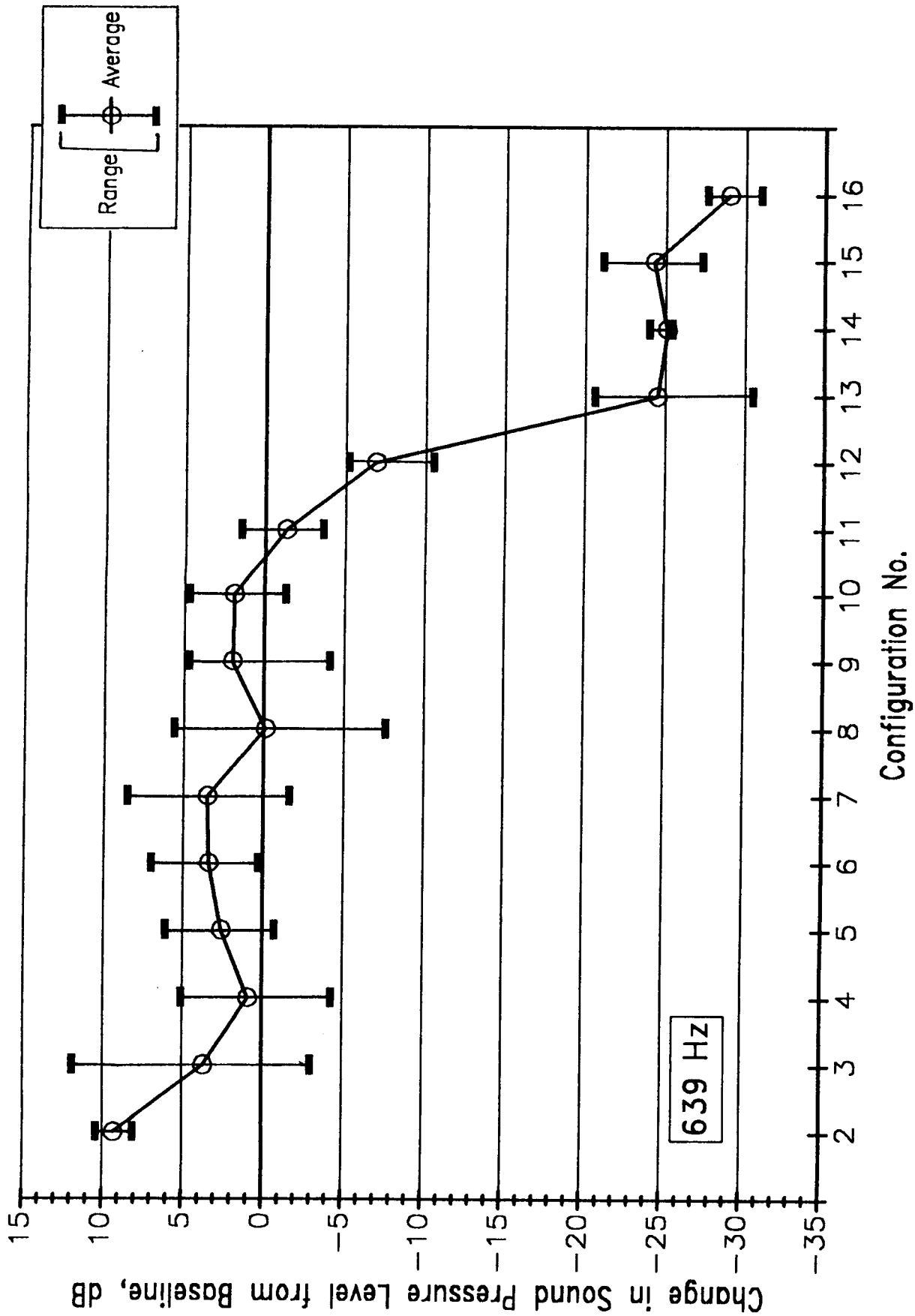


Figure 6-16 Comparison of Average Sound Pressure Levels for All Treatment Configurations, Tonal Acoustic Excitation, 639 Hz

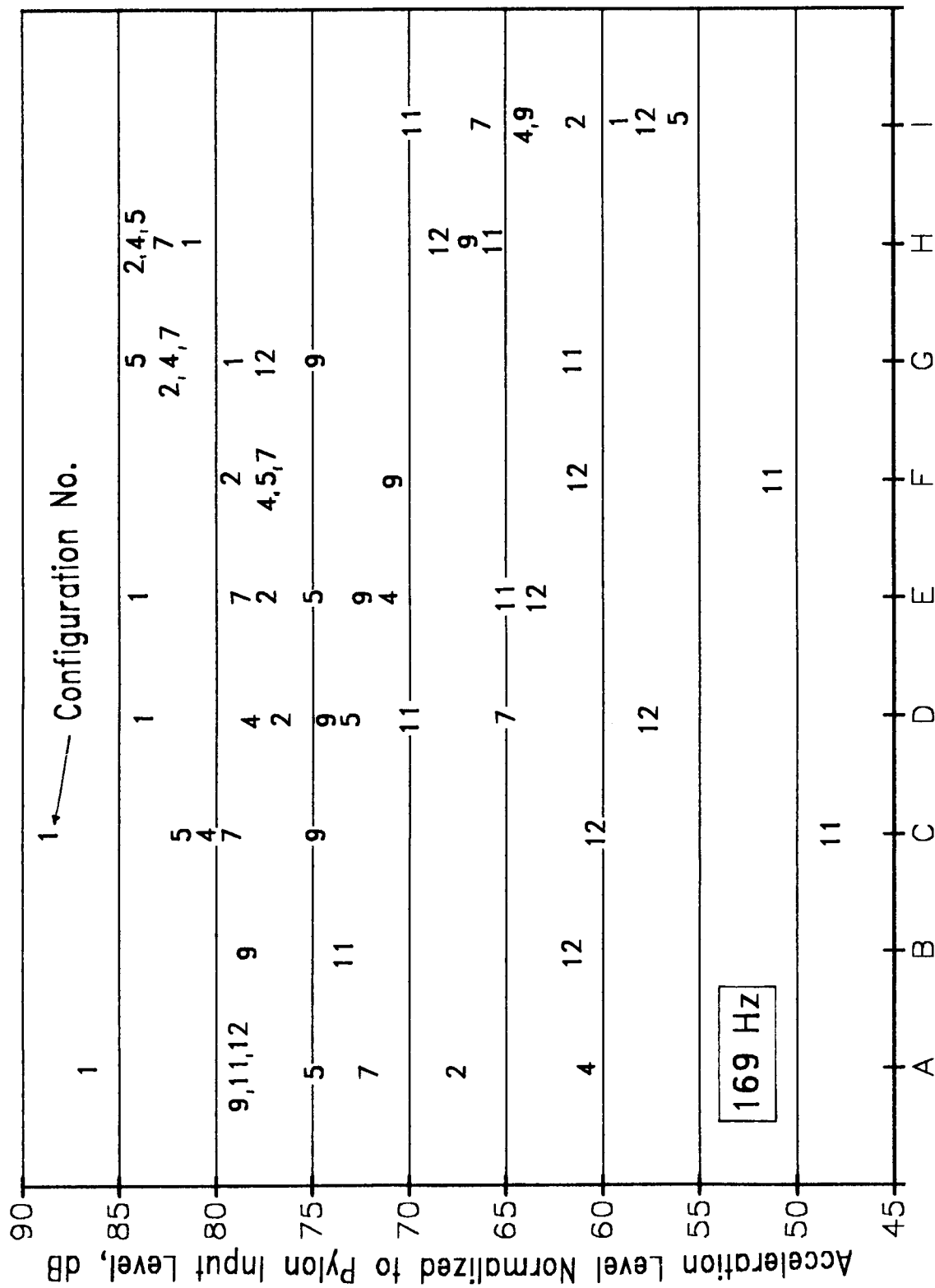
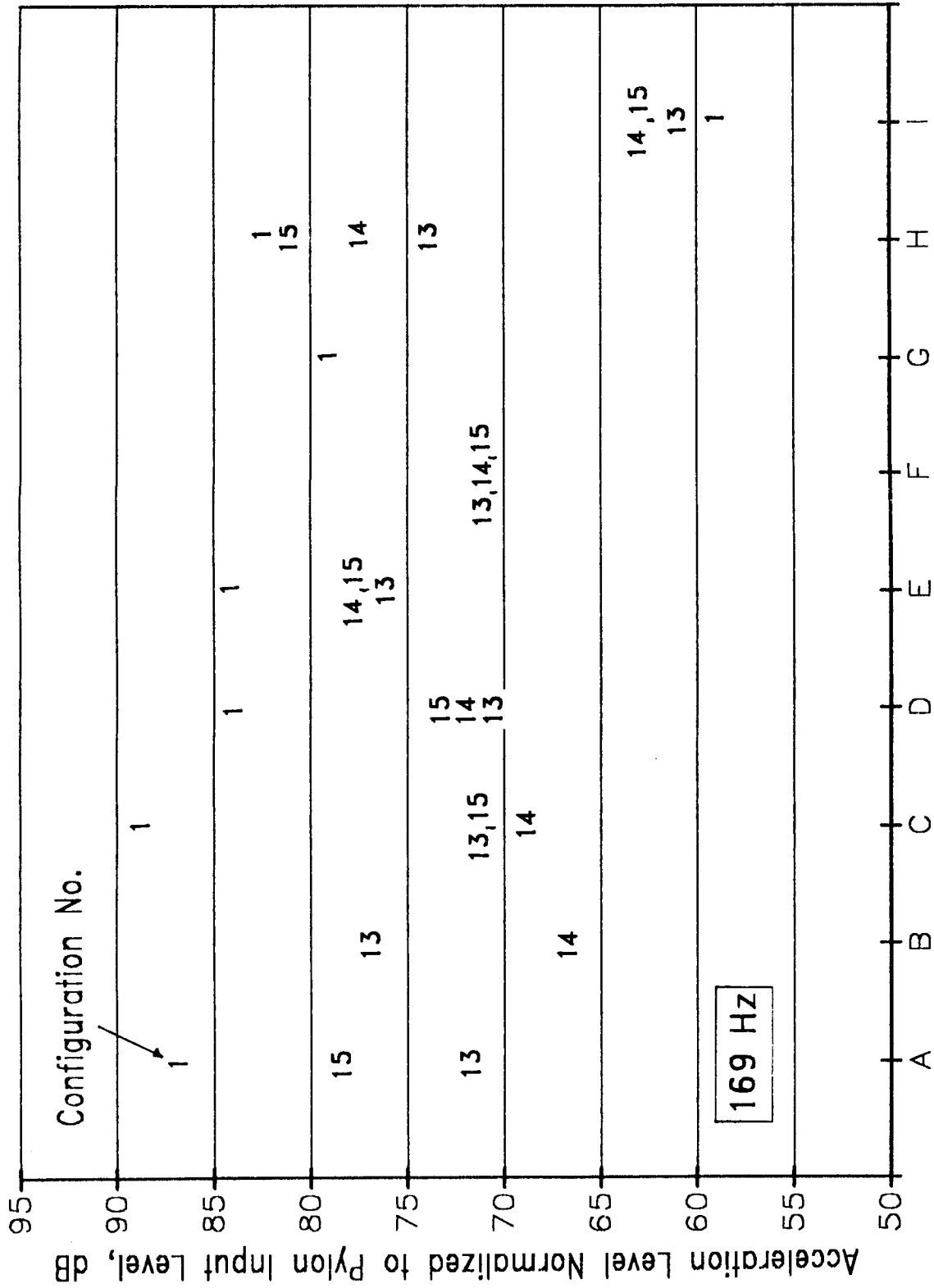


Figure 6-17 Measured Acceleration Levels for Tonal Vibration Excitation, Baseline and Structural Modifications Phases, 169 Hz



Accelerometer Location at Station 718

Figure 6-18 Measured Acceleration Levels for Tonal Vibration Excitation, Baseline and Furnished Fuselage Phases, 169 Hz

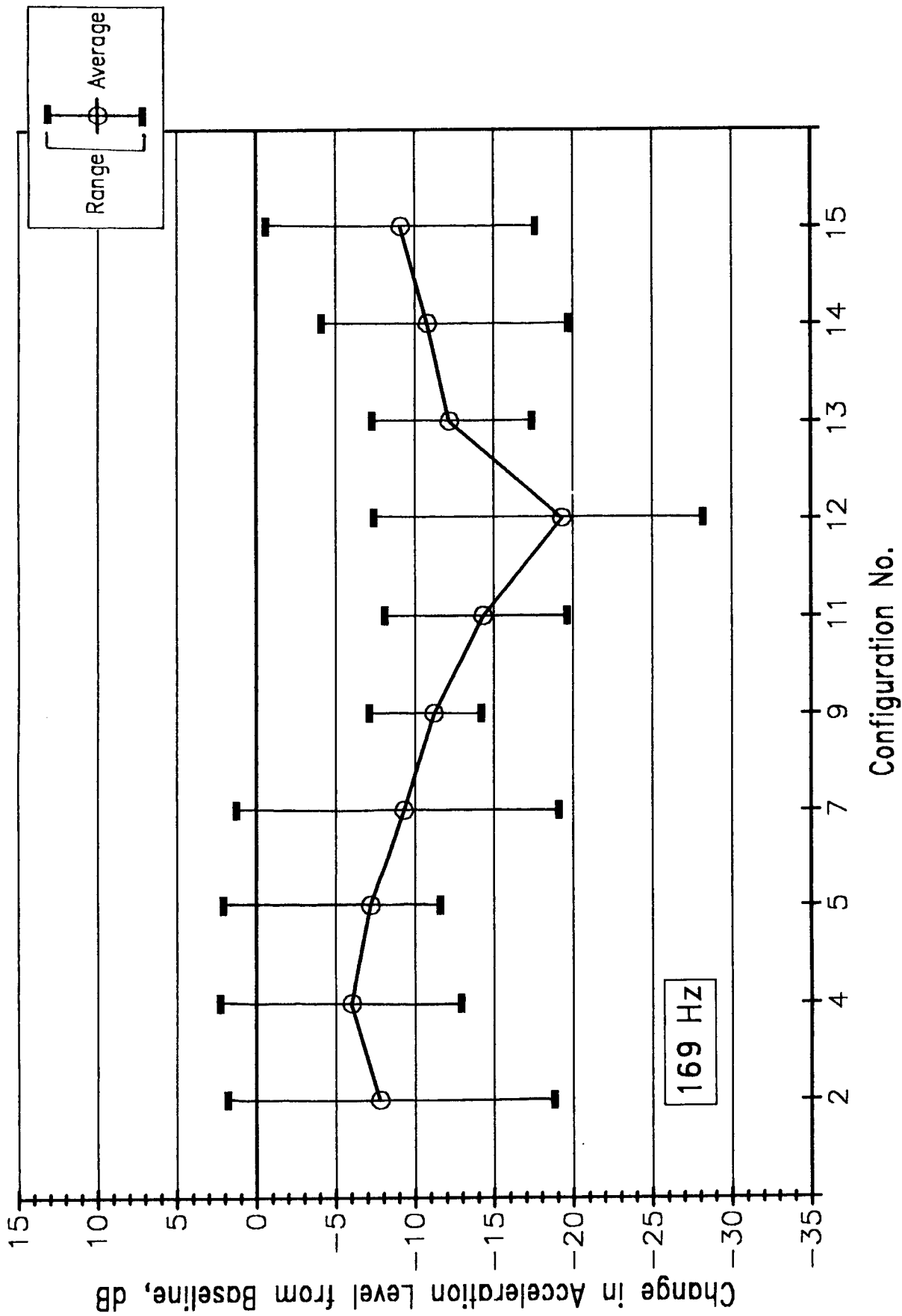


Figure 6-19 Comparison of Average Measured Acceleration Levels for All Treatment Configurations, Tonal Vibration Excitation, Station 718, 169 Hz

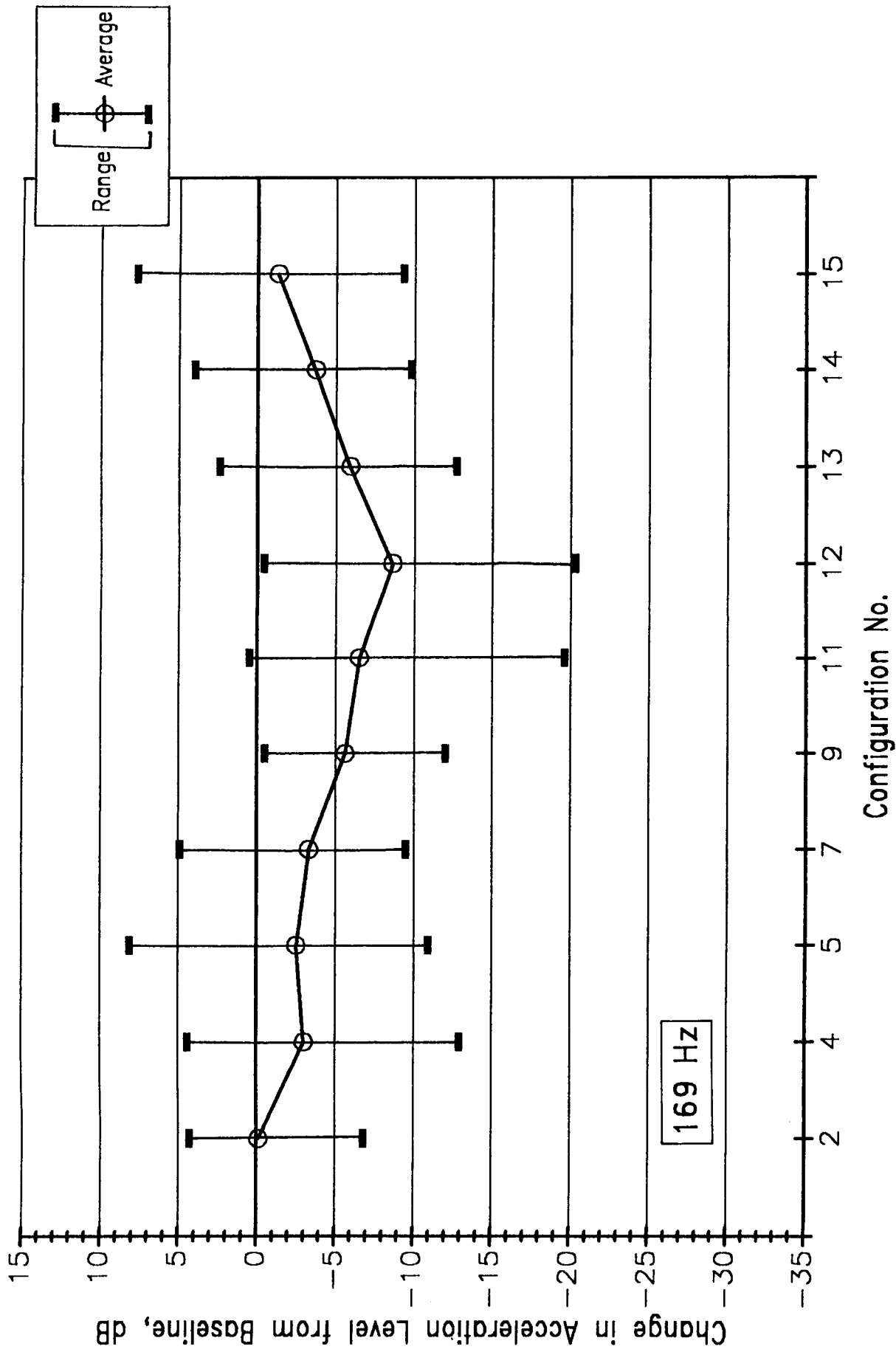


Figure 6-20 Comparison of Average Measured Acceleration Levels for All Treatment Configurations, Tonal Vibration Excitation, Longeron 10, 169 Hz

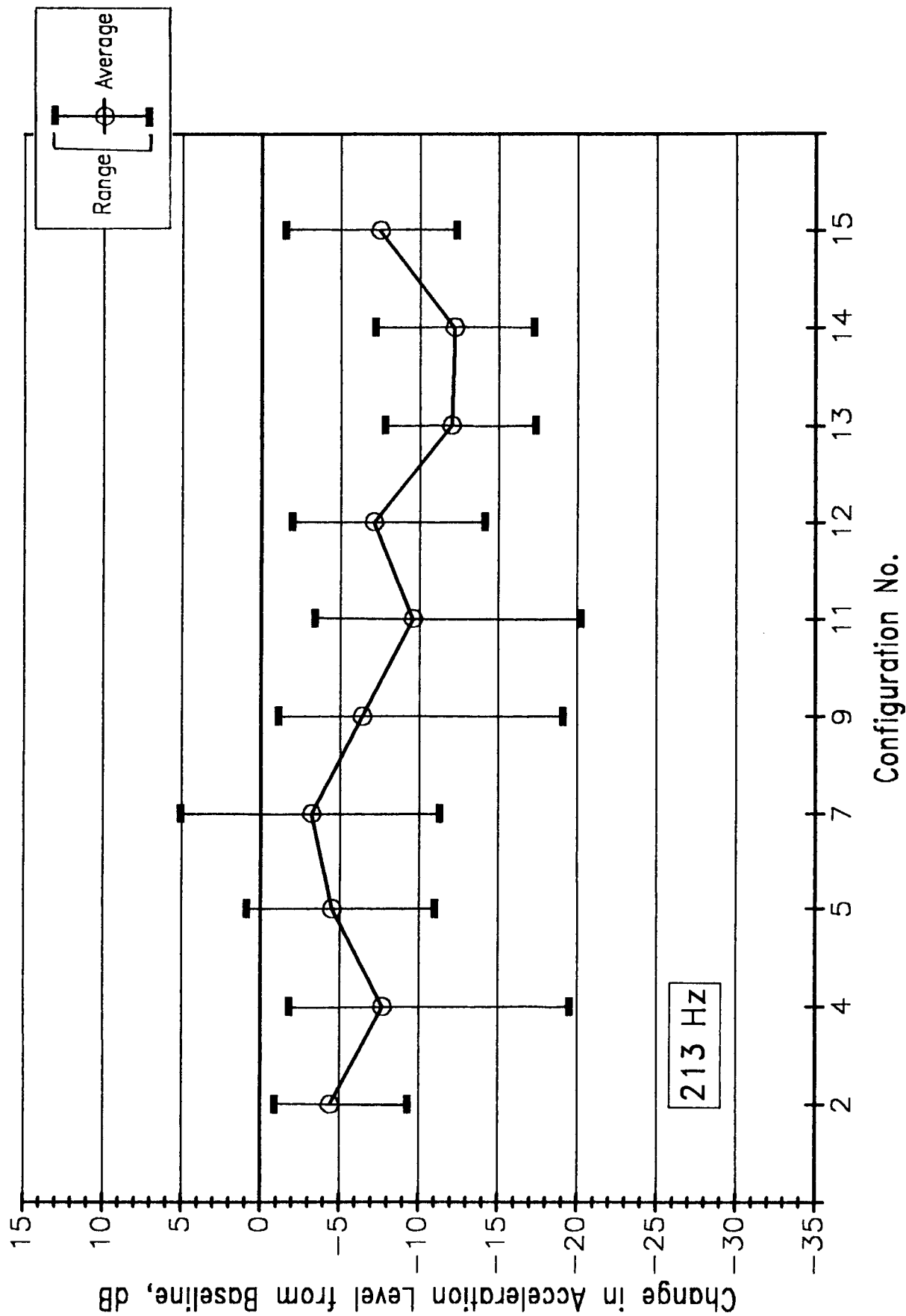


Figure 6-21 Comparison of Average Measured Acceleration Levels for All Treatment Configurations, Tonal Vibration Excitation, Station 718, 213 Hz

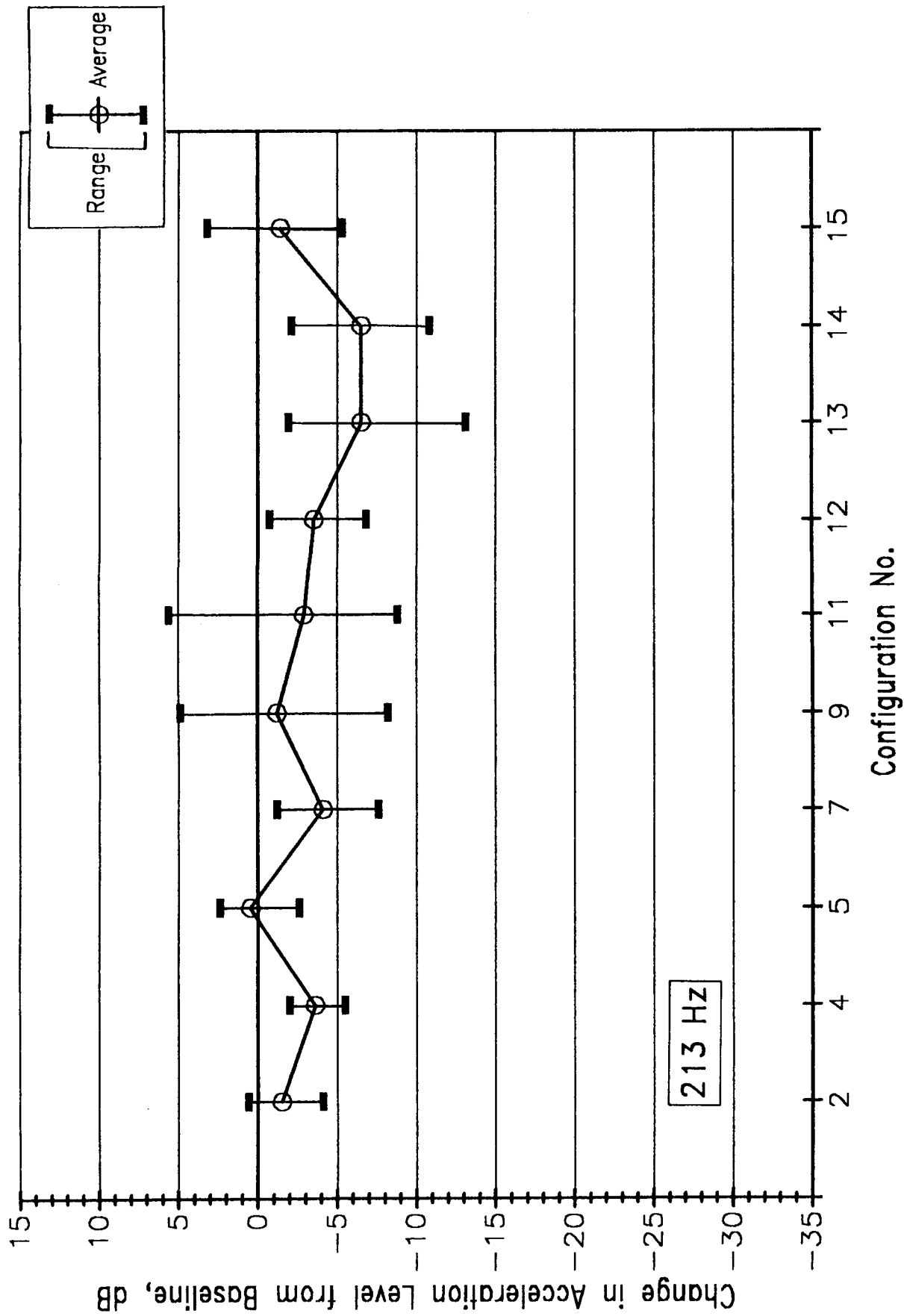


Figure 6-22 Comparison of Average Measured Acceleration Levels for All Treatment Configurations, Tonal Vibration Excitation, Longeron 10, 213 Hz

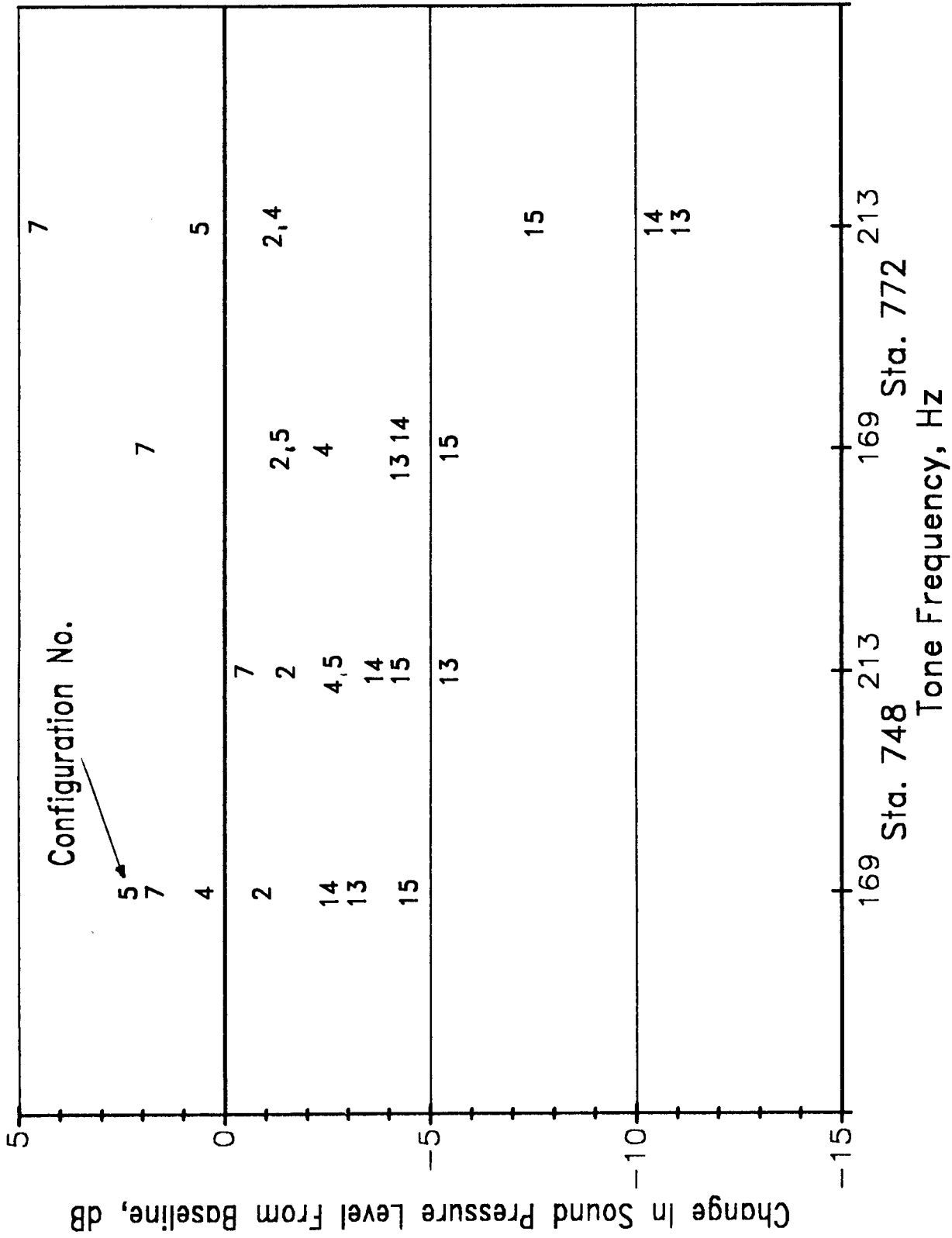


Figure 6-23 Measured Sound Pressure Levels for Tonal Vibration Excitation, Structural Modifications and Furnished Fuselage Phases, Stations 748, 772

## 7 Transmission Path Tests

Preliminary analysis of the noise data collected during the UHB Demonstrator flight test program indicated that the major transmission paths to the fuselage interior were slightly different than originally expected. Cabin noise levels consist of a tonal component from the UHB engine and a broadband component from the turbulent boundary layer. As shown in Figure 7-1, these components are transmitted into the cabin along the following paths:

- An airborne path for the UHB tones (the BPF's and harmonics) through the fuselage into the aft unpressurized section, and then through the pressure bulkhead into the cabin.
- An airborne path for the turbulent boundary layer through the cabin sidewall.
- A structureborne path for the UHB tones (the BPF's and harmonics) through the pylon and fuselage structure and then radiating into the cabin.

A series of three tests was then conducted in FARF to examine the effectiveness of selected treatments along these three paths. These tests are described in the sections below.

### 7.1 Pressure Bulkhead Path

The purpose of these tests was to compare the effectiveness of various treatments applied to the pressure bulkhead in reducing transmission from the aft unpressurized section into the cabin area. Six configurations were studied, starting with the last two configurations used in the forced response tests. For all configurations the cabin is fully furnished, including lavatories; changes are made to the pressure bulkhead only. The treatment configurations were:

**Configuration 15.** The double wall bulkhead treatment is not installed. The pressure bulkhead is in its standard, untreated condition.

**Configuration 16.** The double wall bulkhead treatment is installed. This configuration represents the fully treated cabin studied in the forced response tests.

**Configuration 17.** The double wall bulkhead treatment is removed, and the absorption blanket used in Configuration 10 is applied to the unpressurized side of the pressure bulkhead.

**Configuration 18.** The absorption blanket is removed, and damping material (EAR type SD-40AL/3202-50PSA) is applied to the pressurized side of the pressure bulkhead (except for the door area). The double wall bulkhead treatment is not installed.

**Configuration 19.** The double wall bulkhead treatment is partially installed, covering the two side areas of the pressure bulkhead but not the bulkhead door.

**Configuration 20.** The full double wall bulkhead treatment is installed, and the absorption blanket is applied to the unpressurized side of the pressure bulkhead.

### 7.1.1 Measurement and Analysis Procedures

As shown in Figure 7-2, the tests were conducted using a loudspeaker located in the aft unpressurized section, approximately 3 ft behind the pressure bulkhead and in line with the center of the bulkhead door. A microphone was positioned just behind the door at this center point, to measure the impinging acoustic energy. In the cabin, microphones were positioned at all five seats in the last seat row, and at a single position in the aisle between the lavatories, about 1 ft in front of the bulkhead door and in line with the center of the door.

For each configuration, a broadband signal was played through the loudspeaker and noise levels were measured at each microphone. Two sets of data were collected, one with seat microphones at seat back height (40 in above the floor), and one with seat microphones 8 in above seat back height.

The measured data were processed in one-third octave bands from 100 to 1000 Hz. Two different measures of noise reduction were computed. The noise reduction "through the door" is the difference between the levels measured behind the door and the levels measured in the aisle in front of the door. The noise reduction "into the cabin" is the difference between the levels measured behind the door and the average of the levels measured among all five seat positions. Since the levels measured at the two heights at each seat were usually quite close, the "into the cabin" noise reduction is based on an average of the data collected at both heights.

### 7.1.2 Measurement Results

Figures 7-3 and 7-4 show the computed "through the door" and "into the cabin" noise reductions, respectively, for all configurations. The effectiveness of the various treatments relative to the untreated bulkhead (configuration 15) can be seen primarily in the frequency range above 200 Hz. At 200 Hz there is a dip in the "through the door" noise reduction spectra, likely due to a structural resonance of the bulkhead. Below

200 Hz, both sets of noise reduction spectra show inconsistent trends. This may be due to the modal characteristics of the bulkhead, as well as the cavity mode characteristics in the aft unpressurized section. It may also be indicative of poor performance of the various treatments for the lower frequencies.

Above 200 Hz, the double wall bulkhead (configuration 16) and the double wall with absorption blanket (configuration 20) are both seen to provide increases in noise reduction relative to the untreated bulkhead, with the absorption blanket improving on the effectiveness of the double wall treatment. The absorption blanket alone (configuration 17) also yields some benefit relative to the untreated bulkhead, but primarily in terms of reductions "through the door". For these three configurations, there is a general trend of increasing noise reduction with higher frequency, as expected.

The partial bulkhead treatment (configuration 19) is seen to be more effective than the untreated bulkhead for frequencies of 400 Hz and above, but significantly less effective than the full double wall bulkhead (configuration 16). The damping treatment (configuration 18) is seen to yield minor improvements over the untreated bulkhead. Both of these treatments are applied to the side areas of the pressure bulkhead; their effectiveness is thus limited by transmission through the (untreated) bulkhead door.

## 7.2 Cabin Sidewall Path

These tests were designed to further evaluate the effectiveness of the damping treatments applied to the fuselage skin and interior trim panels in reducing transmission through the cabin sidewall. Four different treatment configurations were studied:

**Configuration 16.** The cabin sidewall includes damping applied to the fuselage skin (Soundcoat type 10MS/10LT12 and EAR type SD-40AL/3202-50PSA, see description of configurations 11 and 12 for details), and to the trim panels (EAR type SD-40ALPSA, see description of configuration 15 for details). This configuration represents the fully treated sidewall studied in the forced response tests.

**Configuration 21.** The damping on the trim panels on the left sidewall is removed; the skin damping remains.

**Configuration 22.** The skin damping on the left sidewall between the bag racks and the floor is removed. The damping on the trim panels is reinstalled.

**Configuration 23.** The trim panel damping is again removed. The left cabin sidewall is now in the standard sidewall condition.

### 7.2.1 Measurement and Analysis Procedures

For each test, a loudspeaker was located approximately 8 ft away from the left side of the fuselage at station 690, centered at exterior microphone row B (see Figure 5-1). Exterior fuselage microphones and interior seat microphones were used to measure the noise levels resulting from the broadband signal played through the loudspeaker. Figure 7-5 shows the locations of the various microphones and the loudspeaker.

All measured data were processed in one-third octave bands from 100 to 1000 Hz. Within each band, exterior levels were the highest at microphone E-690-C and were lower by 2 to 5 dB at the other exterior measurement locations, resulting in a relatively uniform distribution of levels on the fuselage surface outside the cabin.

The levels at E-690-C were used as a reference for the noise reduction calculations; that is, for each configuration the levels at selected interior microphones were subtracted from the E-690-C levels. The average of the levels at all interior microphones was also subtracted from the E-690-C levels to obtain the average sidewall noise reduction.

### 7.2.2 Measurement Results

Based on the treatments applied in the various configurations, configuration 16 with both skin and trim panel damping would be expected to have the highest noise reduction values, while configuration 23 with neither damping treatment would be expected to have the lowest noise reduction values. In the higher portion of the frequency range, transmission loss mass law would indicate that configuration 16 should provide about 5 dB higher noise reduction than configuration 23; configurations 21 and 22 should provide about 3 and 2 dB higher noise reductions than configuration 23, respectively.

The actual measured one-third octave band noise reductions for all four configurations are shown in Figures 7-6 through 7-8. The noise reduction levels shown in Figure 7-6 are based on the average levels among all the interior microphones, while the noise reduction levels shown in Figures 7-7 and 7-8 are based on microphone I-672-B and I-672-F levels, respectively.

These three figures show that at 500 Hz and below, there is little consistent difference among the various configurations. Above 500 Hz, the expected increases in noise reduction from configuration 23 to the other configurations can be seen most clearly in Figure 7-7, for a location away from the treated sidewall through which the sound is transmitted. In Figure 7-8, for a location immediately adjacent to this sidewall, the trend is less pronounced, and it is least clear for the averaged data (Figure 7-6).

The effectiveness of the damping treatments may be compromised by transmission through the cabin windows. This performance degradation would likely occur close to

the windows; this might explain the difference in effectiveness demonstrated between Figures 7-7 and 7-8. There may also be some flanking paths into the cabin through other portions of the fuselage surface, which would have the effect of minimizing differences in levels among the configurations.

### **7.3 Fuselage Structural Path**

In section 7.2, tests of the effectiveness of skin and trim panel damping treatments in reducing airborne transmission through the cabin sidewall were described. In this section, tests of the effectiveness of the same four configurations (16, 21, 22 and 23) in reducing the propagation of vibration energy transmitted through the fuselage structure are discussed.

#### **7.3.1 Measurement and Analysis Procedures**

For these tests, a shaker was attached to the forward engine mount on the left pylon (as for the forced response tests). The vibration signal consisted of sine tones at 169 and 185 Hz; the former corresponds to the BPF of an eight-bladed UHB propulsor, and the latter corresponds to the rotational frequency of the low pressure stage of the UHB engine core. This latter tone at 185 Hz was observed in the interior noise spectra measured during UHB Demonstrator flight tests, and can only arise from structural propagation. Shaker input forces of 10, 20 and 40 lbs were used, to provide data on the variation of noise and acceleration levels with vibration load.

Acceleration levels were measured at several locations on longeron 10, and at several locations on frame 718 (see Figure 5-3). Cabin noise levels were measured simultaneously at the microphone positions shown in Figure 7-5.

#### **7.3.2 Measurement Results**

For configuration 23 with the standard, untreated sidewall, Figures 7-9 and 7-10 show the measured acceleration levels on longeron 10 and on frame 718, respectively, for each input force. Data for 170 and 185 Hz are shown in separate graphs on each figure.

These graphs show a relatively constant increment of approximately 6 dB between the 10 lb and 20 lb data, and again between the 20 lb and 40 lb data, for both frequencies and all accelerometers. Since a 6 dB increase in acceleration levels corresponds to a doubling of acceleration, this is consistent with a doubling of input force. The variation in level along longeron 10 as well as on frame 718 for 170 Hz is very similar to the

variation for 185 Hz, except for an abrupt dip in level for 185 Hz at frame 718 location D. These various trends also occur in the data for the other three configurations, but at different levels.

In order to compare the data for all four configurations, the acceleration levels were normalized to a reference input vertical acceleration level on the pylon of 1 g. The results of this normalization are presented in Figures 7-11 and 7-12, for the longeron 10 and frame 718 data, respectively, for the 20 lb input force. These figures show that within a few decibels, configurations 21, 22, and 23 produce the same acceleration levels at a specific location. Configuration 16, on the other hand, produces consistently lower acceleration levels, by 5 to 10 dB. It appears that the two damping treatments are relatively ineffective by themselves, but when used together do provide significant reduction in vibration energy. The acceleration data for 10 and 40 lb input force levels show similar results.

Interior noise levels arising from the shaker input should demonstrate the same trends with configuration. Indeed, Figures 7-13 and 7-14 confirm this expectation. In these figures, the interior noise levels at the vibration input frequencies have been normalized in the same manner as the acceleration levels in the previous figures. This normalization removes the dependence of noise level on input force, so that measured levels for the 10, 20 and 40 lb input forces shown in the figures represent duplicate data points. Figure 7-13 presents interior noise data for both frequencies based on an average of the levels at all of the measurement microphones. Figure 7-14 presents similar data for the microphone location with typically the highest level for each frequency (I-737-F for 170 Hz and I-737-E for 185 Hz). Again, the levels for configurations 21, 22, and 23 exhibit minor differences, but the levels for configuration 16 are nominally 5 to 8 dB lower.

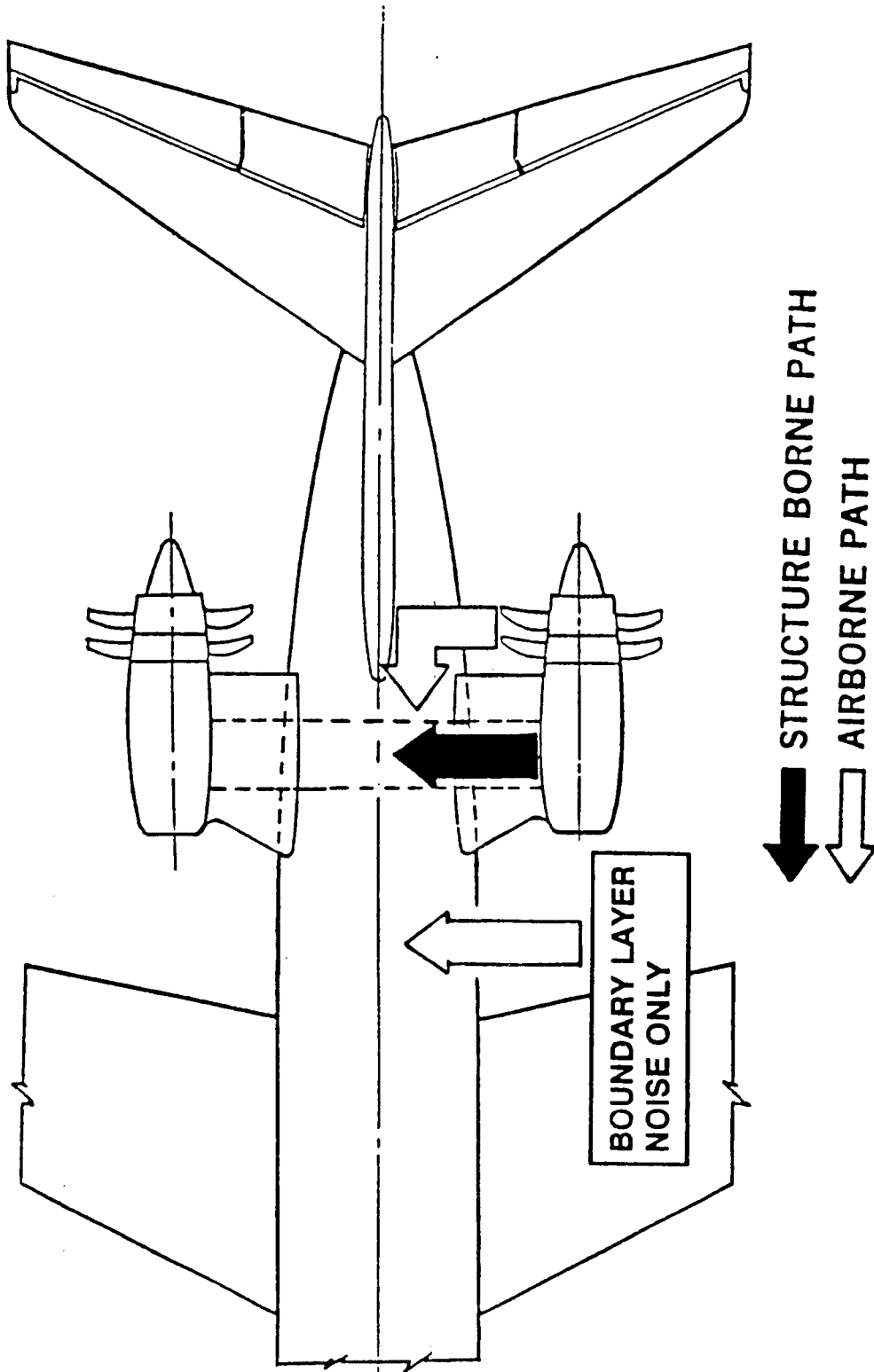
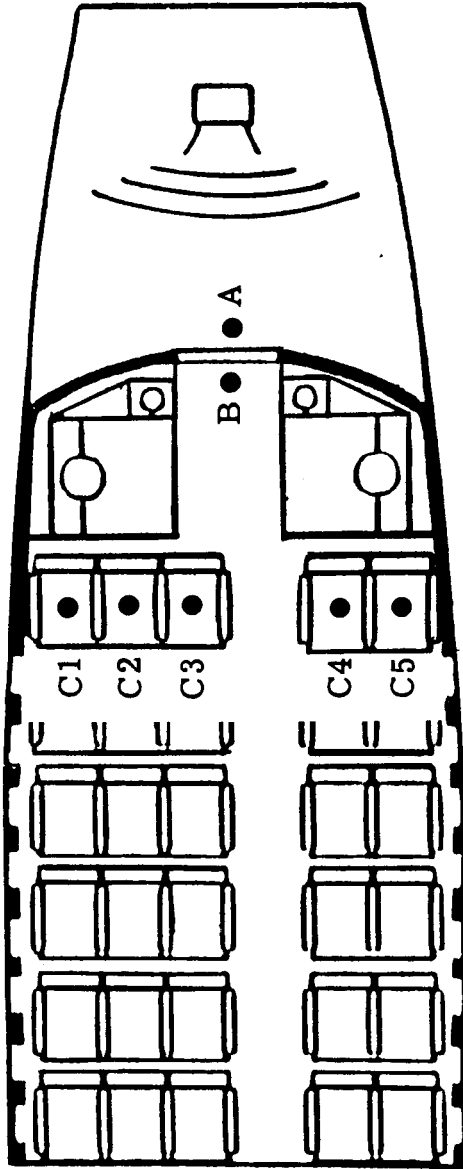


Figure 7-1 UHB Noise Transmission Paths (Based on Demo Data)



"THROUGH THE DOOR" NOISE REDUCTION:  $SPL_A - SPL_B$

"INTO THE CABIN" NOISE REDUCTION:  $SPL_A - \overline{SPL_C}$

Figure 7-2 Pressure Bulkhead Path Test Configuration

Configuration No.
⊗ 15
✱ 16
◇ 17
⊙ 18
⊕ 19
□ 20

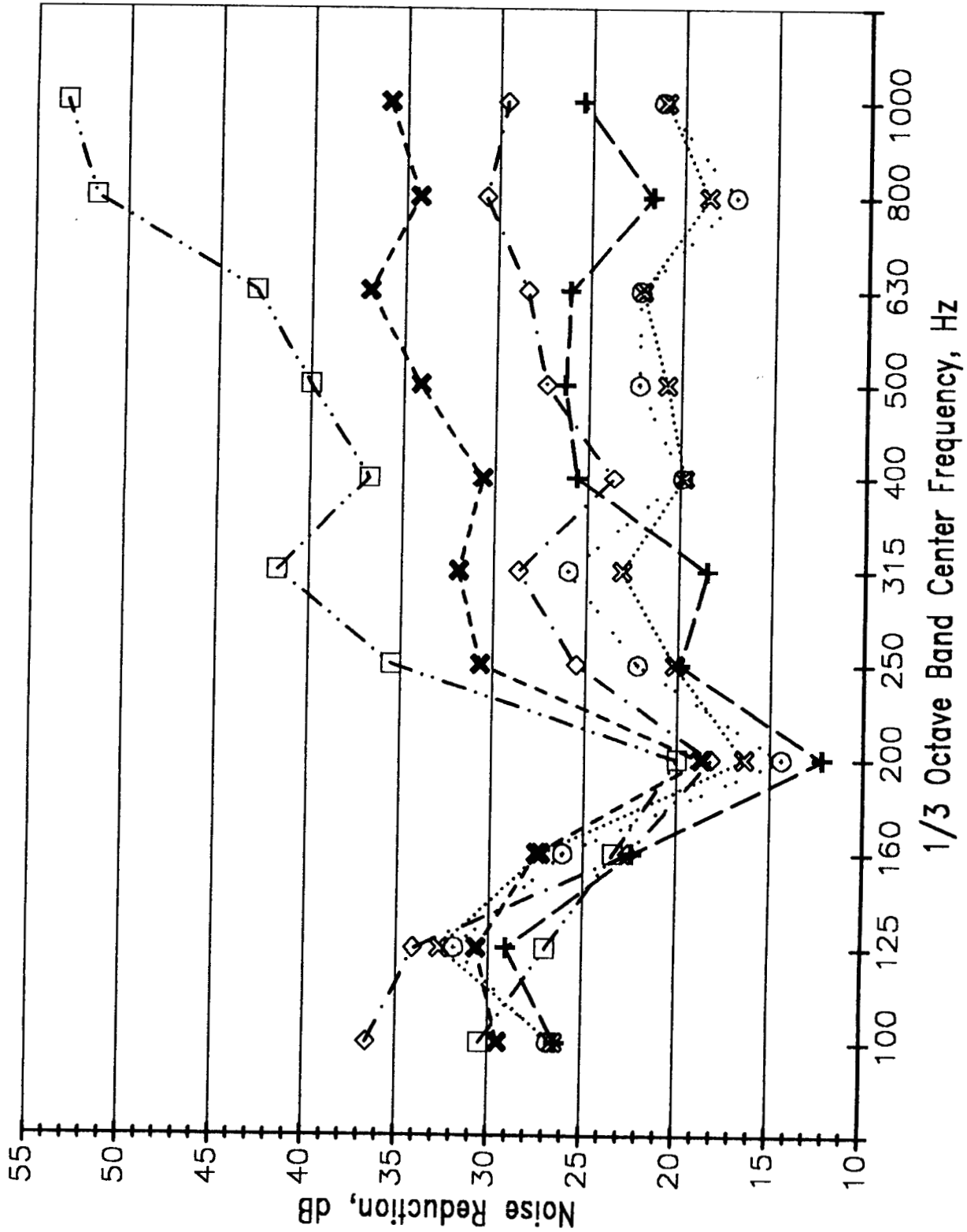


Figure 7-3 Pressure Bulkhead "Through the Door" Noise Reduction

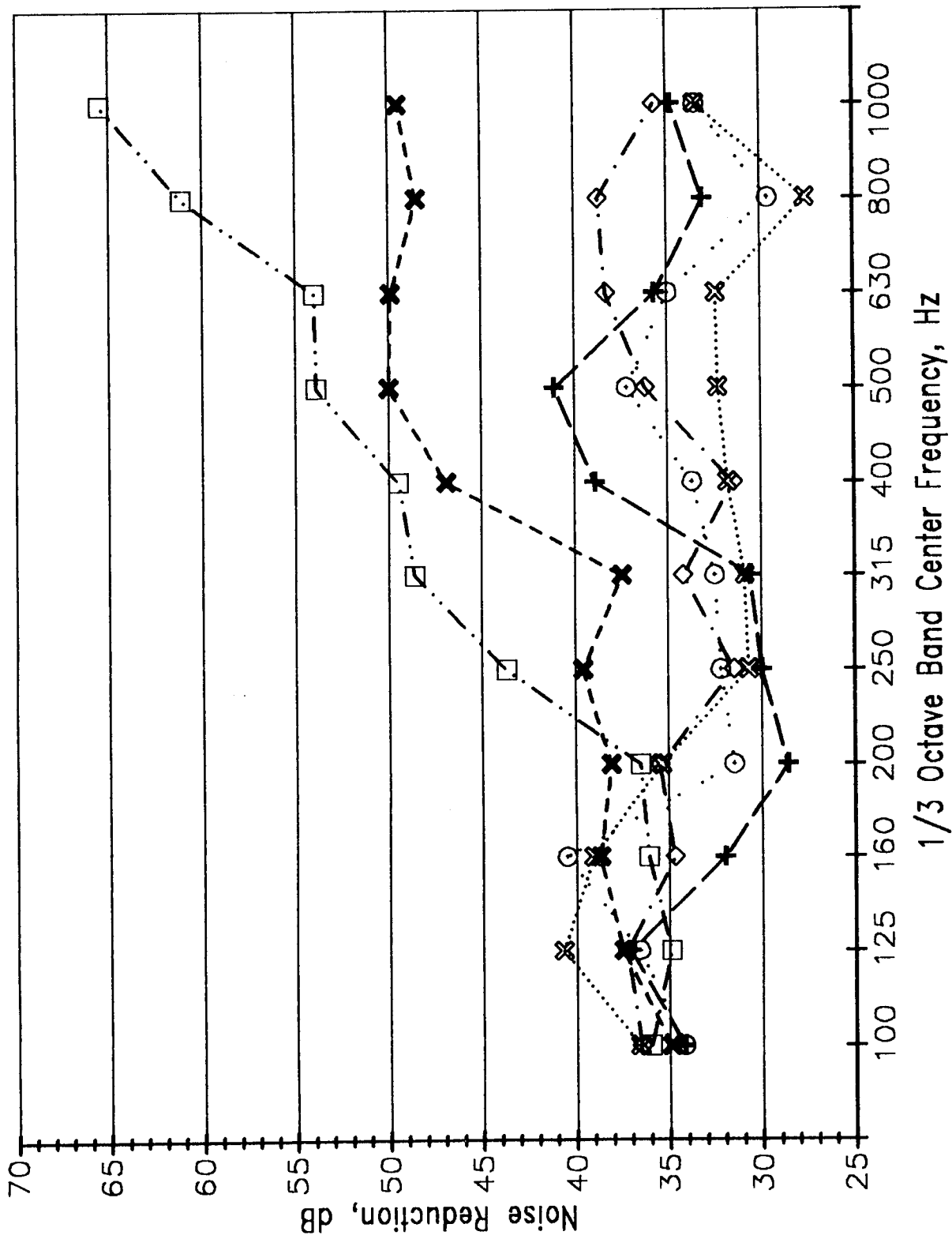


Figure 7-4 Pressure Bulkhead "Into the Cabin" Noise Reduction

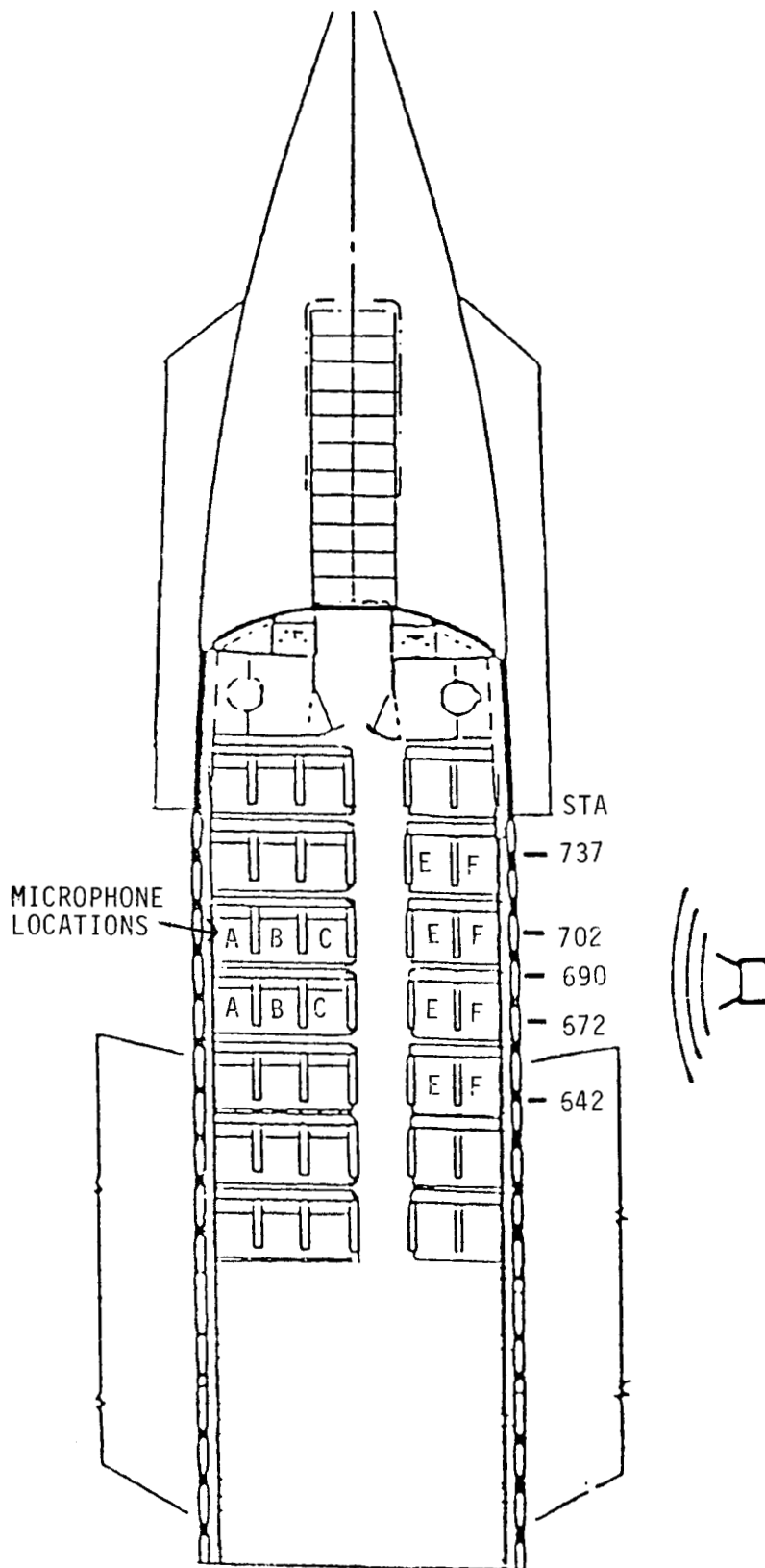


Figure 7-5 Cabin Sidewall Path Test Configuration

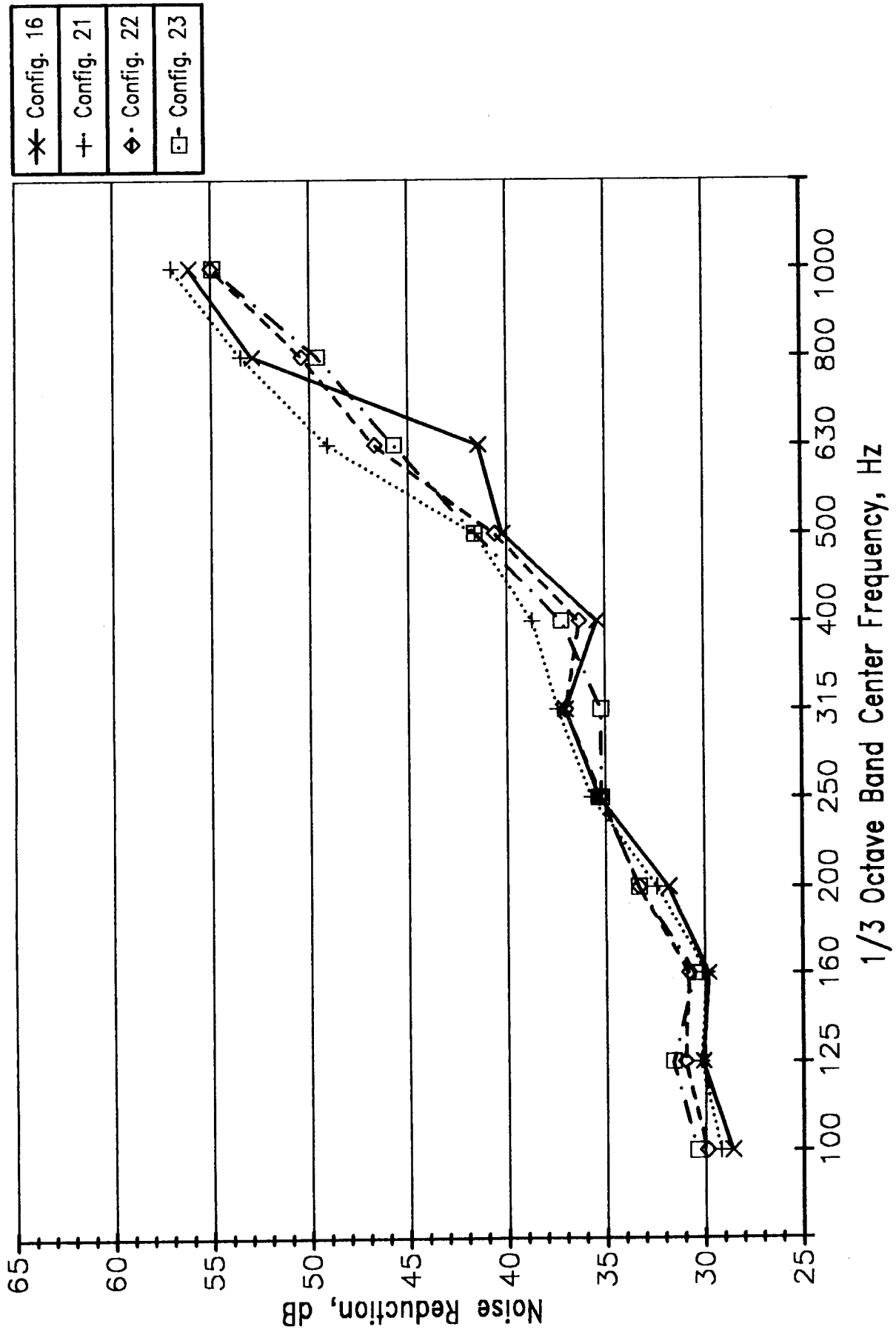


Figure 7-6 Sidewall Noise Reduction (Average for All Mics)

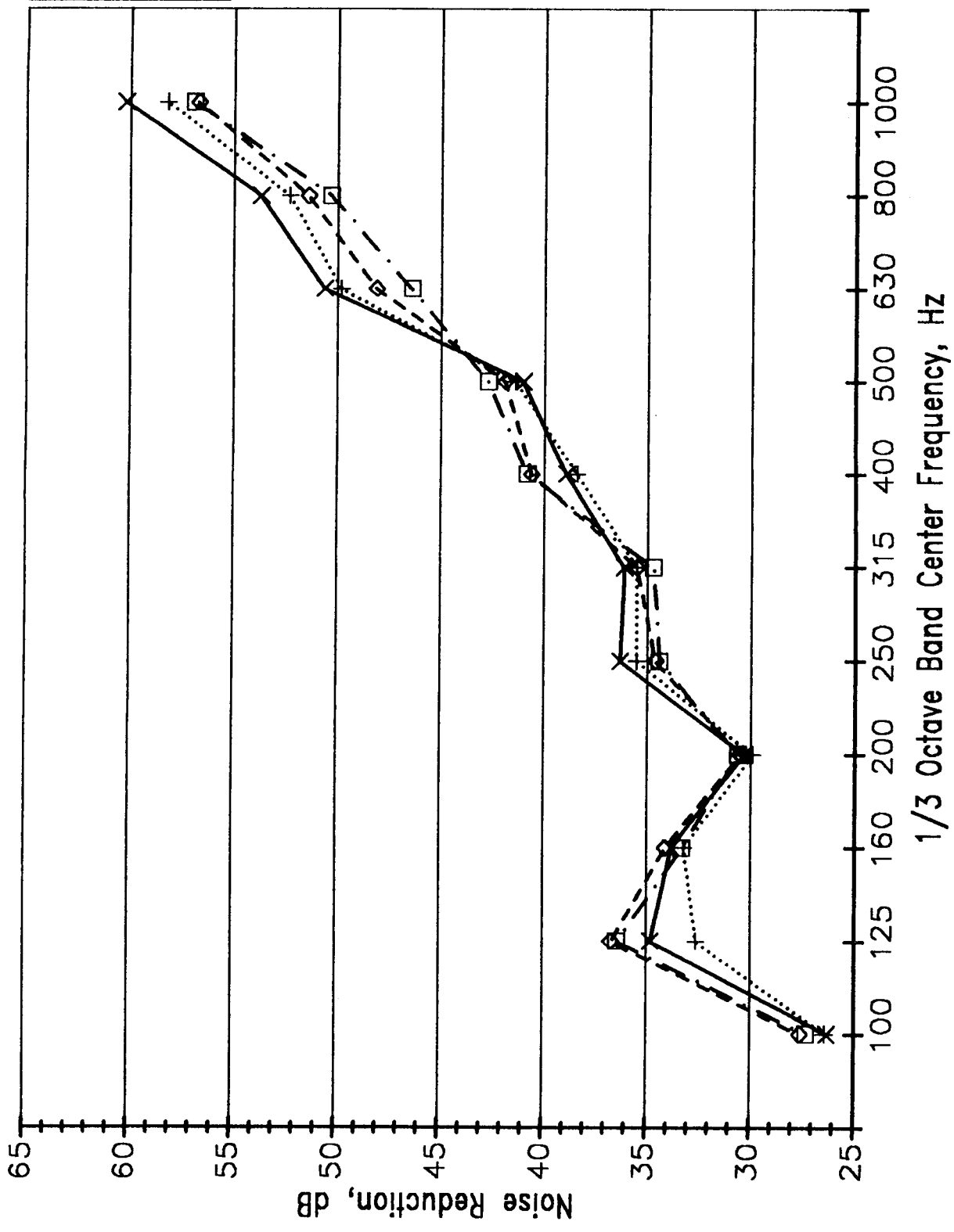


Figure 7-7 Sidewall Noise Reduction (To Mic I-672-B)

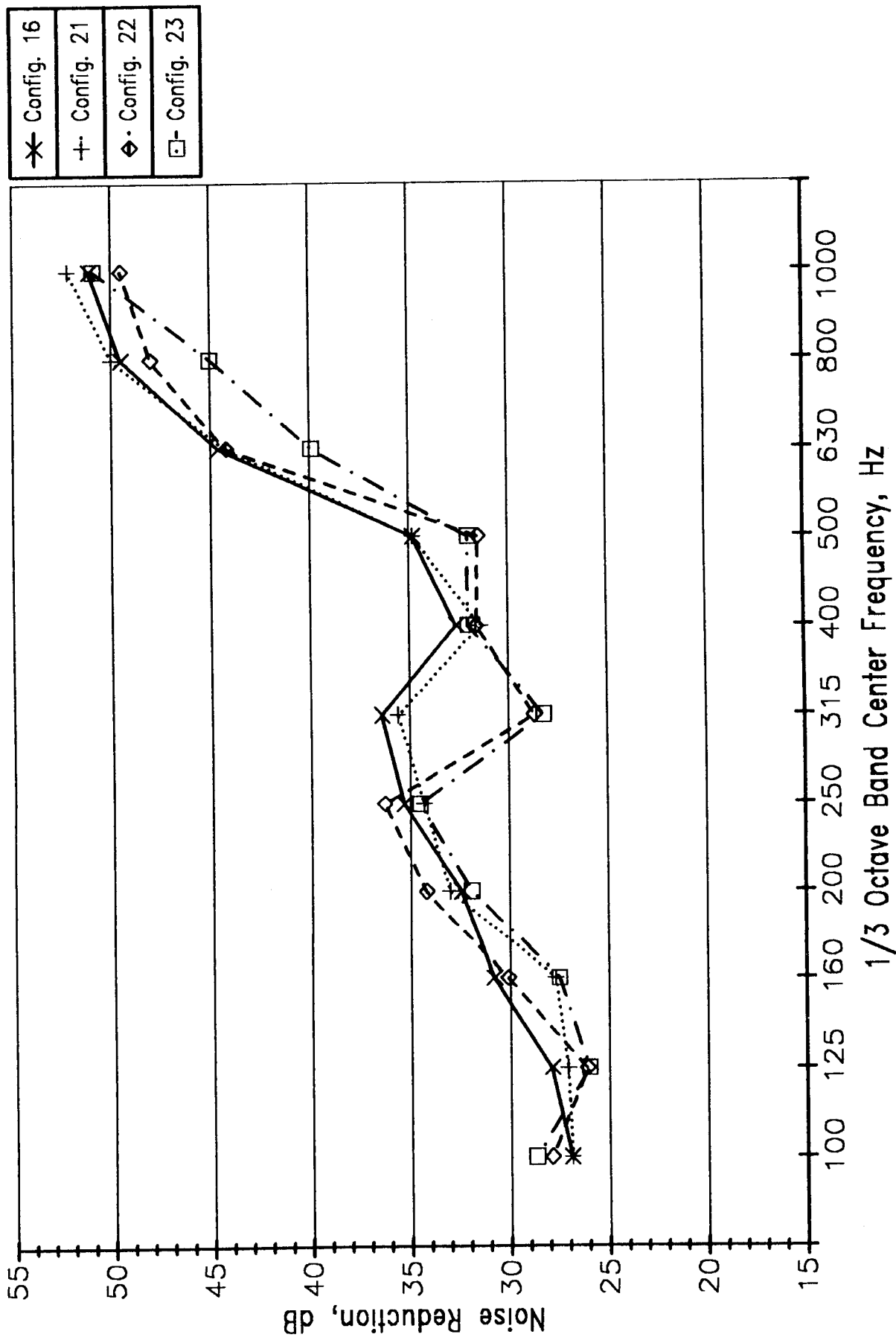


Figure 7-8 Sidewall Noise Reduction (To Mic 1-672-F)

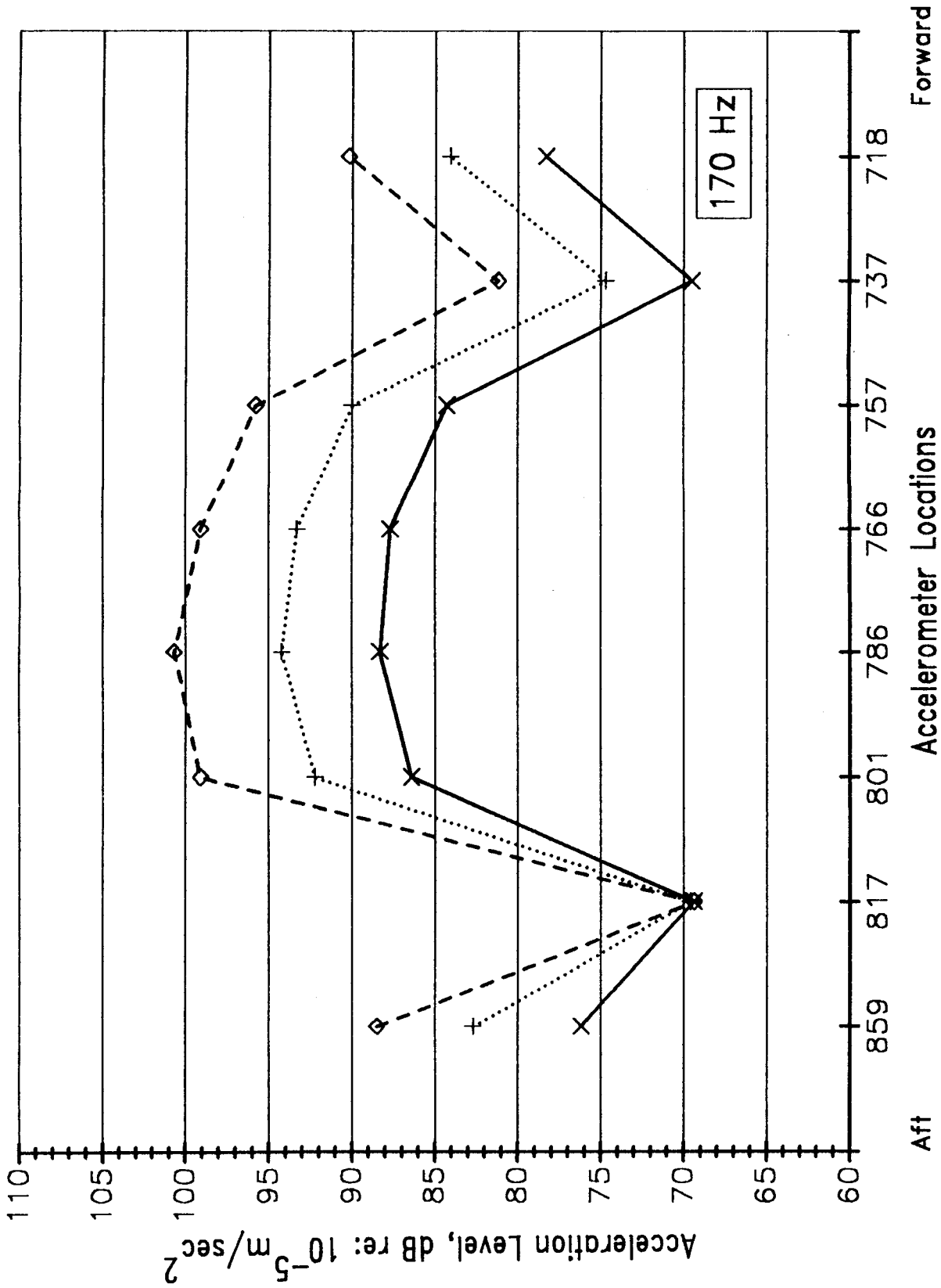


Figure 7-9a Longeron 10 Acceleration Levels, Configuration 23  
(Input at Frame 786, Longeron 15)

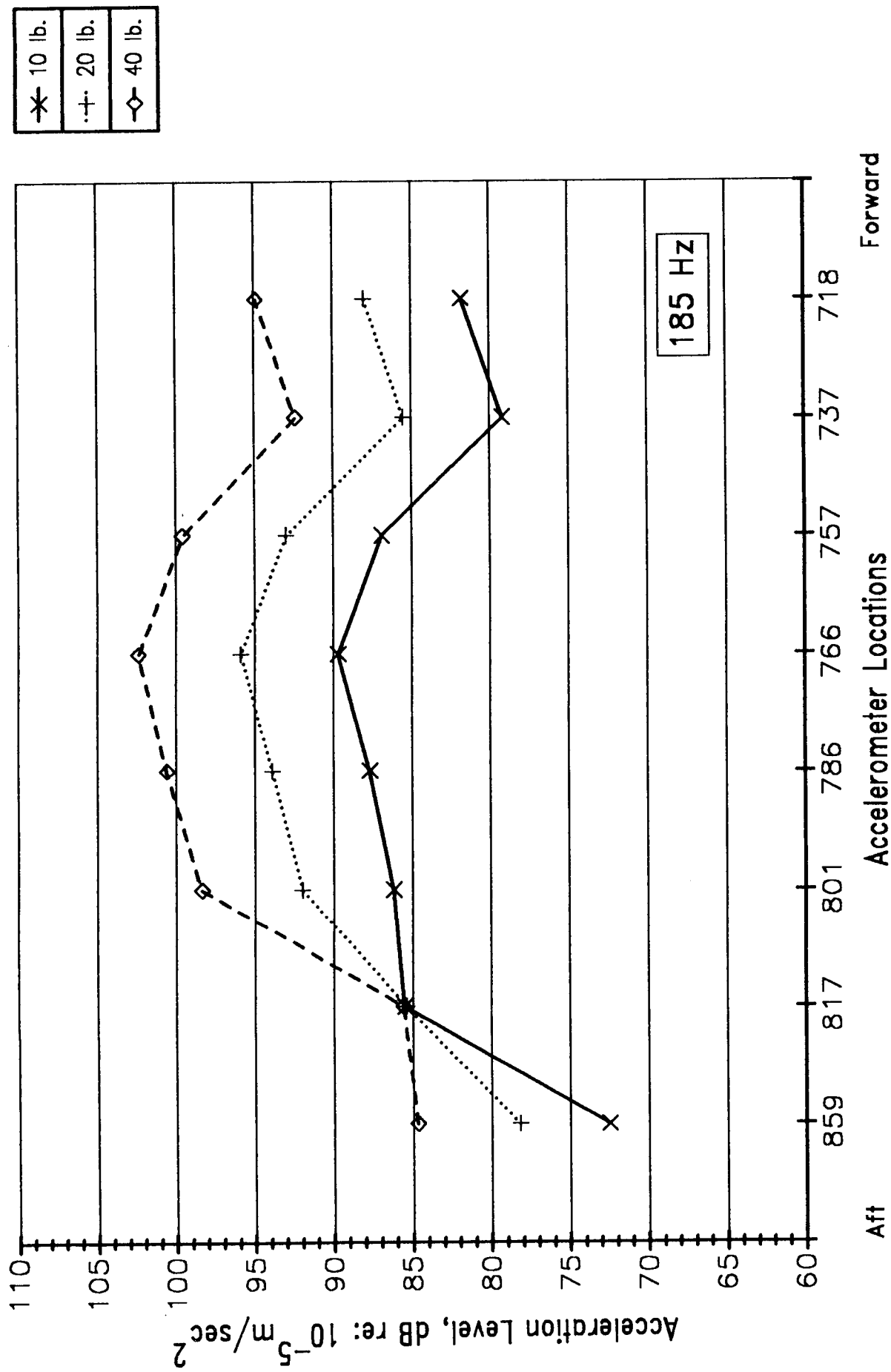


Figure 7-9b Longeron 10 Acceleration Levels, Configuration 23  
(Input at Frame 786, Longeron 15)

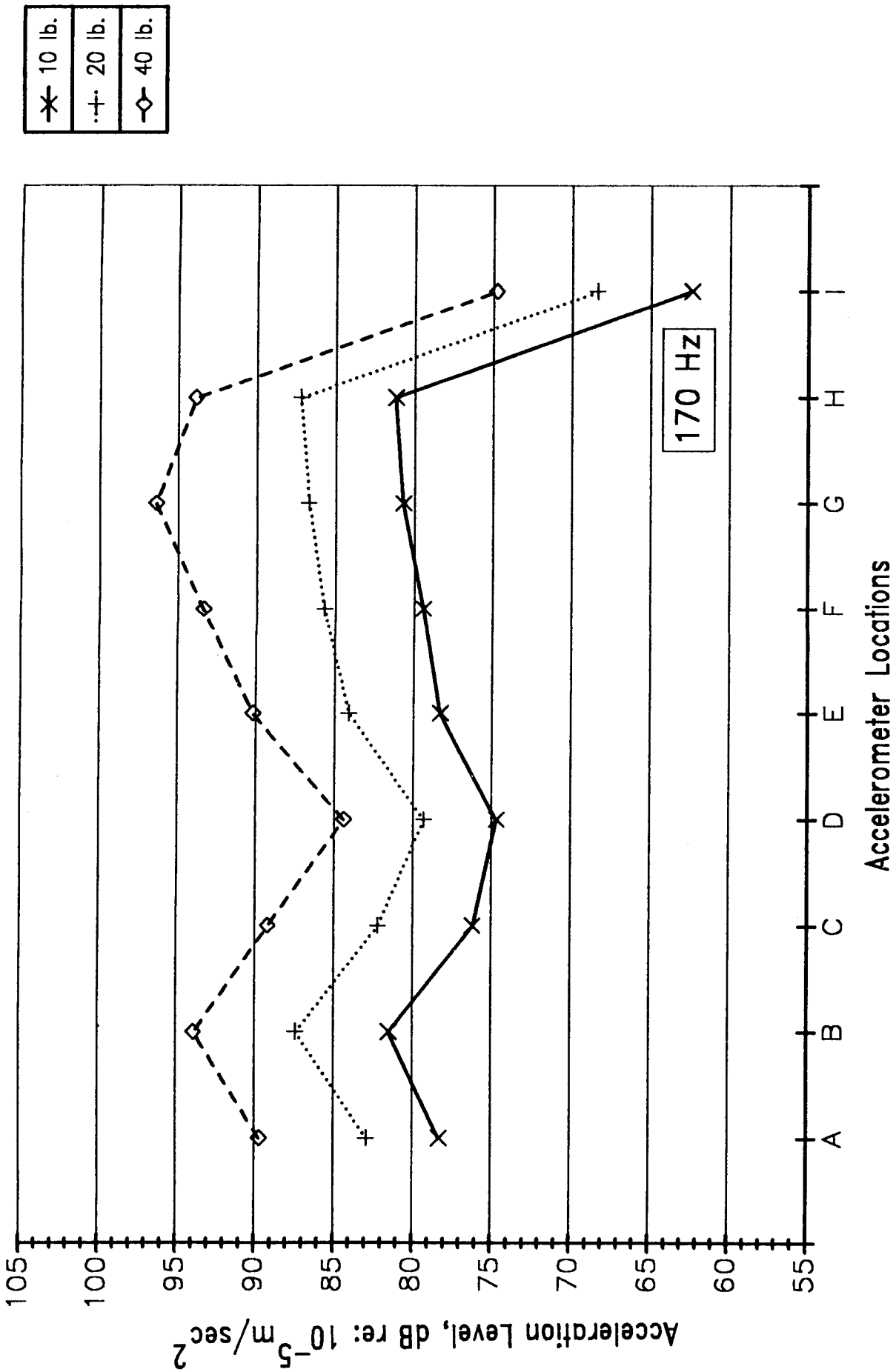


Figure 7-10a Frame 718 Acceleration Levels, Configuration 23  
 (Input at Frame 786, Longeror 15)

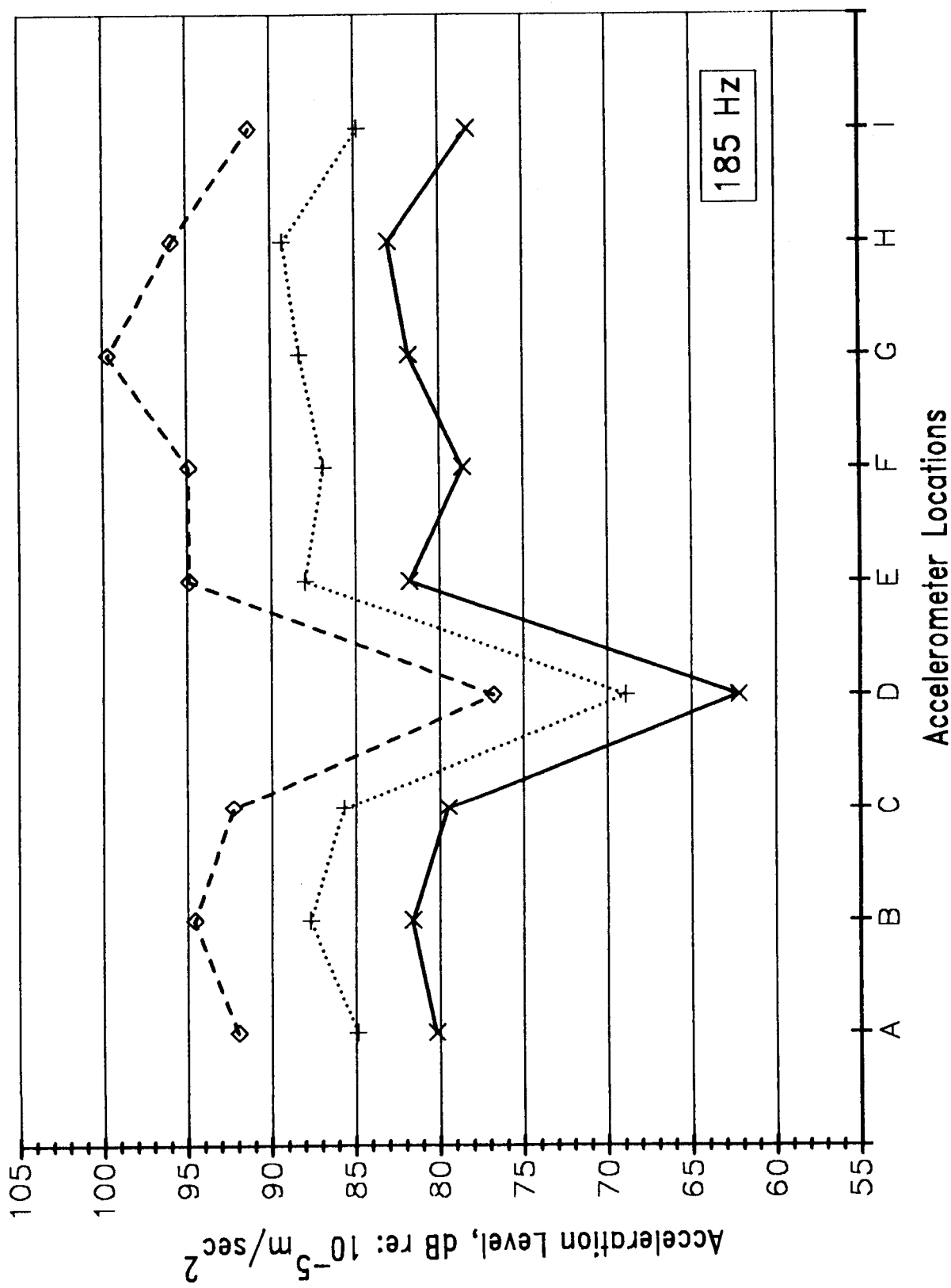


Figure 7-10b Frame 718 Acceleration Levels, Configuration 23  
 (Input at Frame 786, Longeron 15)

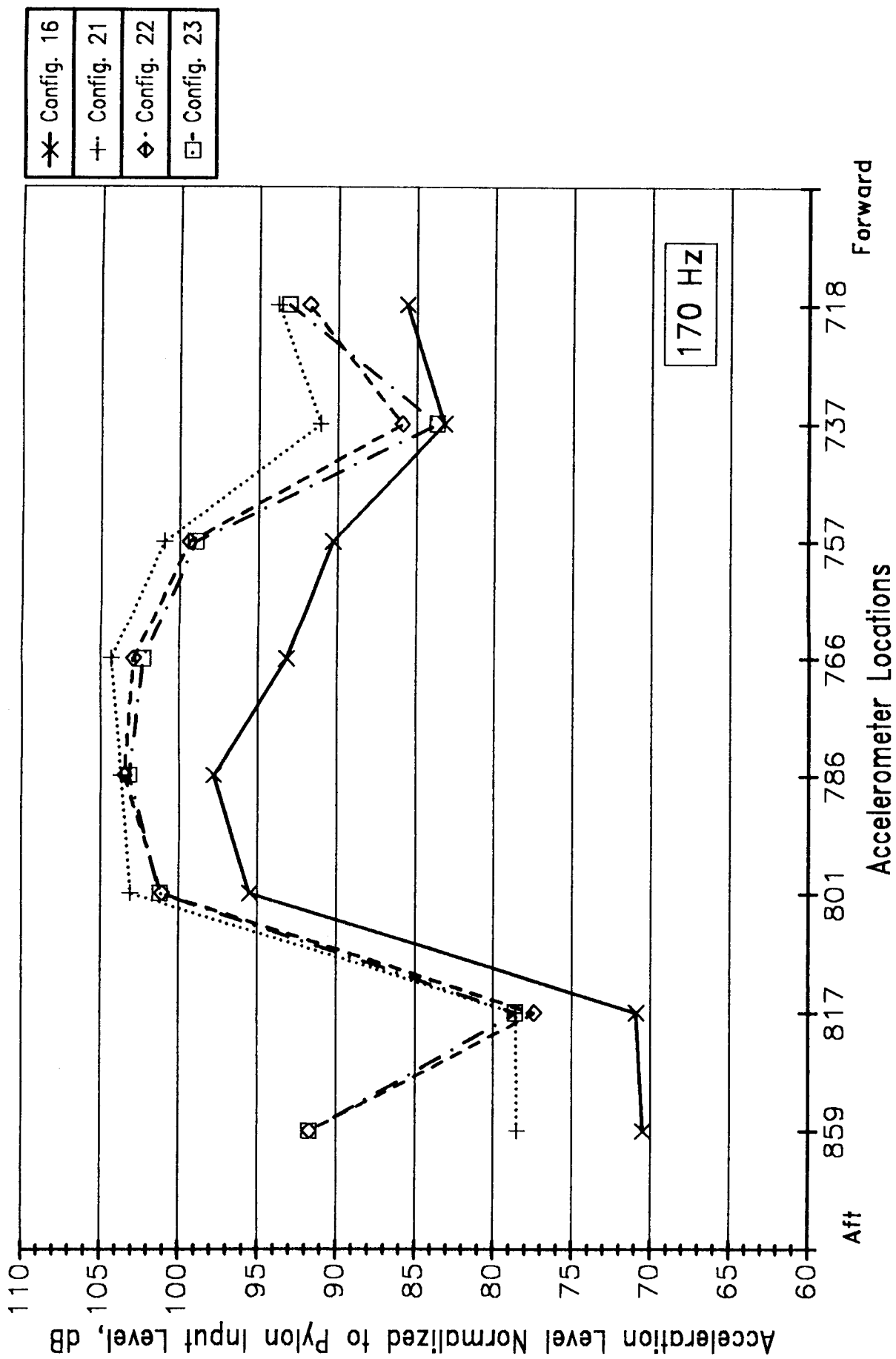


Figure 7-11a Longeron 10 Normalized Acceleration Levels (20 lb Force)  
 (Input at Frame 786, Longeron 15)

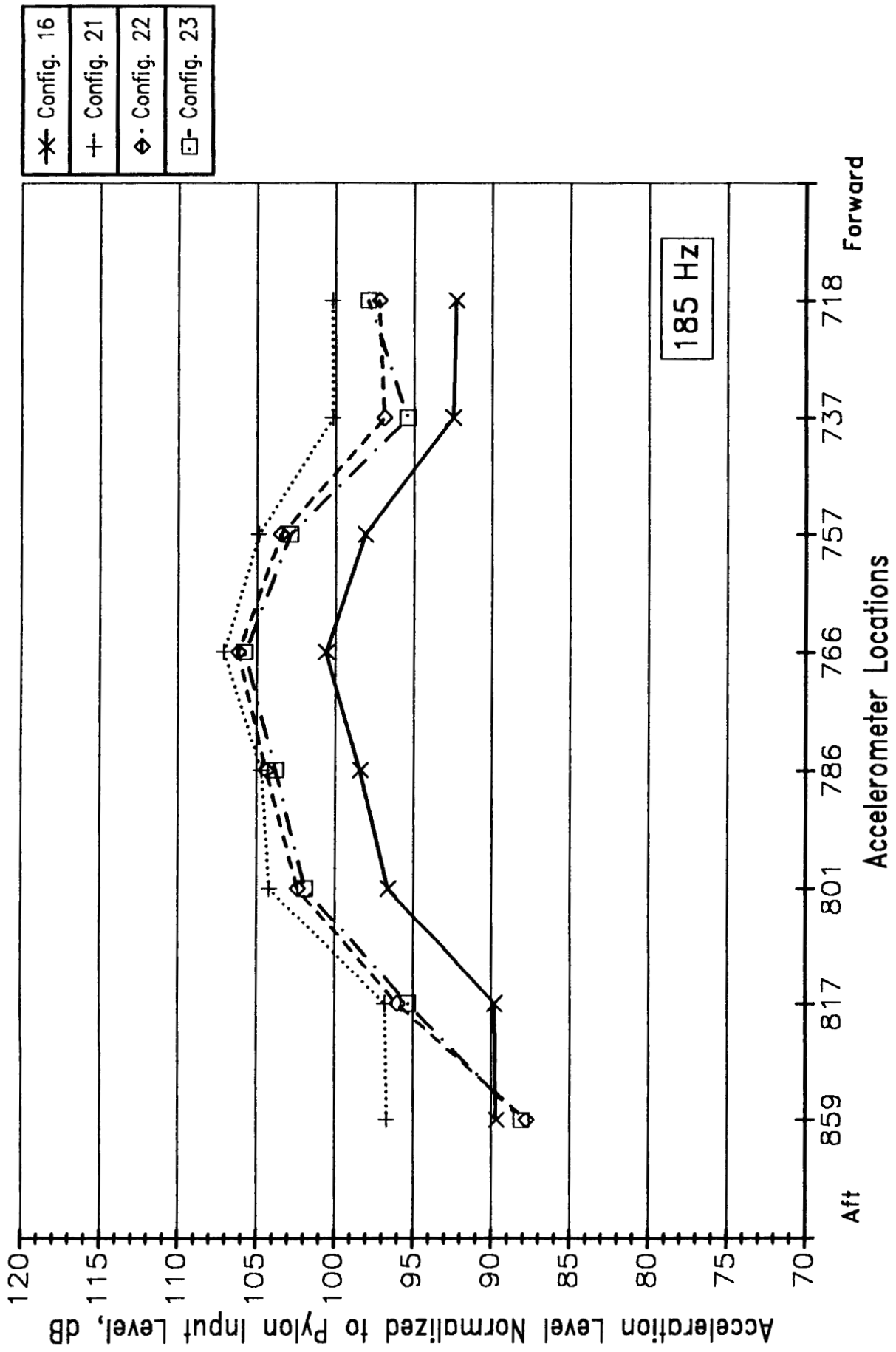


Figure 7-11b Longeron 10 Normalized Acceleration Levels (20 lb Force)  
 (Input at Frame 786, Longeron 15)

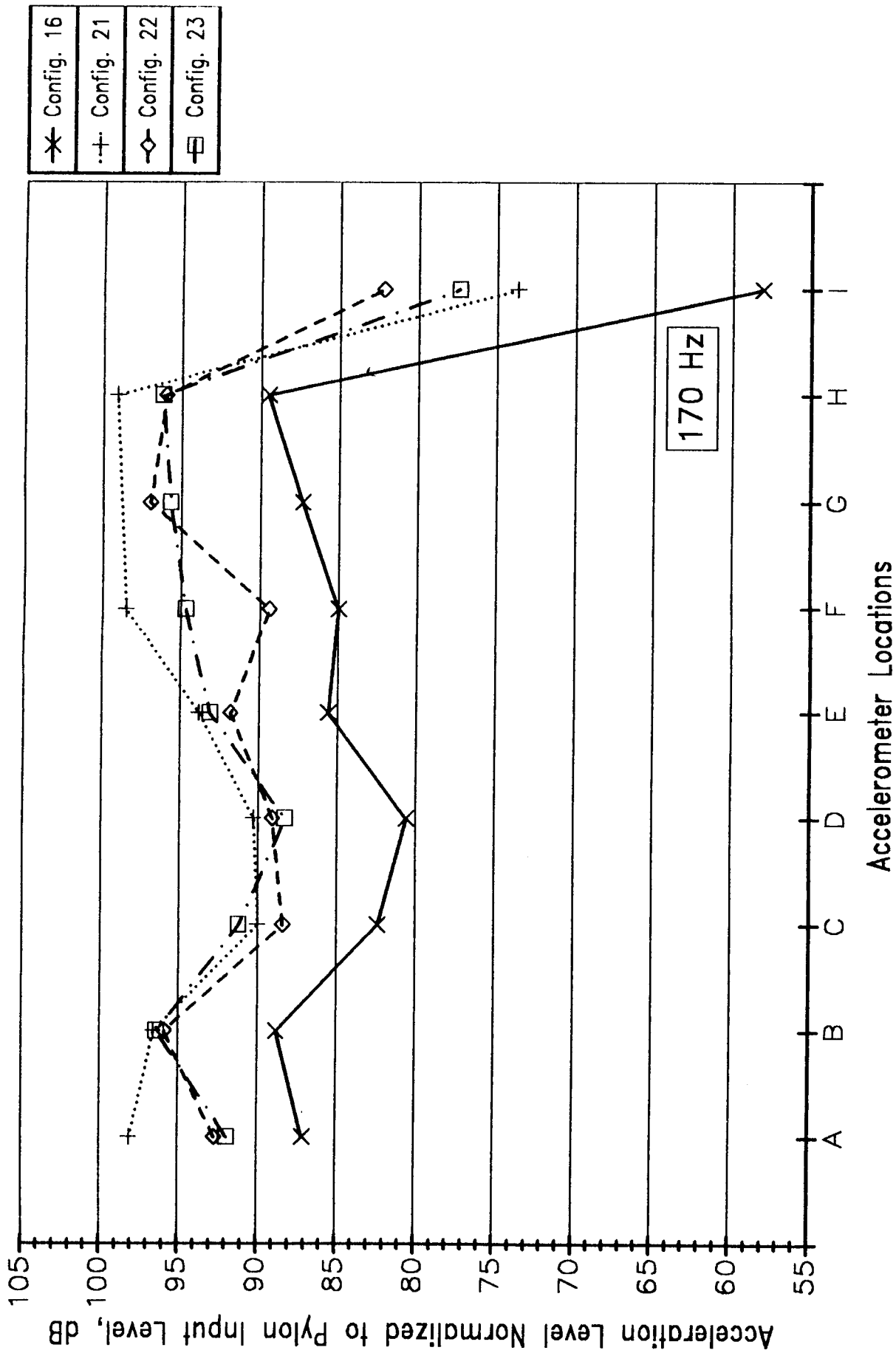


Figure 7-12a Frame 718 Normalized Acceleration Levels (20 lb Force)  
 (Input at Frame 786, Longeron 15)

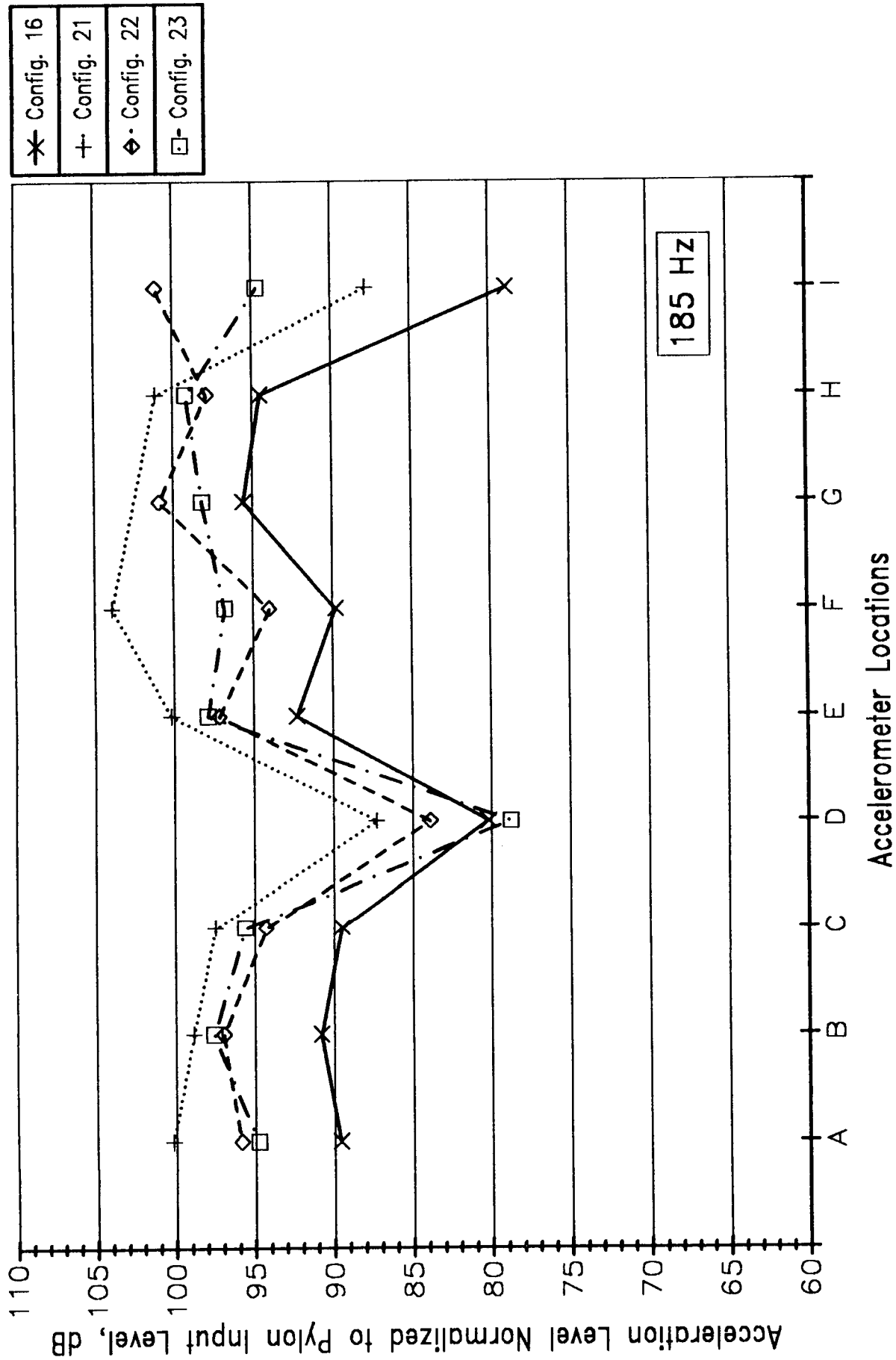


Figure 7-12b Frame 718 Normalized Acceleration Levels (20 lb Force)  
 (Input at Frame 786, Longeron 15)

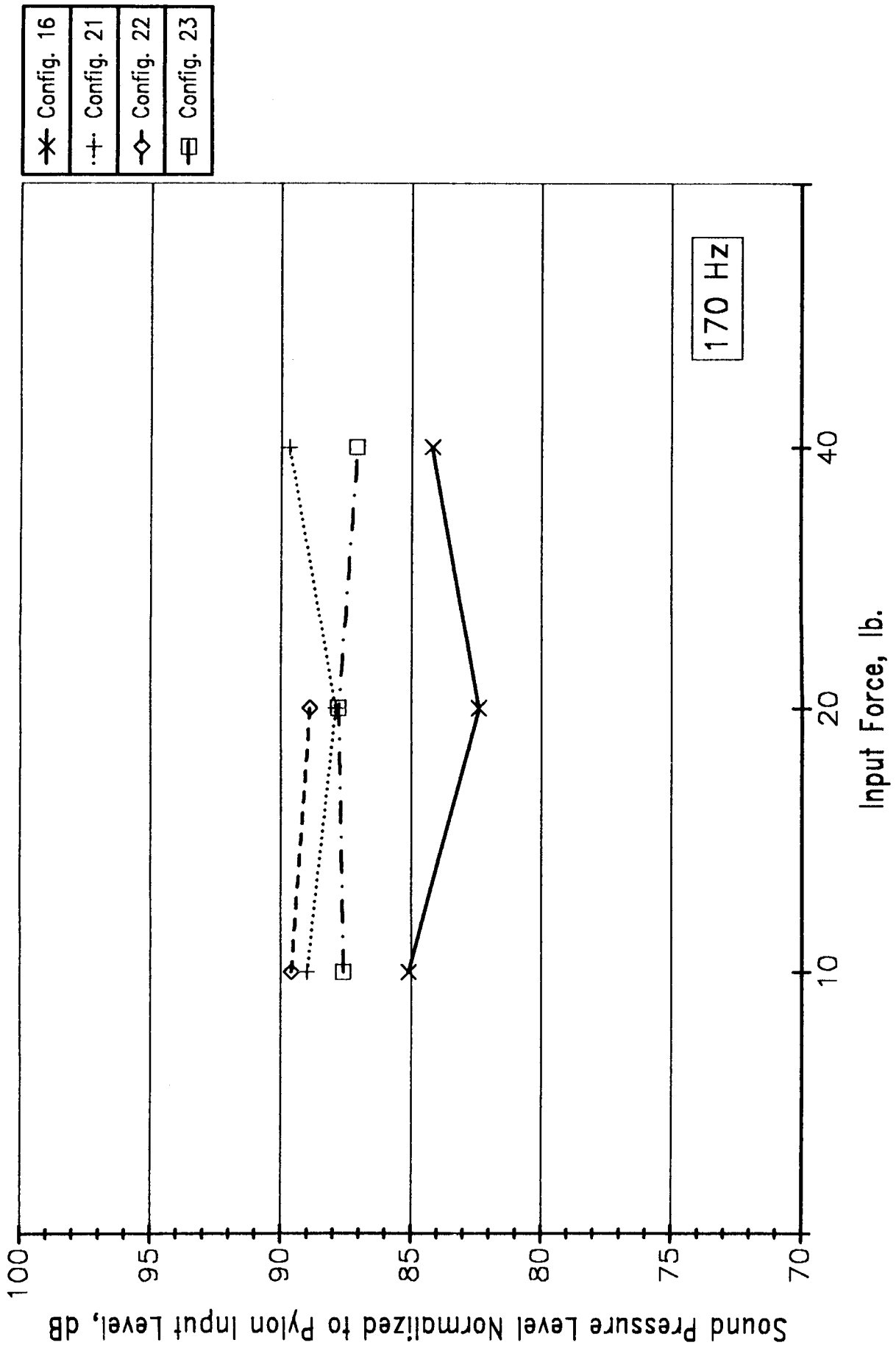


Figure 7-13a Normalized Sound Pressure Levels (Average for All Mics)

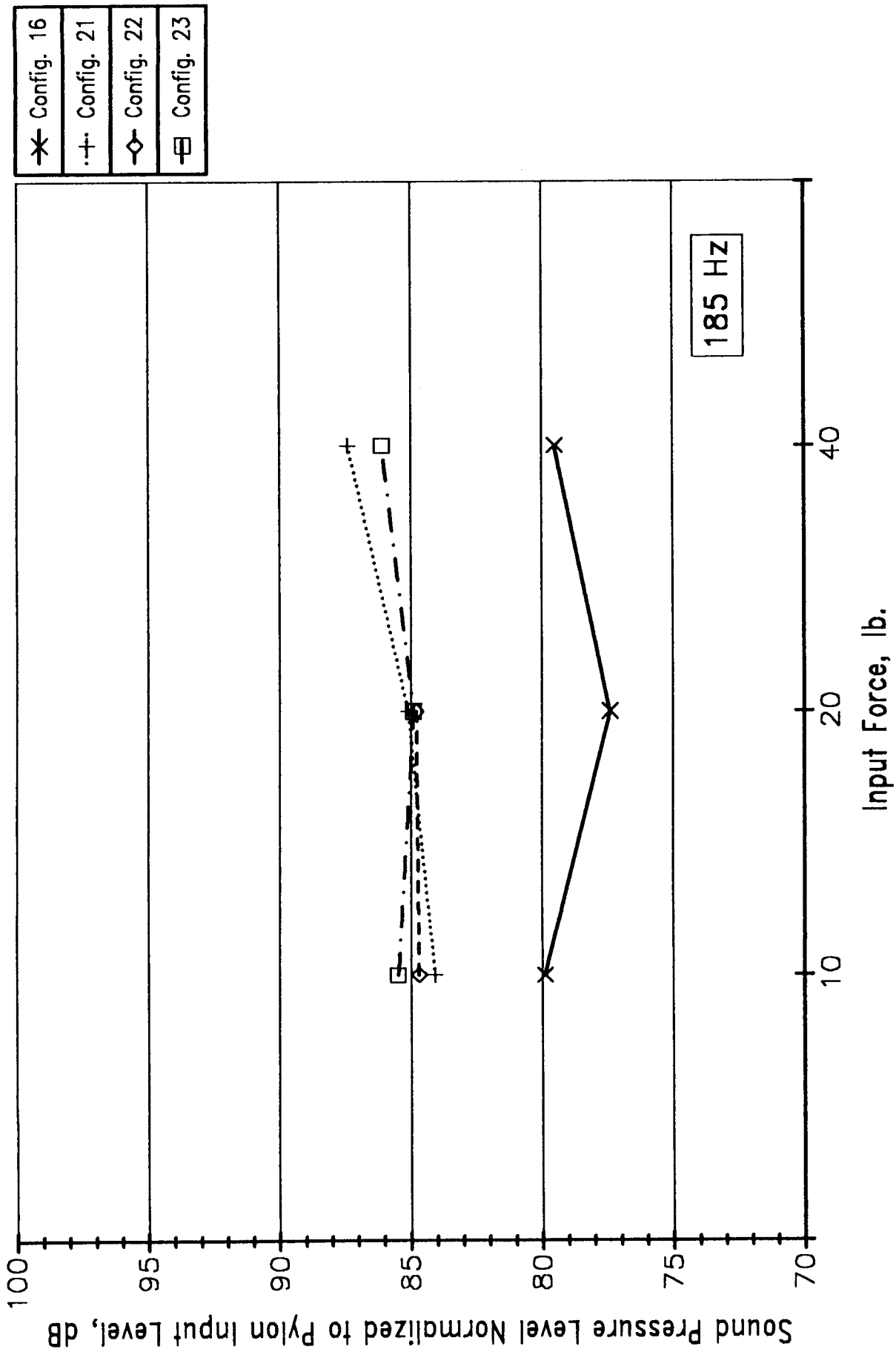


Figure 7-13b Normalized Sound Pressure Levels (Average for All Mics)

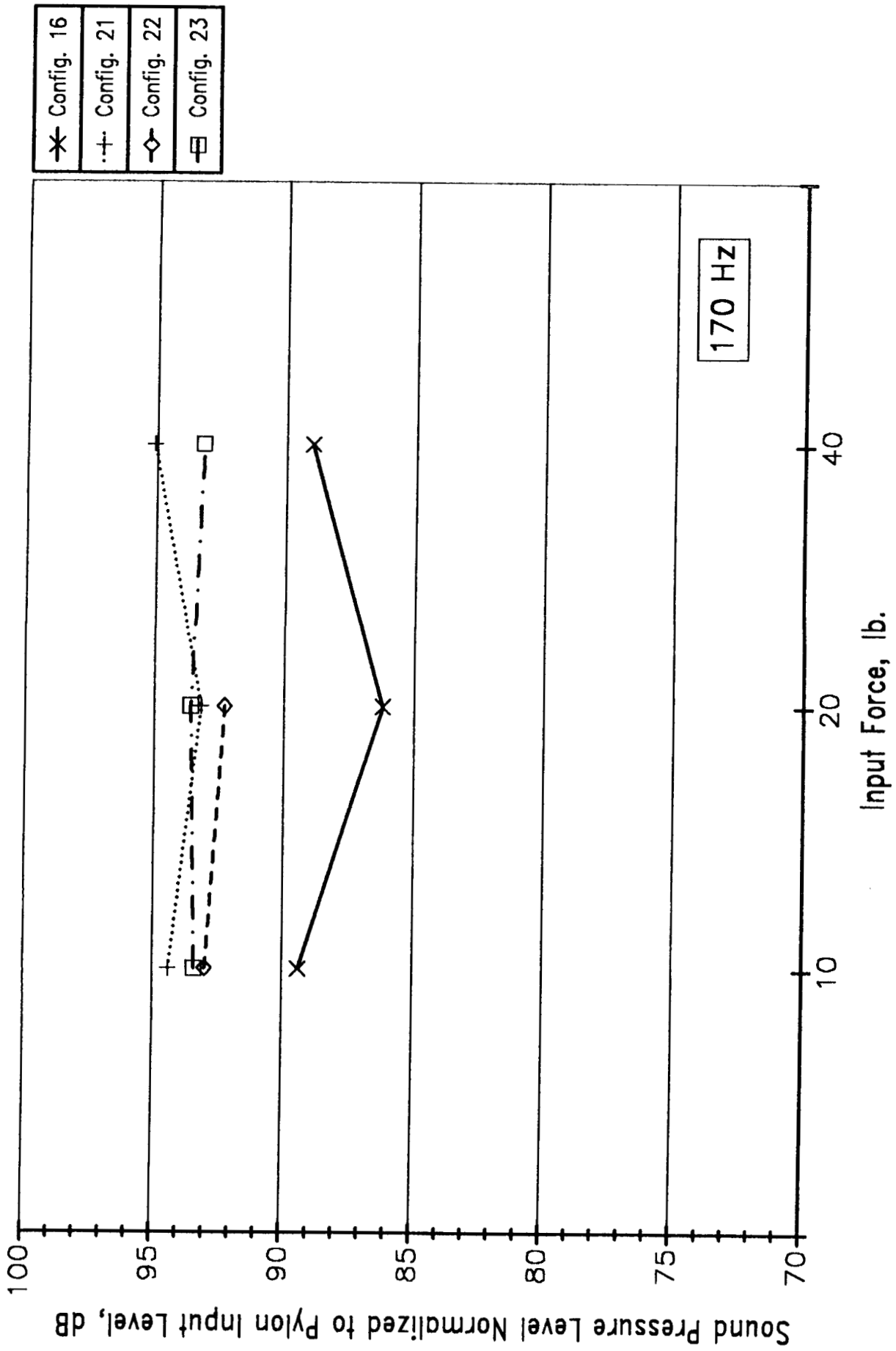


Figure 7-14a Normalized Sound Pressure Levels (At Mic I-737-F)

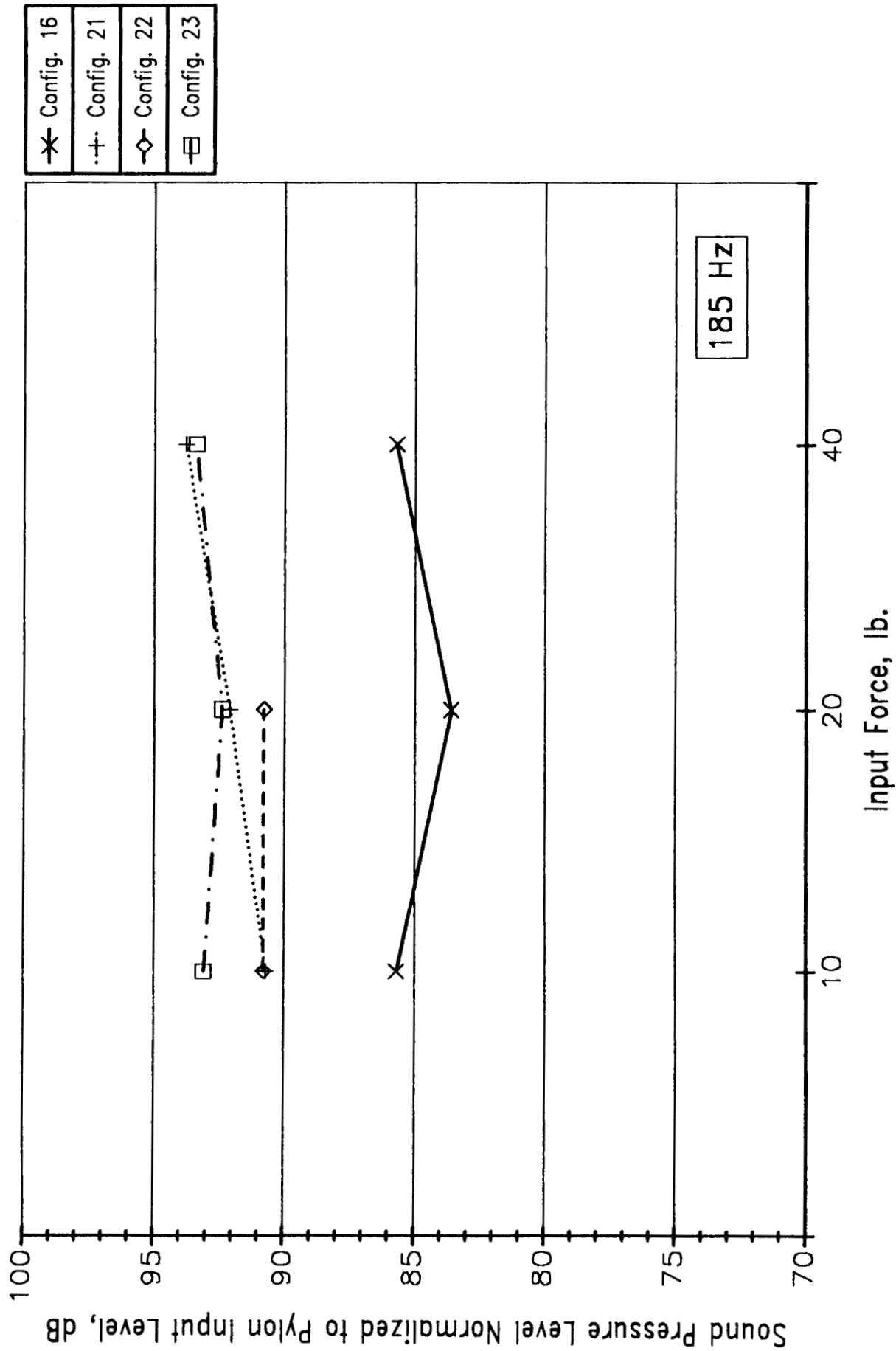


Figure 7-14b Normalized Sound Pressure Levels (At Mic I-737-E)

## 8 Sound Intensity Surveys

Sound intensity surveys were conducted in the aft cabin area for both bare and fully furnished configurations. The main objective of these surveys was to identify the major transmission paths into the cabin for acoustic and vibration excitation. A secondary objective was to further evaluate the effectiveness of selected treatments.

### 8.1 Measurement and Analysis Procedures

#### 8.1.1 Bare Cabin Survey

For the bare cabin measurements, portions of the right sidewall, floor and pressure bulkhead were surveyed. Figure 8-1 shows these cabin surfaces, while Figure 8-2 depicts the survey grids (with grid cells typically 4 sq ft in area) used for each surface. Broadband, random noise was played through the right bank of loudspeakers (pass 2 loudspeakers active), centered at station 908 as in the forced response tests. Because of the highly reverberant nature of the cabin in the bare configuration, several layers of Sonex foam were placed on the left sidewall and hung along the cabin centerline to decrease the reactivity of the interior acoustic environment.

A B & K model 3519 sound intensity probe was used for the measurements. The probe scanned each grid cell at a distance of 4 in from the surface being measured. The measured data were processed with a B & K model 2032 real-time analyzer to yield narrow band intensity levels for each cell, from which the corresponding one-third octave band intensity levels and sound power levels from 100 to 1000 Hz were subsequently calculated.

The measurement system also provides sound pressure level data; from these the pressure-intensity (PI) index was determined for each cell. The PI index is the numerical difference in decibels between the sound pressure level and the sound intensity level, and as such is a measure of the reverberant field in the cabin. If the PI index is more than 15 dB in a particular frequency band, the reflected energy in the cabin in that frequency range is excessive, indicating that the measured intensity level is inaccurate. If the PI index is between 10 and 15 dB, the reflected energy is high, indicating that the accuracy of the measured intensity level is in question. If the PI index is 10 dB or less, the reflected energy is sufficiently low so as not to interfere with the measured intensity level.

## 8.1.2 Furnished Cabin Surveys

For the furnished cabin measurements, portions of the left sidewall, bag racks, floor, ceiling, left pylon bulkhead and pressure bulkhead door were surveyed. An additional set of sound intensity measurements were made of the pressure bulkhead door, with the double wall treatment over the door removed. Figures 8-3 and 8-4 show the survey areas and survey grids, respectively.

The cabin was fully furnished (Configuration 16), except that the seats were removed to permit access to the measurement surfaces and the carpeting was removed from the floor and pylon bulkhead so that it would not affect the sound intensity. As for the bare cabin survey, sonex foam was used in the cabin to reduce the reverberent field (see Figure 8-5).

Two separate furnished cabin surveys were performed, to study airborne and structureborne paths. The airborne path survey utilized the right and left banks of loudspeakers, both centered at station 908 (pass 2 loudspeakers active). The structureborne path survey utilized a shaker attached to the left pylon at the forward engine mount. Broadband, random signals were used for both types of excitation.

The surveys were conducted with a Norwegian Electronics model 216 sound intensity probe; data were processed with a Norwegian Electronics model 830 real-time analyzer to yield one-third octave band sound intensity levels and sound power levels for each cell.

## 8.2 Measurement Results

### 8.2.1 Bare Cabin Survey

Figures 8-6 and 8-7 show sample sound power levels for each grid cell surveyed during the bare cabin measurements. On these and subsequent figures, positive values indicate that acoustic energy is flowing into the cabin (i.e., the surface is an energy source), while negative values indicate that acoustic energy is flowing out of the cabin (the surface is an energy sink). Values with an asterisk (\*) have a PI index greater than 15 dB and are thus suspect.

The two figures depict the sound power levels in the 160 and 200 Hz one-third octave bands, which contain the two BPF's (nominally 169 and 213 Hz, respectively) for a 10x8 UHB engine.

Analysis of the bare cabin survey data shows that the areas with the highest sound power levels in each frequency band are as follows:

100 Hz - upper sidewall  
125 Hz - upper sidewall  
160 Hz - upper sidewall and pressure bulkhead  
200 Hz - pressure bulkhead  
250 Hz - pressure bulkhead  
315 Hz - pressure bulkhead and bulkhead door  
400 Hz - pressure bulkhead  
500 Hz - pressure bulkhead and aft sidewall  
630 Hz - pressure bulkhead and aft sidewall  
800 Hz - sidewall  
1000 Hz - sidewall

The aft pressure bulkhead appears to be the dominant source for much of the frequency range. This is not surprising, since the acoustic loads on the aft portion of the fuselage (behind the pressure bulkhead) are greater than the loads on the fuselage forward of the pressure bulkhead, and the transmission loss of the aft fuselage (into the unpressurized section) is less than the transmission loss of the fuselage sidewall into the cabin.

At 125 and 160 Hz, the upper two portions of the sidewall have significantly higher levels (by about 10 dB at 125 Hz and 4 dB at 160 Hz) than the lower two portions. Also, the forward areas of the sidewall have higher levels than the aft areas at 125 and 250 Hz. These results may reflect the greater transmission loss of the lower and aft sidewall sections in the lower frequency range due to the increased stiffness occurring at the floor-sidewall and bulkhead-sidewall interfaces.

The aft bulkhead has significantly higher levels (5 to 10 dB depending on frequency) than the bulkhead door from 315 to 1000 Hz, likely because the greater mass and stiffness of the door causes higher transmission loss in this frequency range than the transmission loss of the bulkhead.

The floor functions as a sound sink (i.e., has negative sound intensity) at all frequencies of interest.

It should be noted that from 500 Hz to 1000 Hz, the PI index is very high for most of the measurement surfaces. Thus in this frequency range the measured levels should only be used to identify gross trends.

### **8.2.2 Furnished Cabin Surveys**

For the airborne and structureborne path surveys, Figures 8-8 through 8-11 show sample sound power levels measured in each grid cell. Figures 8-8 and 8-9 show the

160 and 200 Hz sound power levels, respectively, for the airborne path survey; similar data are presented in Figures 8-10 and 8-11 for the structureborne path survey.

The airborne path survey data show, in general, that without the pressure bulkhead double wall treatment the bulkhead door is the major source in all the frequency bands; for 100 and 125 Hz the upper sidewall also is a major source. With the bulkhead treatment installed, however, the data show that the bulkhead door is no longer the major source, demonstrating the effectiveness of the double wall treatment for airborne excitation. The surfaces which have the highest power levels in this configuration are as follows:

- 100 Hz - upper sidewall
- 125 Hz - upper sidewall
- 160 Hz - floor
- 200 Hz - multiple
- 250 Hz - upper and lower sidewall
- 315 Hz - pressure bulkhead
- 400 Hz - multiple
- 500 Hz - multiple
- 630 Hz - multiple
- 800 Hz - multiple
- 1000 Hz - floor

The term "multiple" means that several surfaces have about the same power levels. Thus, with the bulkhead treatment, the furnished interior is fairly well balanced in that there are no dominant sources at most frequencies.

The relative contributions from these various surfaces are further illustrated in Figures 8-12 and 8-13. In these and subsequent figures, sound intensity levels are shown rather than sound power levels in order to compare the power flow through grid cells of different areas. (These sound intensity levels are 2 to 6 dB higher than the corresponding sound power levels, depending on grid cell size.) Also in these figures, levels with a PI index greater than 15 dB are excluded.

In Figure 8-12, the measured sound intensity levels for two upper sidewall survey grid cells (F17 and F19) are plotted. For comparison, the measured sound intensity levels for comparable cells (B26 and B28) in the bare cabin are also plotted. The decrease in intensity levels from bare to furnished conditions apparent on the figure is comparable to the noise reduction obtained with the installation of the final furnished fuselage configurations relative to the baseline configuration, see Section 6. (Note that the bare cabin data on the figure have been normalized to the same exterior levels as for the furnished cabin data, and to two-sided loudspeaker excitation).

In Figure 8-13, the measured sound intensity levels for an aft bulkhead cell is plotted for conditions with and without the double bulkhead treatment (cells F4 and F3, respectively). Again the benefit of this treatment can be seen. The measured sound intensity levels for the comparable cell in the bare cabin (B6) are also shown, and as for the sidewall comparison in the previous figure, the decrease in intensity levels from bare to furnished conditions is clear.

Comparison of the levels for the treated bulkhead area on Figure 8-13 with the levels for the two upper sidewalls on Figure 8-12 highlights the observation made earlier that with the double wall treatment in the furnished cabin, the various surfaces provide comparable power levels.

The structureborne path survey data show that the engine pylon bulkhead and the upper and lower sidewall areas are the major sources in most of the frequency bands, for vibration excitation. Installation of the double wall treatment reduces the power levels from the bulkhead door for some frequencies, but does not alter the radiation from the pylon bulkhead or upper sidewall.

To illustrate these observations, Figure 8-14 shows the measured sound intensity levels for the aft bulkhead with and without the double wall treatment (cells F4 and F3); the effectiveness of the bulkhead treatment seen earlier for acoustic excitation is not as great for vibration excitation. In Figure 8-15 the sound intensity levels measured for the two upper sidewall areas (F17 and F19) are compared with the levels measured for the pylon bulkhead (F7). Below 400 Hz, the sidewalls have higher intensity levels, while above 400 Hz the pylon bulkhead has higher intensity levels. Comparing these levels with the treated and untreated aft bulkhead levels of the previous figure, it can be seen that for vibration excitation the sidewall and pylon bulkhead surfaces have higher levels than the aft bulkhead, at all frequencies.

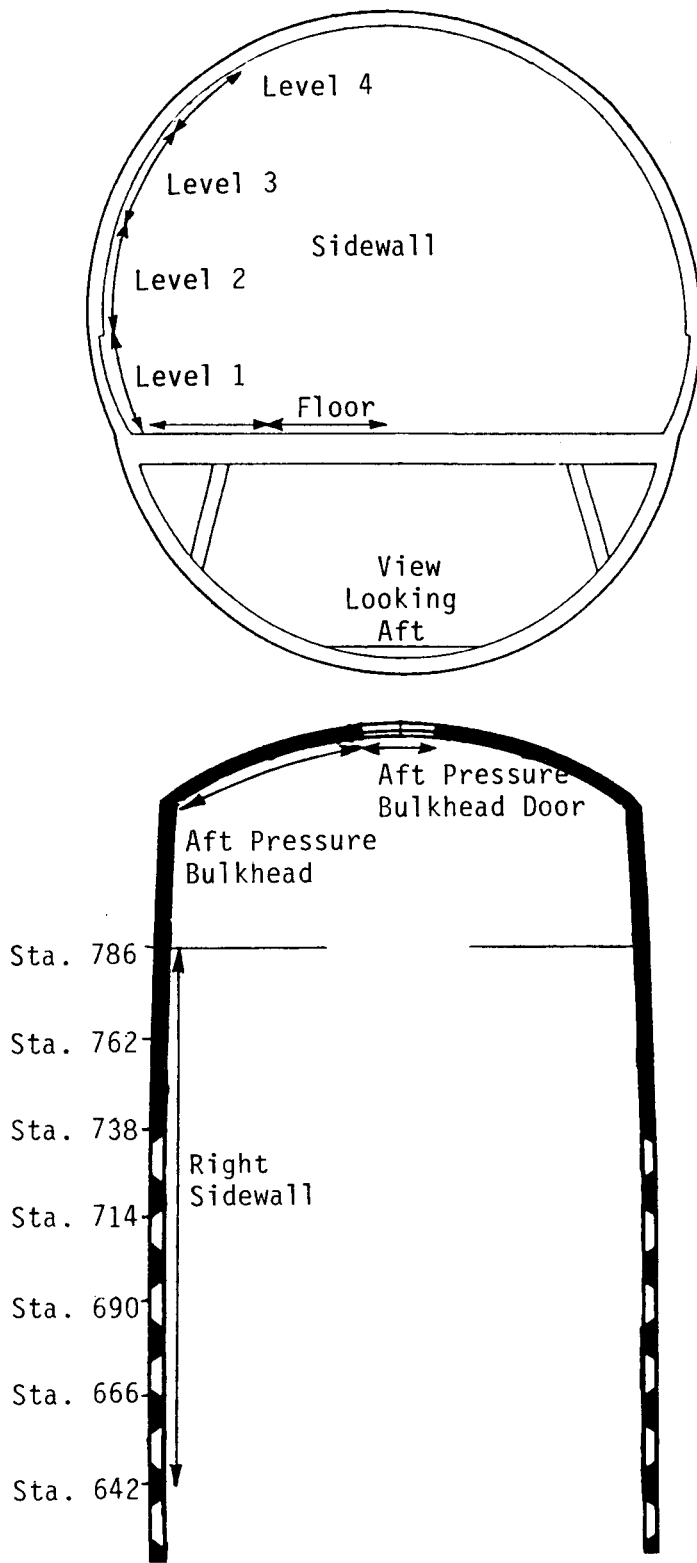


Figure 8-1 Sound Intensity Survey Areas in the Bare Cabin



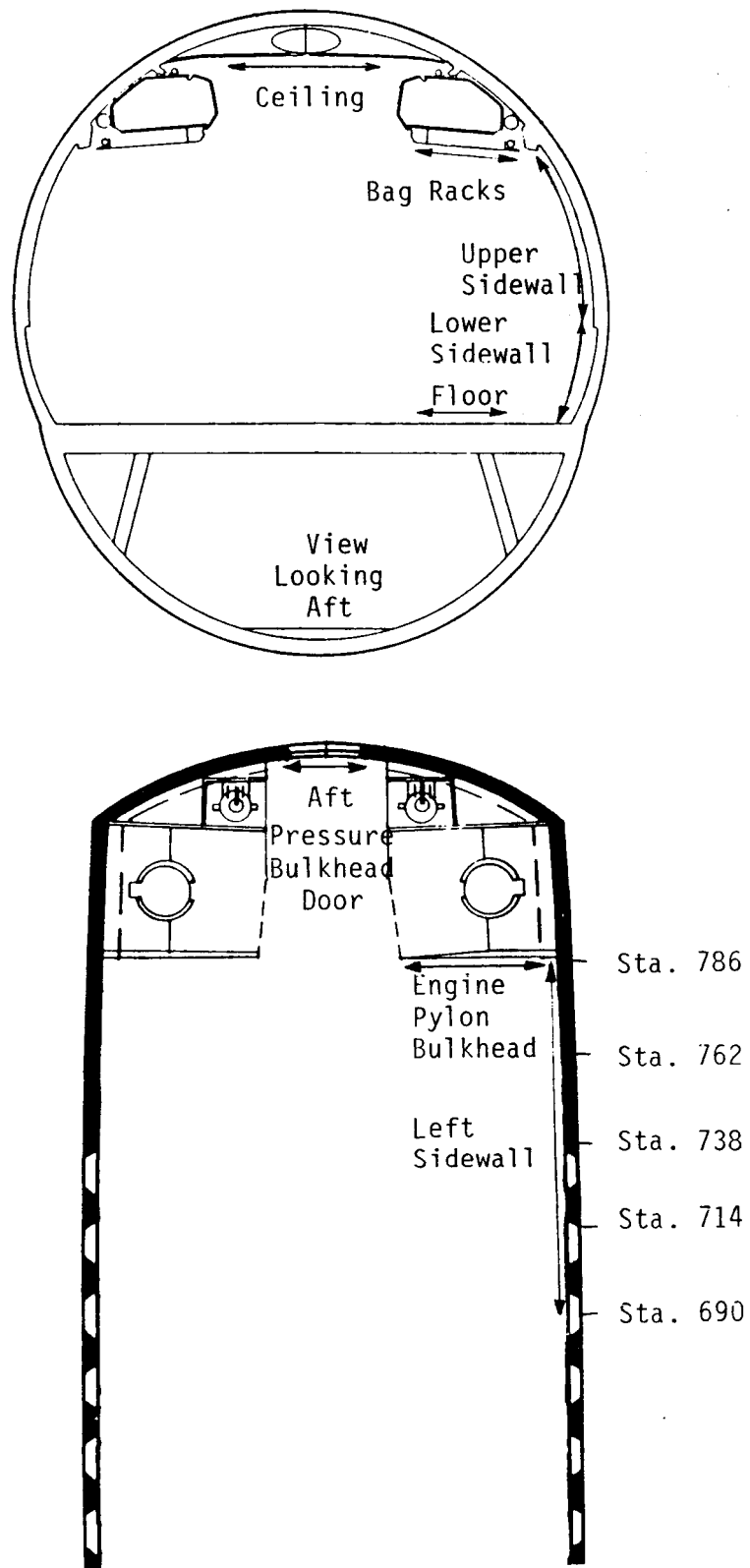
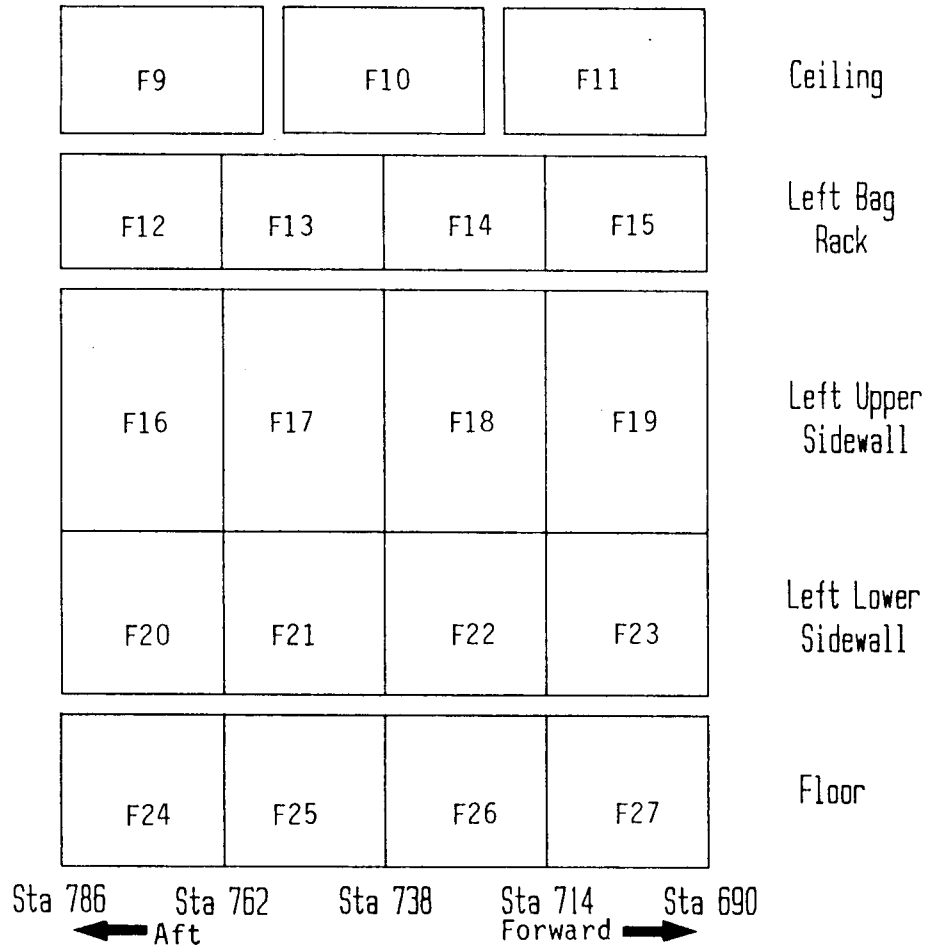
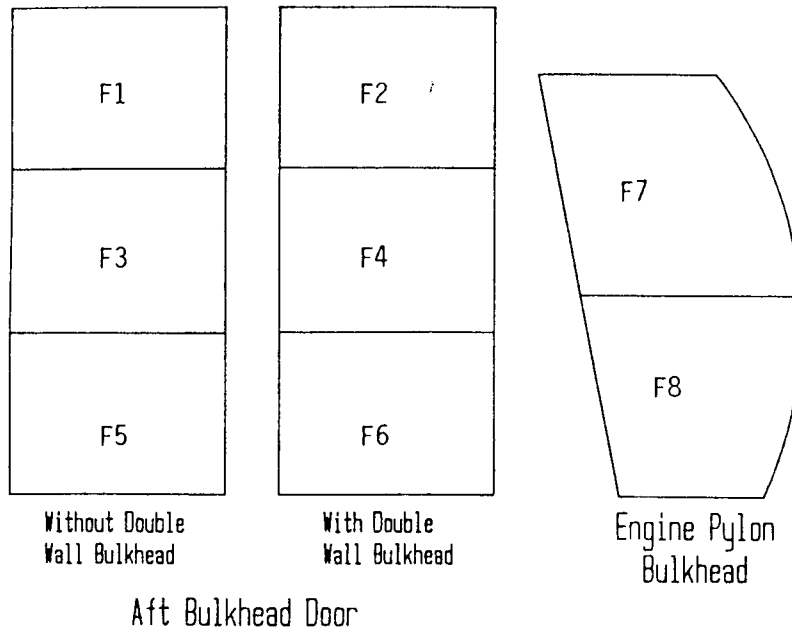


Figure 8-3 Sound Intensity Survey Areas in the Furnished Cabin



**Figure 8-4 Survey Grid Cells, Furnished Cabin**

ORIGINAL PAGE  
BLACK AND WHITE PHOTOGRAPH



Figure 8-5 View of the Furnished Cabin  
Survey Area





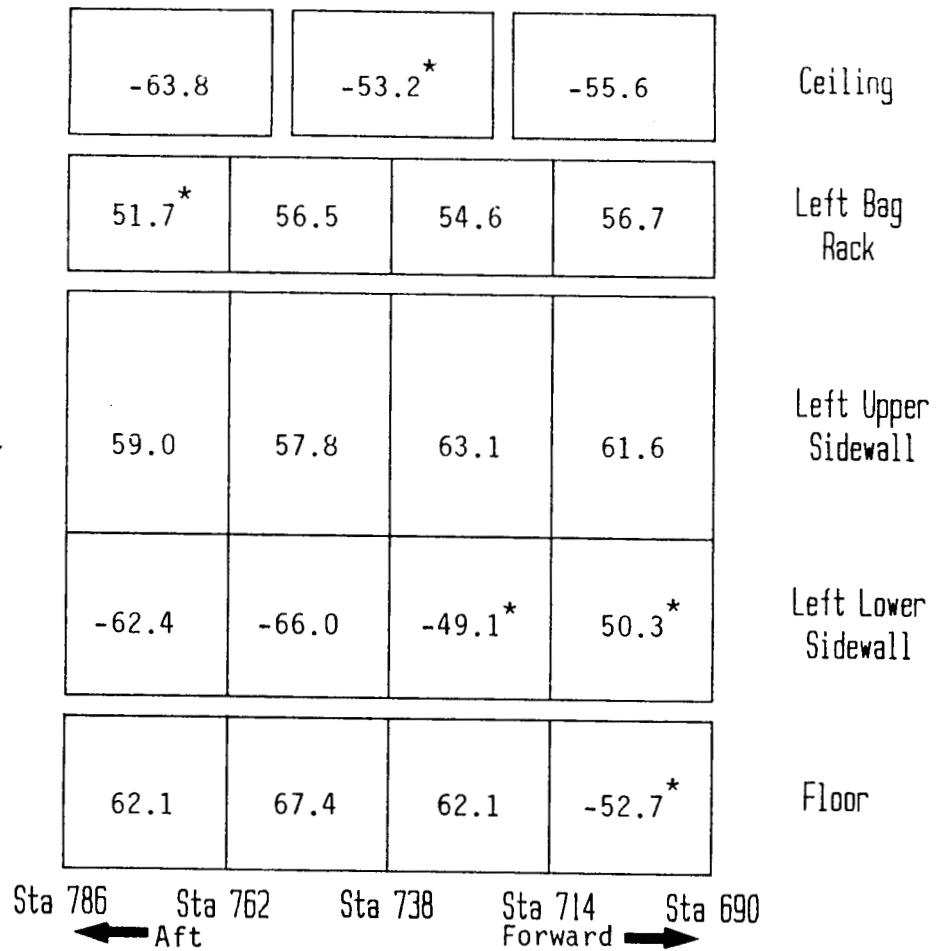
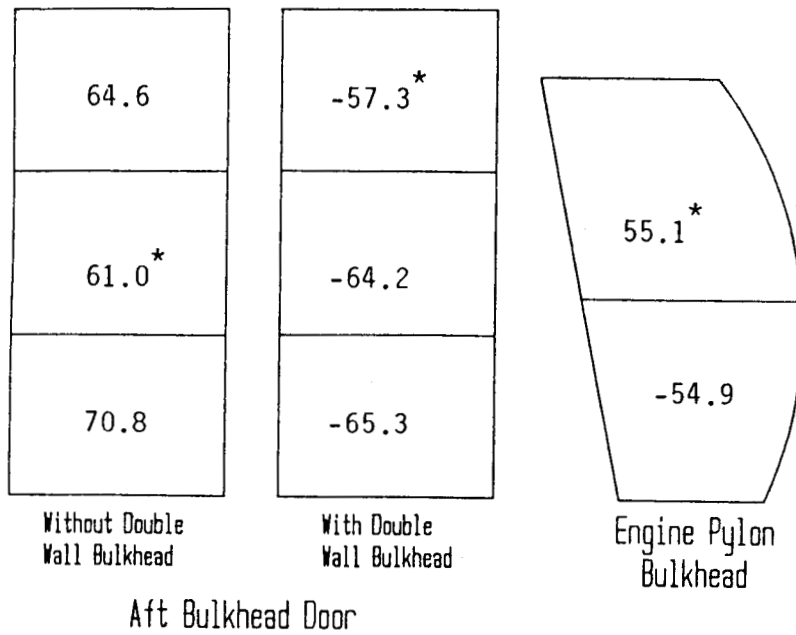


Figure 8-8 Sound Power Levels in the 160 Hz Band, Airborne Path Survey, Furnished Cabin







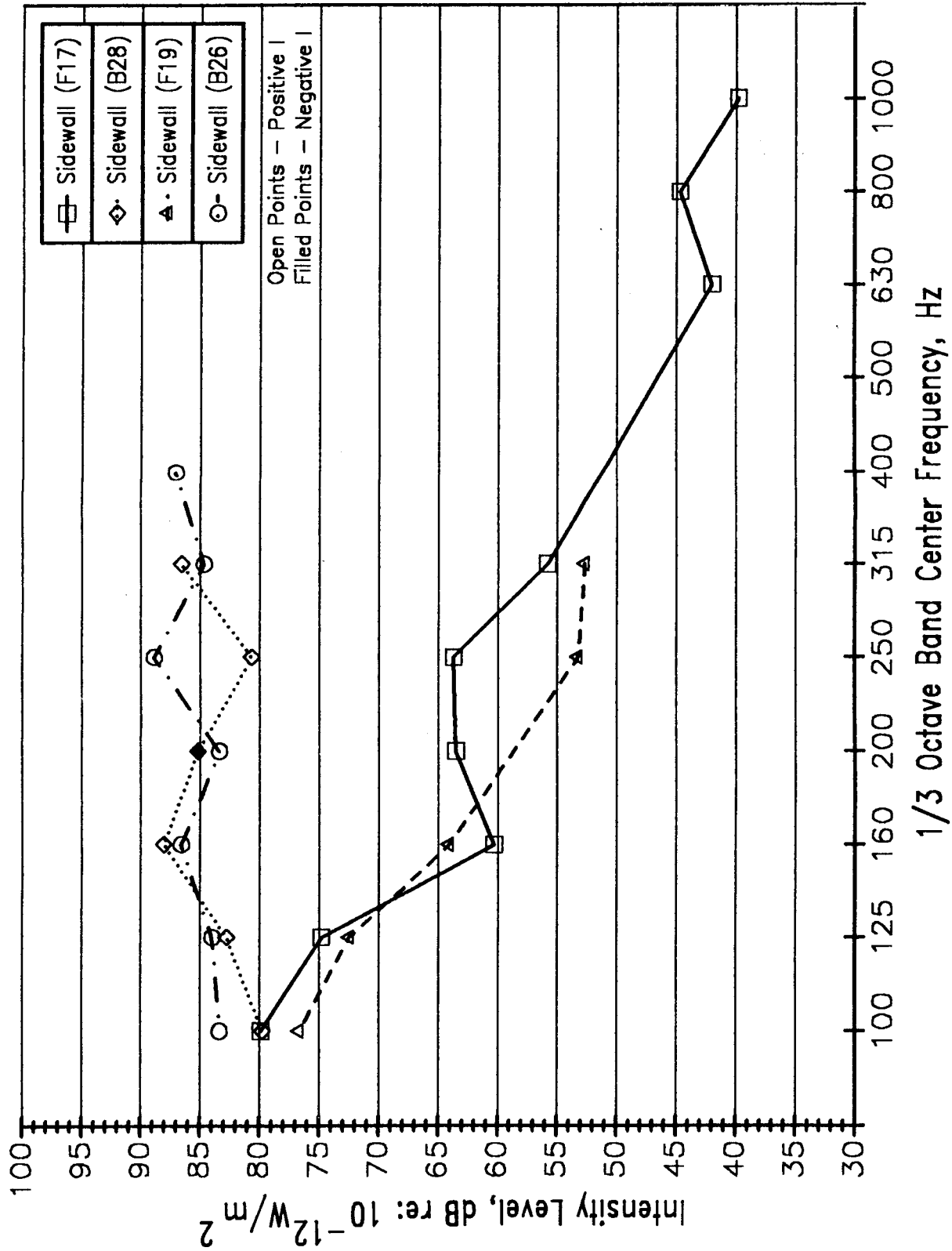


Figure 8-12 Comparison of Sidewall Intensity Levels, Airborne Path Surveys

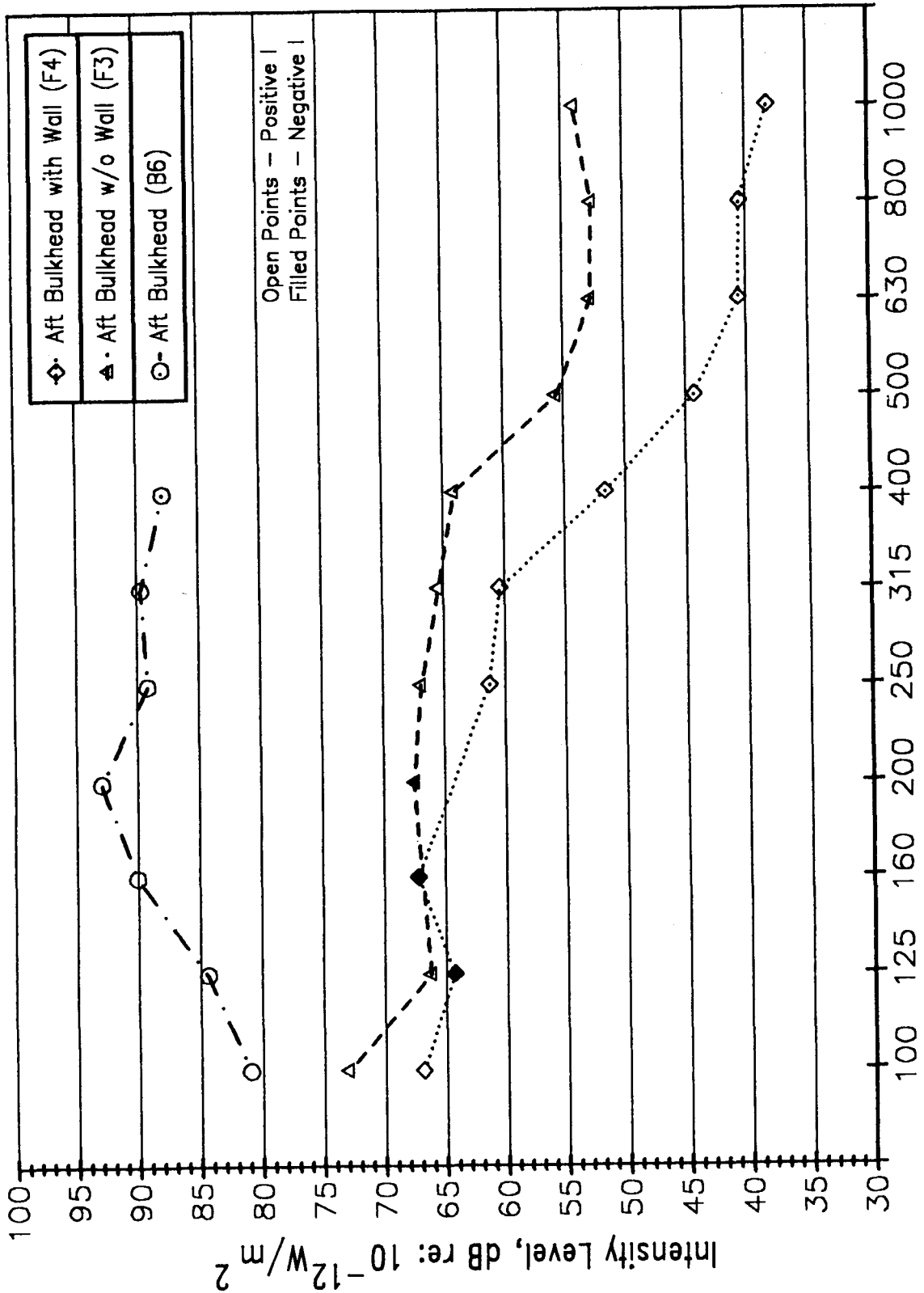


Figure 8-13 Comparison of Pressure Bulkhead Intensity Levels, Airborne Path Surveys

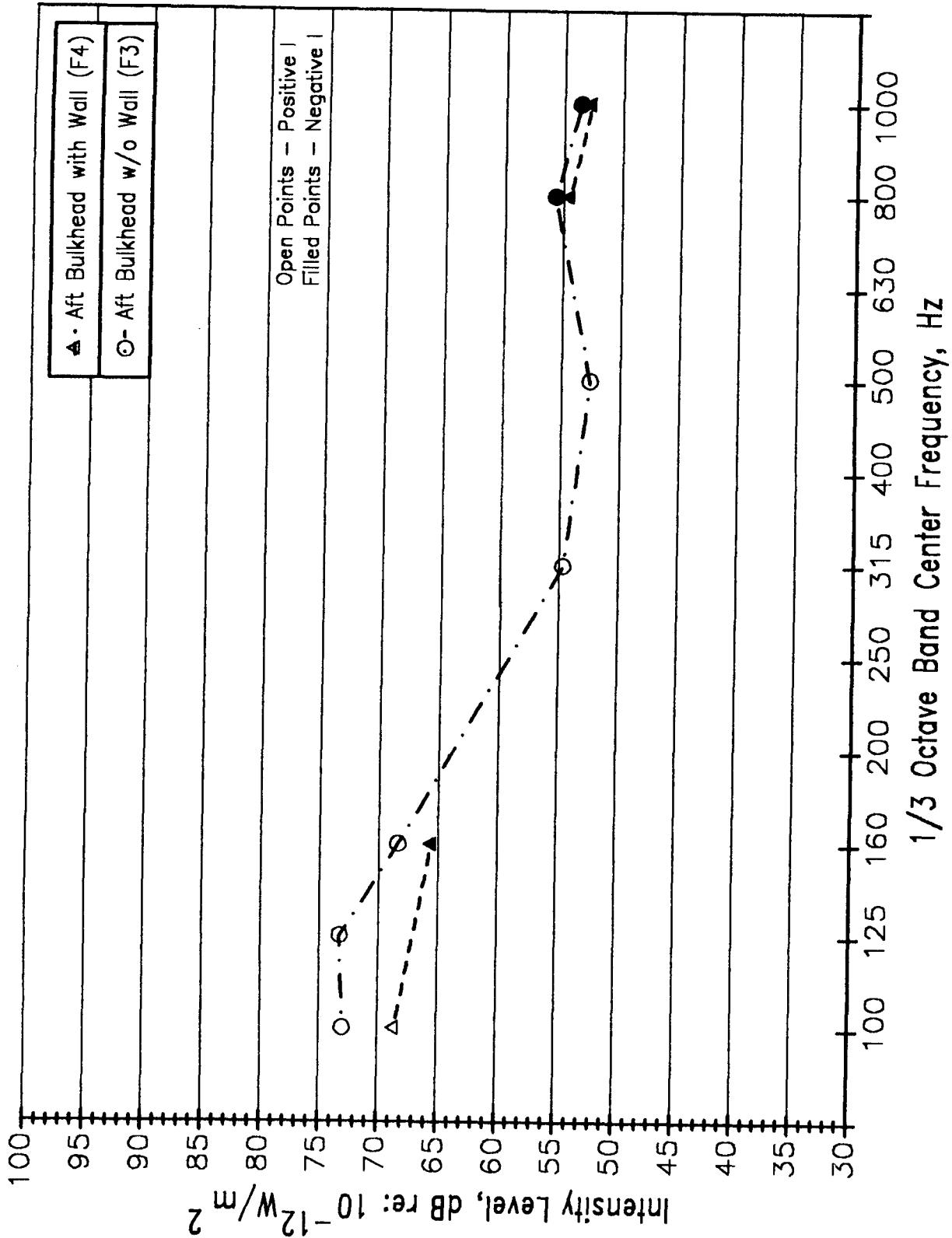


Figure 8-14 Comparison of Pressure Bulkhead Intensity Levels, Structureborne Path Surveys

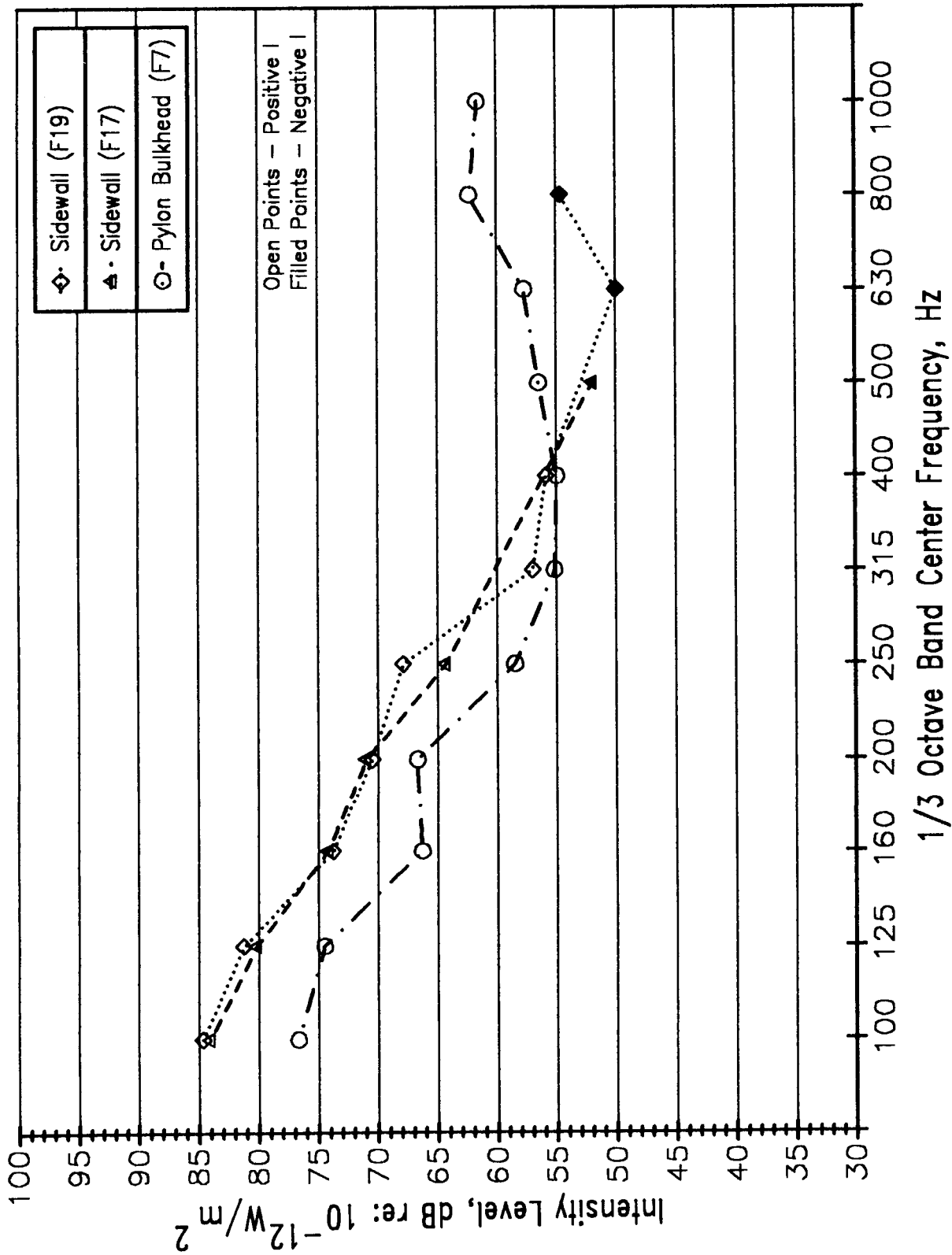


Figure 8-15 Comparison of Sidewall and Pylon Bulkhead Intensity Levels, Structureborne Path Surveys

## 9 Summary and Conclusions

This report documents several sets of tests conducted in the Douglas Aircraft Company Fuselage Acoustic Research Facility, using the aft section of a DC-9 aircraft as the test article. The tests were designed to investigate the interior noise environment of aircraft powered by aft-mounted, advanced turboprop engines, and focused on measurement of the fuselage response characteristics and the effectiveness of selected interior noise control treatments under simulated advanced turboprop excitation.

Fuselage structural mode surveys and acoustic cavity mode surveys of the bare and furnished cabin were conducted to identify the modal response characteristics of the aft fuselage and to support development of analytical models. Both types of surveys showed a high modal density, with many structural and cavity modes occurring in the frequency range where the blade passage frequency of advanced turboprop propellers will occur. The measured structural modes generally showed good agreement with analytical predictions, but there was inconsistent agreement between measured and predicted cavity modes.

Forced response tests were conducted using acoustic and vibration excitations that simulate the expected excitations of a UHB aircraft with a 10x8 propulsor configuration. Several structural and furnished cabin noise control treatment configurations were sequentially installed on the fuselage. Interior noise levels and frame and longeron acceleration levels were measured for the untreated aircraft and for each treatment configuration under similar excitation levels, and compared in order to evaluate the effectiveness of each treatment in reducing noise and vibration levels. The test data showed that treatment effectiveness was often frequency dependent, and also dependent on type of excitation. The major results of these tests are as follows:

- The torque box causes increased noise levels in the cabin at all frequencies for acoustic excitation, but causes substantial reduction in acceleration level for vibration excitation.
- The two extra frames decrease noise levels, and levels generally decrease further with the installation of a second set of two extra frames. The four frames also provide reduced acceleration levels for vibration excitation.
- The frame damping treatment has no effect on interior noise levels and a relatively minor reduction in acceleration levels. The same conclusions apply to application of damping to the torque box, and to disabling the torque box.
- The double wall pressure bulkhead reduces interior noise levels for the higher excitation frequencies.

- Dynamic absorbers tuned to 169 Hz have no significant effect on interior noise levels but reduce acceleration levels at this frequency, and to a lesser extent at 213 Hz, for vibration excitation.
- The absorption blanket has no significant effect on noise levels for acoustic excitation.
- The sonic fatigue damping and the skin acoustic damping treatments both provide reductions in noise levels and acceleration levels, depending on frequency. For acoustic excitation, the benefits of the sonic fatigue damping begin above 213 Hz, while additional noise level reductions due to the skin acoustic damping begin above 426 Hz. For vibration excitation, both treatments reduce acceleration levels at 169 Hz, but only the sonic fatigue damping reduces levels at 213 Hz.
- Installing the cabin furnishings significantly reduces interior noise levels at all frequencies for acoustic excitation. The individual Furnished Fuselage configurations generally provide increasing benefits at the higher excitation frequencies; at the lower frequencies addition of the trim panel damping reduces interior levels. In contrast, for vibration excitation, acceleration levels do not decrease significantly (and in fact increase at 169 Hz). Noise levels measured during vibration excitation, however, show small decreases for both frequencies with the installation of the cabin furnishings.

Additional tests of treatment effectiveness were conducted for excitation along three specific transmission paths. Following are the results of these tests:

- For the pressure bulkhead path, the effectiveness of various treatments applied to this bulkhead was found to occur for frequencies above 200 Hz. In this frequency range, the double wall bulkhead treatment causes significant reduction in level relative to the untreated bulkhead. Adding absorption blankets to the bulkhead further decreases interior noise levels; this result is in disagreement with the results of the forced response tests, which showed that the absorption blankets increase interior levels for certain frequencies.
- For the cabin sidewall path, the effectiveness of skin and trim panel damping applied individually and at the same time varied with measurement location in the cabin. For the locations where the differences among the various configurations were the greatest, benefits occurred above 500 Hz. The reductions in interior noise levels resulting from the damping treatments appeared to follow predictions based on mass law, with a maximum reduction of 5 dB for the combined skin and trim panel damping.

- For the fuselage structural path, the effectiveness of the same skin and trim panel damping treatments was evaluated on the basis of reductions in frame and longeron acceleration levels and interior noise levels, under vibration excitation at 169 and 185 Hz. The noise and acceleration data both showed negligible changes in level for each individual damping treatment compared to the undamped configuration, but a sizeable reduction in level (5 to 10 dB) when the two damping treatments were installed at the same time.

Finally, sound intensity surveys were conducted in the bare and furnished cabin to identify major transmission paths for acoustic and vibration excitation. The bare cabin acoustic excitation survey showed that transmission through the (untreated) pressure bulkhead was the major path for most frequencies. For the lowest frequencies, transmission through the upper portion of the sidewall was also important.

The furnished cabin survey for acoustic excitation without the pressure bulkhead double wall treatment installed showed transmission path results similar to the bare cabin survey, but with uniformly lower levels. However, with this treatment in place the major path into the cabin was eliminated, and various sidewall, floor, and pressure bulkhead areas generally have comparable levels for much of the frequency range.

The furnished cabin survey for vibration excitation showed that the major transmission paths were through the engine pylon bulkhead and the upper and lower sidewall, for most frequency bands.

The various tests and test results described in this report have demonstrated the usefulness of the Fuselage Acoustic Research Facility for studying fuselage response characteristics and evaluating the effectiveness of different types of noise control treatments. For an aft-engine mount advanced turboprop aircraft, structural and cavity modes have been identified, and major acoustic and structural transmission paths have been defined. The performance of individual treatments in reducing advanced turboprop acoustic and vibration excitation has been tested, with the various treatments installed in the fuselage as they would be on a real aircraft.

For vibration excitation, several treatments were found to be effective in decreasing acceleration levels and resulting structureborne noise levels in the cabin for the major UHB excitation frequencies. These include the fuselage stiffening treatments (the torque box and the additional frames), the tuned absorbers, and the damping treatments applied to the fuselage skin. For acoustic excitation, however, none of the treatments were found to be particularly effective in reducing cabin noise levels at the lower UHB frequencies (169 and 213 Hz). For the higher UHB frequencies, several treatments proved effective; in particular the double wall bulkhead provided substantial reductions in noise level for transmission from the unpressurized section through the pressure bulkhead, and the combined skin and trim panel damping treatments reduced

noise levels transmitted through the cabin sidewall.

The need still exists to identify and test lightweight and compact treatments which effectively reduce cabin noise levels resulting from acoustic excitation at frequencies below 250 Hz. There is also a need to better understand the acoustic characteristics of the cabin cavity, and the interaction of the structural and cavity response characteristics, in this frequency range.



# Report Documentation Page

1. Report No. NASA CR-181819		2. Government Accession No.		3. Recipient's Catalog No.	
4. Title and Subtitle Interior Noise Control Ground Test Studies for Advanced Turboprop Aircraft Applications			5. Report Date April 1989		
			6. Performing Organization Code		
7. Author(s) Myles, A. Simpson, Mark R. Cannon, Paul L. Burge, and Robert P. Boyd			8. Performing Organization Report No.		
			10. Work Unit No. 535-03-11-04		
9. Performing Organization Name and Address Douglas Aircraft Company McDonnell Douglas Corporation 3855 Lakewood Blvd. Long Beach, California 90846			11. Contract or Grant No. NAS1-18037		
			13. Type of Report and Period Covered Contractor Report		
12. Sponsoring Agency Name and Address National Aeronautics and Space Administration Langley Research Center Hampton, VA 23665-5225			14. Sponsoring Agency Code		
			15. Supplementary Notes  Langley Technical Monitor: Kevin P. Shepherd Final Report		
16. Abstract <p>This report documents measurement and analysis procedures and summarizes the results of interior noise control ground tests conducted on a DC-9 aircraft test section at Douglas Aircraft Company. The objectives of these tests were (1) to study the fuselage response characteristics of treated and untreated aircraft with aft-mount advanced turboprop engines, and (2) to analyze the effectiveness of selected noise control treatments in reducing passenger cabin noise on these aircraft. The results of fuselage structural mode surveys, cabin cavity surveys and sound intensity surveys are presented. The performance of various structural and cabin sidewall treatments is assessed, based on measurements of the resulting interior noise levels under simulated advanced turboprop excitation.</p>					
17. Key Words (Suggested by Author(s)) Acoustics Advanced Turboprop Aircraft Aircraft Noise Interior Noise Noise Control			18. Distribution Statement  Unclassified - Unlimited Subject Category 71		
19. Security Classif. (of this report) Unclassified		20. Security Classif. (of this page) Unclassified		21. No. of pages 148	22. Price A07